Ultrasound Stimulated Release of Liposomes

Mercy Afadzi

July 14, 2008

Professor: Bjørn Angelsen
Professor: Catharina de Lange Davies

Department of Physics

Abstract

A prerequisite for successful cancer therapy (drug delivery) is that the cytotoxic agents reach all cancer cells and inactivates them and this requires triggerable release of liposomes in order to delivery a high local dose to the cancer cells. The overall aim of this project is to improve the delivery of liposomal drug by combining ultrasound and liposomal drug delivery: Thus, to investigate the effect of ultrasound on release of liposomal drug at various frequencies, intensities, exposure time and medium and also to design an experimental setup to investigate this task. In vitro studies using liposomal calcein as a model for the therapeutic molecules was carried out using four ultrasound transducers (200kHz, 500kHz, 1MHz and 2MHz) at different intensities, exposure time and medium (PBS and HEPES) and release was studied by measuring the fluorescent intensity with a spectrophotometer. Drug release was found to be dependent on frequency, intensity, exposure time and the medium. The optimal frequency was found to be 500kHz at an acoustic intensity of $0.038 mW/cm^2$ and mechanical index of 0.5 which gave 15% average release. Maximum release was obtained at the highest exposure time (600s) for all frequencies and PBS gave higher release than HEPES. The acoustic intensities and mechanical indexes obtained with these transducers suggests the mechanism of release to be stable cavitation.

This research establishes the design of experimental setup and protocols which includes design of ultrasound probes and construction of sample holders used during ultrasound exposure for control release experiment. It confirms the dependency of frequency and acoustic pressure, intensity and exposure time in ultrasonically-triggered drug delivery from liposomes, and finally proposes stable cavitation as the mechanism for the release using the value of the mechanical index as an indicator. This opens the door for further investigations to know the mechanism that is associated with drug release in this field of study.

Preface

This thesis is submitted to the Department of Physics at the Faculty of Natural Sciences at the Norwegian University of Science and Technology (NTNU) in fulfillment of the masters program in the year 2008.

The thesis was carried out at the Department of Circulation and Medical Imaging at the Faculty of Medicine and Department of Physics at NTNU. Supervision of this project was done by Professor Bjørn Angelsen and Professor Catharina de Lange Davies. In fact I give thanks to God for successful completion of this two years program (MSc Medical Technology) and being there for me all the time. My deepest gratitude goes to my two supervisors for being helpful, inspiring and supportive for this work. They never refused giving their time and advice when needed. Sincere thanks goes to Ing. Tonni Franke Johansen and Øyvind Krøvel-Velle Standal for their support and professional advice especially for the laboratory work. I really appreciate all your efforts and time. God richly bless you so much.

To all colleagues and friends for their support in any form through out these years. To Abednego Tetteh, Raymond Doe, David Lamptey, Kofi Hanson and Kingsley Bawfeh, thanks so much for your help and support it is great having you as friends. To the international church at Bethel I say God bless you all for your support in these two years. You were more than a family to me. Finally, my deepest gratitude goes to my family in Ghana, God bless each one of you for your love and care through out my life.

Contents

List of Figures

List of Tables

Chapter 1

INTRODUCTION

There are lot of limitations associated with conventional chemotherapy. The main limitation is, cytostatic drugs used for the treatment of cancer do not target the tumor cell specifically but affect healthy tissues containing dividing cells. Thus small- molecule chemotherapeutic agents have large volume of distribution when administered [1, 57] which often results in narrow therapeutic index (ratio of therapeutic benefit to side effects) due to high level of toxicity in healthy tissues [18]. To overcome the unwanted effect associated with chemotherapy, the therapeutic index could be enhanced by delivering these agents specifically to tumor cells whereby keeping them away from non-malignant cells sensitive to the toxic effects of the drug. This is done by encapsulating drugs in a micromolecular carrier, such as a liposome.

Liposomal drug delivery systems aim to improve drug pharmacokinetics and biodistribution by delaying drug clearance, reducing the distribution volume, retarding drug metabolism and shifting the distribution in favor of diseased tissues due to the leaky capillaries in tumors and lastly to control drug release rate [2, 18, 56, 10, 60]. Studies have shown that hydrophobic drugs release too slowly for therapeutic efficacy[11, 56] so to deliver local high dose, triggerable released would therefore be desirable [25]. Nevertheless, lot of methods for both drug encapsulation and for prolonging the circulation of liposome have been developed unlike procedures for triggered drug release[25, 32, 3].

Some of the strategies proposed for triggered drug release from liposome to increase selectivity includes; inserting pH-responsive copolymers into liposomal membranes and exploiting the acidic environment of endosomes in cancer cells [18], enzyme activated prodrug therapy, methods based on physical phenomena such as electric fields [39], magnetic fields [8], temperature [32] , visible light [4, 38] and ultrasound [25, 40, 36]. This project focuses on drug release triggered by ultrasound. Ultrasound is of special interest because it is non-invasive, can be focused on targeted sites, it can also penetrate into interior of the body without affecting the interposed tissue. Finally it has been shown by studies that ultrasound increases the permeability of blood-tissue barriers

and cell membranes [51]. The exact mechanisms for ultrasound mediated release are poorly understood, but studies [49, 62] have shown cavitation (more on cavitation can be found in Chapter 2) to be a major factor. Also, it has been shown that ultrasound increases the release of liposomal drug, and reduce the volume of tumors growing in mice [40, 41]. Cavitation can cause bubbles to oscillate when exposed to pressure waves and this oscillation may or may not lead to the collapse of the bubble depending on the acoustic intensity (that is, can be stable or inertia cavitation). For effective use of ultrasound in drug delivery, determination of optimal frequency, intensity and duration is of importance. Thus, although it has been shown that release depends on the frequency, pressure, intensity, exposure time and composition of the liposomes [54, 56, 25, 6], the various effects ultrasound have on the delivery may be optimal at different frequencies and intensities and also how much time you apply the ultrasound.

In this project, however, we aim to improve the delivery of liposomal drugs by combining drug delivery and ultrasound. Thus to design an experimental setup for control release experiments and also to investigate the effect of ultrasound on release of liposomal drugs by varying;

- Frequencies $(0.2 - 2MHz)$
- Intensities
- Exposure time
- Medium (HEPES Sucrose buffered solution and Phosphate Buffered Saline (PBS))

As a model for drug delivery, liposomes filled with calcein will be used. The destruction of liposomes by the ultrasound releases calcein into the medium (PBS or HEPES Sucrose buffered solution) so by measuring the fluorescence intensity of emitted light the effect of ultrasound on release can be investigated. Due to quenching of emitted light from nearby calcein molecules, the intensity increases when calcein is released from the liposomes, by relating the intensity after treatment with ultrasound to the intensity registered before ultrasound and the total intensity registered due to addition of triton , the percentage release can be computed.

This report is organized as follows: Chapter two and three explains the theoretical background of the study- the morphology and physiology of tumors, the mechanism by which liposomes are able to deliver drugs to solid tumors and the barriers they face on their way has being dealt with in Chapter two. Chapter three explains the interaction of ultrasound with matter, that is, fundamental physical effects can be found in th first section whereby the second section is about ultrasound transducer and how it works. The last part of the background theory can be found at Chapter four which explains the concept of spectroscopy. The materials and method used in the experiment can be found in Chapter five. The six chapter gives the results obtained from all the experiments whereas Chapter 7 is about how these results were interpreted- discussions on the results. Conclusion of the project has been given in Chapter eight.

Part I

BACKGROUND THEORY

Chapter 2

TUMOR PHYSIOLOGY AND LIPOSOMES

This chapter has two main sections, thus, the first section explains the morphology and physiology of tumors and the final section is about liposomes in drug delivery- the mechanisms associated with the delivery of liposomal drugs has been explained followed by some of the barriers that impedes its progression into the tumor cells.

2.1 Characteristics of Tumors

Cancer is a disease that affects cells of the body and is found to be responsible for about 13% of all deaths [46]. According to the American Cancer Society, 7.6 million people died from cancer in the world during 2007.

Generally, in human tissues, cells division balances with cell differentiation and cell death so there is no net accumulation of dividing cells. However, in tumors, cell division does not balance with cell differentiation and cell death which leads to accumulation of cells so that the normal organization and function of the tissues is disrupted. Based on the differences in the growth patterns of tumors, they can be classified as either benign or malignant. Benign tumors grow in a confined local area and are rarely dangerous and do not grow back when removed. These tumors do not invade the tissues around them, thus do not spread to other parts of the body. Malignant tumors on the other hand are cancerous and so are generally more dangerous than the benign. They can sometimes reappear after it has been removed and can even spread to damage nearby tissues and organs. The cancer cells can spread by breaking from the original tumor, enter the bloodstream or lymphatic system and invade new organs by forming new tumors and damage the organ, example liver, lungs, and brain (metastasis). Summary of these differences can be found in Table 2.1.

Table 2.1: Differences in the microscopic appearance of benign and malignant tumors[31]

Trait	benign	malignant
Nuclear size	small	large
Nuclear to cytoplasmic (N/C) ratio	low	high
Nuclear shape	regular	pleomorphic
Mitotic index	low	high
Tissue organization	normal	disorganised
differentiation	well- differentiated	anaplastic
Tumor boundary	well-defined	poorly defined

2.1.1 *Physiology of tumors*

A solid tumor is made up of tumor cells, blood vessels, the interstitium/extracelluar matrix (substance produced by cells and secreted into the environment in which the cells are embedded; contains collagen, proteoglycans, glycosaminoglycans, and fluid) and stromal cells (Connective tissue cells such as fibroblasts). In order for blood to reach all areas of a tissue, the blood vessels in normal tissues are well organized. Cancer cells initially grow in the midst of normal tissues and make use of the existing vasculature but as the tumor grows, the cancer cells then induce new blood vessels (often leaky) to form within them so that they can receive nutrients to grow. This process of forming new blood vessel is known as angiogenesis. They actually do this by sending out a signal to stimulate the cells lining nearby blood vessels to grow towards them and also to divide faster than usual. Due to their unnaturally quick growth, the new blood vessels are usually not quite normal (leaky) and much less effective at carrying blood (slow flow rate), but they can still provide the necessary nutrients to the tumor. The vascular system of tumors is therefore made up of vessels coopted from the preexisting network of the host vascualature and vessels resulting from the angiogenic response of the host vessels to cancer cells [22]. This leads to disorganized vascular system resulting in uneven or chaotic blood supply in tumors [29, 30]. The slow flow rate combine with compression of tumor cells leads to high pressure in the blood vessels and is normally called high microvascular pressure (MVP). Fluid then flows out of these vessels into the interstitium/extracellular matrix and because there is no lymphatic system in tumors, interstitial fluid pressure is elevated as the fluid builds up. That is, high interstitial fluid pressure (IFP) reflects high microvascular pressure (MVP) [17] . However, interstitial fluid pressure at the tumor periphery is almost zero as the transcapillary pressure gradient. Studies have shown both experimentally and mathematically that the pressure increases $(0.4 - 0.6mm)$ as you move from the periphery of the tumor to the tumor interior [30]. In addition to this, the disorganized nature of the tumor blood vessel can result in limited diffusion from functional blood vessels (diffusion-limited or chronic hypoxia) and interruptions (heterogeneity) in blood flow can also lead to transient hypoxia (a situation where some part of

the tumor receives blood for some time and another moment no blood flow). There are therefore four main regions in tumors, that is, the necrotic region, seminecrotic region, stabilised microcirculation region and advancing front due to this chaotic blood supply [20](see Fig.2.1). The lack of diffusion may also lead cancer cells to secrete high levels of lactic acid (low pH).

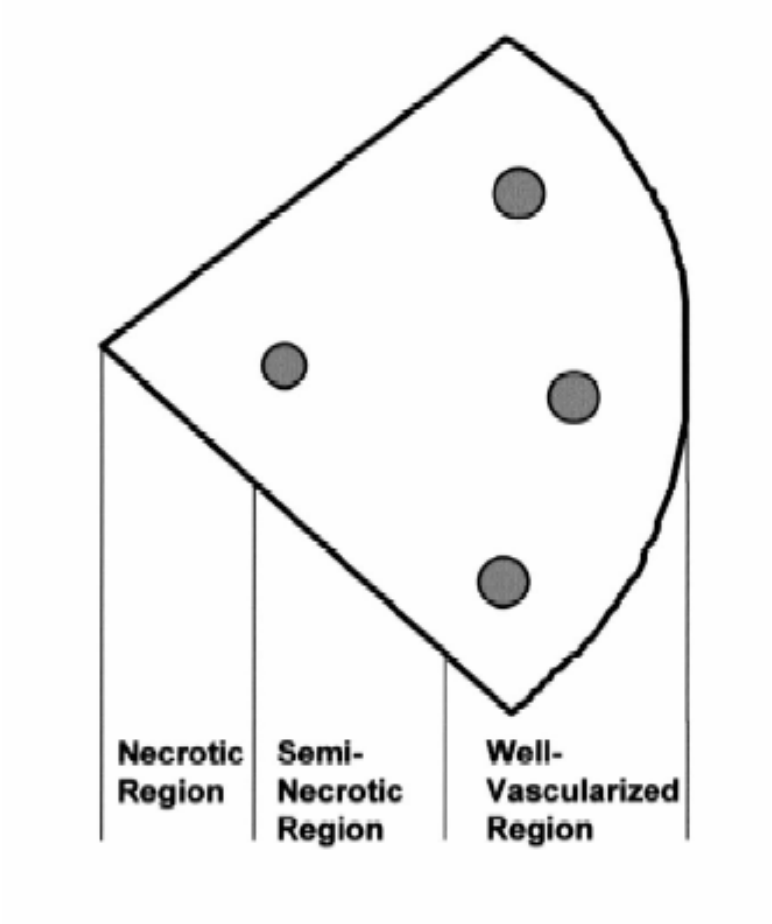

Figure 2.1: Schematic diagram of a heterogeneously perfused tumor showing well-vasculaized periphery, seminecrotic or intermediate zone and a central necrotic region [29].

2.2 Liposomes in Drug Delivery

Liposomes are non-toxic biodegradable and ion -immunogenic drug delivery vehicle which was discovered about 30 years ago by Bangham [9]. They are the smallest artificial vesicles of spherical shape produced from natural untoxic phospholipids and cholesterol which can be used in a lot of applications (clinical, cosmetics etc). Thus they are made

up of one or more concentric bilayer of phospholipid with each enclosing an aqueous compartment as shown in Fig. 2.2. The molecular shape of a phospholipid consist of water-loving head and two oil-loving tails as can be seen in Fig. 2.2c. When a large number of these molecules are placed in a small space, the heads will spontaneously be arranged together and the tails will also come together and this makes them suitable for delivery both hydrophilic and lipophilic drugs. The bilayer is impermeable to large molecules such as proteins and enzymes whereby it has low permeability to charged molecules, including ions. It can also be loaded with a great variety of molecules, such as small drug molecules, nucleotides and even plasmids.

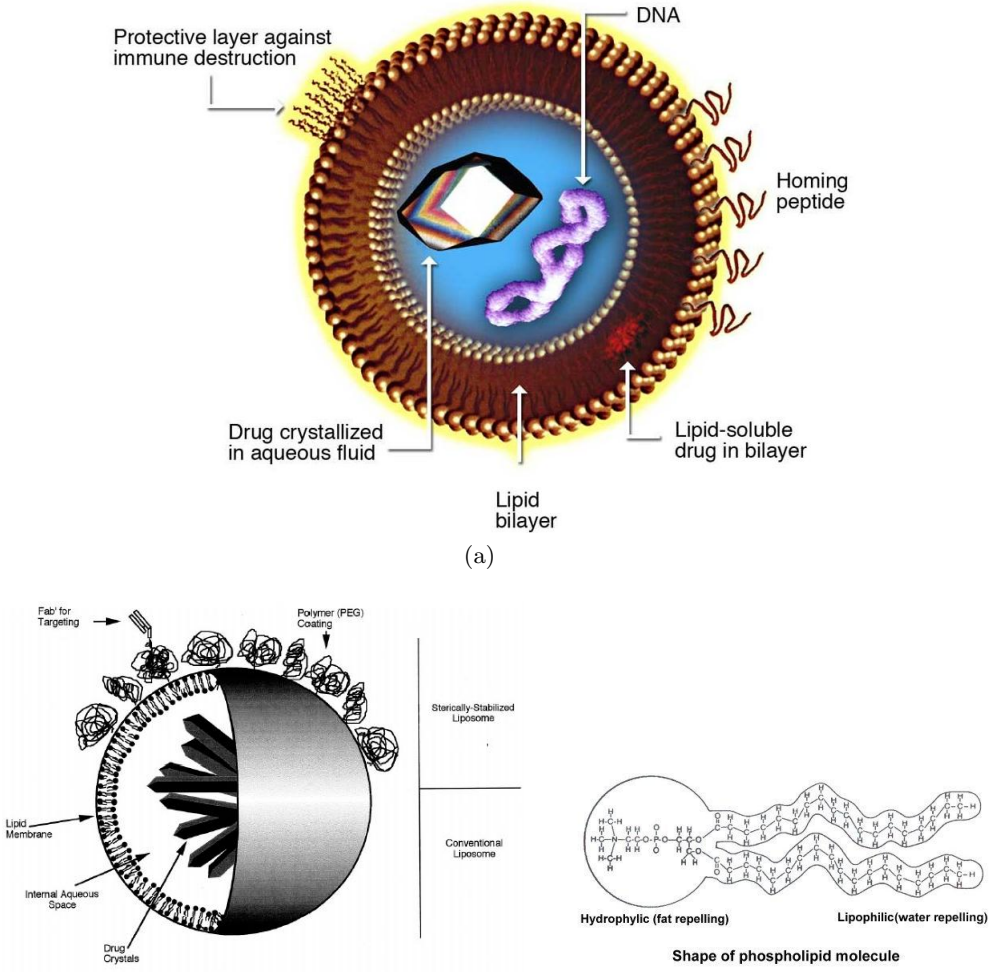

Figure 2.2: Structure of Liposome for drug delivery (a and b),(c) Shape of a phospholipid molecule [9].

The average diameter of a liposome is 50 to 100nm [2] which means that they can be formulated in a large range of sizes. They have a lot of properties that make them versatile drug carriers for either water-soluble or lipid-soluble drugs. For instance, liposomes have the ability to change the pharmacokinetics of drugs incorporated into it and this makes them valuable as drug systems as compare to free drugs or the same drug in aqueous solution. Thus there are significant changes in the uptake, biodistribution and clearance of liposomes-associated drugs which leads to dramatic effects on both the efficacy and toxicity of the compound entrapped [2]. In addition to these changes, liposomes also have long circulation half life since the clearance rate is substantially reduced especially when they are pegylated (as the ones used in this research) to prevent them from been taken up by cells of the reticuloendothelial system and also to prevent leakage while in circulation. It has also been observed that increase in circulation times of liposome-associated drug increases their localization into diseased tissues [24, 47]. Since the capillaries of solid tumor have increased permeability compared to normal vessels the drug is able to localize in greater quantities in the tumor than in normal tissues as a result of long circulation times. After localization of liposomal drug in the solid tumor, the drug is then released from the liposome in the extracelluar matrix or the interstitium followed by uptake of the drug in its free form by the tumor cells.

2.2.1 *Some barriers encountered by liposomal drugs*

An ideal liposome should be able to travel through the bloodstream and cross the capillary wall to their target after they have been administered orally or by injection. To be able to eradicate the tumor completely, the liposomal drug must disperse throughout the tumor in sufficient concentrations to eliminate every deadly cell. Thus before the drug can attack the tumor cells, liposomes have to make their way through the blood vessels in the tumor, must be able to cross the walls of the vessels into the interstitium and then finally, move through the interstitium to the cancer cells [29] (see Fig. 2.3).

The first barrier to drug delivery is the chaotic blood supply in solid tumor [29, 30] since movement of molecules through the vascular system is dependent on the length, diameter, the number, the geometric arrangement of the blood vessels and the blood flow-rate. Also, due to the uneven distribution of blood vessels, regions lacking vessels (necrotic area) will not be able to receive drug directly from circulation and this result in a decrease in uptake of drug in general. In other words, the average uptake of drug decreases with an increase in tumor weight [29, 30]. In addition to this, the twisted nature of the vessels leads to slow blood flow which also hinders delivery of drugs to poorly perfused regions of the tumor. The second barrier is the mechanism by which the drugs are delivered to the tumor cells namely; diffusion and convection

Diffusion depends on the concentration gradient in the interstitium whereby convection is dependent on the pressure gradient in the interstitium. As stated earlier on, there is high interstitial fluid pressure in the center of the solid tumors as compared to the periphery

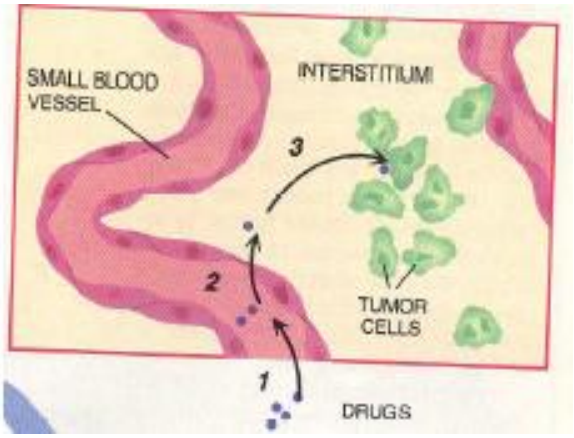

Figure 2.3: Three critical steps for cancer drugs to get to their targets successfully [29]

and surrounding tissues. Elevated interstitial fluid pressure (IFP) is believed to be one of the main reasons to low uptake and heterogeneous distribution of macromolecular therapeutic agents in tumors. The reason being that, interstitial fluid flows from the tumor's periphery into the surrounding normal tissue so macromolecule at the tumor's periphery has to overcome this outward convention to diffuse into the tumor. Those macromolecule which are able to make their way into the interstitium will face the difficulty of spreading evenly throughout the interstitium to be able to reach cells which are not directly fed by blood vessels due to the collagen content and structure which may impede the diffusion of large molecules in tumors. This can in turn contribute to the low concentration of drug molecules in the extracellular matrix [29]. It would therefore be desirable to trigger the liposomes to release their content such that the local concentration is high enough to mediate an effective therapeutic effect.

Chapter 3

THEORY OF ULTRASOUND

This Chapter describes the various effects that is being produced as a result of interaction of ultrasound with a medium. The first section begins with discussions on the fundamental physical effects, that is, the wave motion, intensity and energy deposition. This is followed by a brief discussion on the secondary effects induced by ultrasound as it propagates through a medium. The last two sections describe acoustic heating and cavitation (principles behind bubble collapse). Finally, a brief description of the ultrasound transducer can be found in the last section.

3.1 Ultrasound Interaction with Matter

The name ultrasound (US) is used to describe sound waves with frequencies above the audible range, that is, above $15 - 20kHz$. It can be used in a number of applications in the clinic and the industry (including welding and processing and non-destructive evaluation). Like any other sound waves, US is a mechanical wave that requires a material medium (such as air or liquid) for its propagation. Medical US usually operates in the range $2 - 20MHz$ [5]. In medicine, ultrasound is used for therapy, to detect changes in appearance and function of organs, tissues, or abnormal masses, such as tumors. Currently, US imaging is widespread in clinical use and it accounts for about one in four of all imaging procedures worldwide [61] with a wide range of therapeutic applications currently under considerations [26].

3.1.1 *Fundamental physical effects of ultrasound*

The theory in this section is cited from [26] and Chapter 1 and 2 of [5]. Acoustic waves can arise from the application of a time-varying stress to a medium. In a material where by acoustic parameters (mass density and compressibility) are independent of position

and direction (isotropic homogeneous medium), the propagation of sound waves is due to the elastic properties of the medium. When a wave travels through an isotropic medium, it causes cyclic compression and expansion of the material as can be seen in Fig. 3.1. Thus for a longitudinal wave, the particle motion is along the direction of the wave motion. The wave motion will cause each plane wave to vibrate around its equilibrium position, with displacement $\xi(z,t)$ from its equilibrium position. The vibration velocity and the acceleration are given as;

$$\begin{aligned} u(z,t) &= \frac{\partial \xi(z,t)}{\partial t} \\ a(z,t) &= \frac{\partial u(z,t)}{\partial t} \end{aligned} \tag{3.1}$$

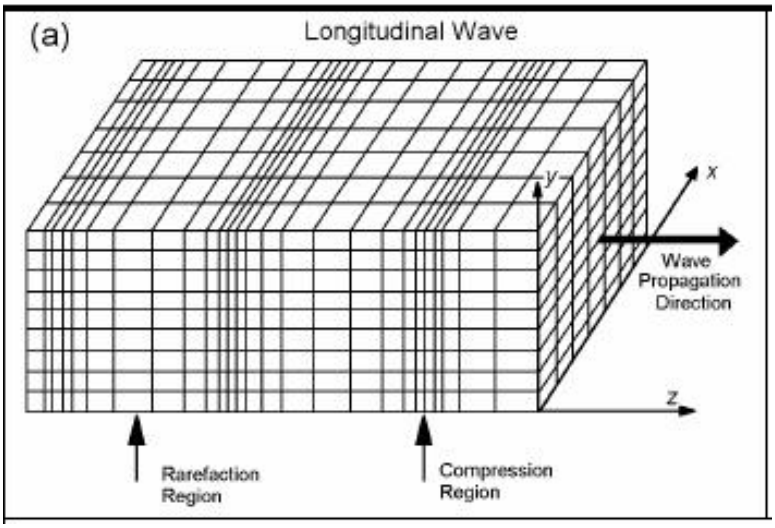

Figure 3.1: Particle displacement for a plane longitudinal wave propagating in the z-direction of an isotropic solid medium [15].

The varying displacement also leads to compression of the material which generates pressure. The volume compression of the element in a short term is given as [5];

$$\begin{aligned} \delta V &= \left\{ \xi(z,t) + \Delta z \frac{\partial \xi}{\partial z} - \xi(z,t) \right\} A \\ \frac{\delta V}{\Delta V} &= \frac{\partial \xi}{\partial z} \end{aligned} \tag{3.2}$$

where $\Delta V = \Delta z A$ is the volume in the unstrained material.

The volume compression is also dependent on the pressure so assuming a linear relationship will lead to;

$$p \approx -\frac{1}{\kappa}\frac{\partial \xi}{\partial z} \tag{3.3}$$

where κ is the bulk or volume compressibility

Differentiating with time and using Eq. 3.1 yields;

$$\frac{\partial p(z,t)}{\partial t} = -\frac{1}{\kappa}\frac{\partial u(z,t)}{\partial z} \tag{3.4}$$

From Newtons second law, the kinetic energy can be given as;

$$\rho \frac{\partial u}{\partial t} = -\frac{\partial p(z,t)}{\partial z} \tag{3.5}$$

Combining Eq. 3.5 and Eq. 3.6 gives the wave equation;

$$\begin{aligned} \frac{\partial^2 u}{\partial z^2} - \frac{1}{c^2}\frac{\partial^2 u}{\partial t^2} &= 0 \\ \frac{\partial^2 p}{\partial z^2} - \frac{1}{c^2}\frac{\partial^2 p}{\partial t^2} &= 0 \end{aligned} \tag{3.6}$$

where $c^2 = \frac{1}{\rho\kappa}$ is the propagation velocity and have also assumed constant compressibility κ and density ρ of the medium. This equation describes the wave motion and is based on the cyclic exchange between the potential energy stored in the elastic compression of the material and the kinetic energy based on the Newton acceleration equation.

Variation in particle displacement from their equilibrium positions produces changes in the medium density from the equilibrium density ρ_0 and the pressure in the medium from p_0 to $p_0 + p$. Where p_0 is the ambient pressure and p is the acoustic pressure.

For a harmonic plane wave the pressure is related to the velocity by $p = \rho_0 c_0 u$. The acoustic pressures can exceed the ambient pressure, for instance in fluid because fluids can support an overall negative pressure (tension) for short times based on how long it is applied. If the higher pressure is applied for a longer time the fluid will cavitate with small bubbles forming. Interaction of ultrasound with the material can results in a lot of physical effects namely; intensity and energy deposition, transmission and reflection at interfaces and nonlinear propagation.

3.1.1.1 *Intensity and energy deposition*

Ultrasonic waves can be characterized in terms of their energy density and the rate at which they transmit energy (kinetic energy-particle motion and potential energy- fluid compression). For a plane harmonic wave, acoustic intensity I of a sound wave can be defined as the average rate of flow of energy through a unit area normal to the direction of propagation. In other words, acoustic intensity is defined as follows;

$$I = \frac{1}{2}\frac{p^2}{\rho_0 c_0} \tag{3.7}$$

where $p = p\cos wt$ is the amplitude of the pressure.

Table 3.1: Examples of medical ultrasound diagnostic and therapy applications and their frequencies, peak rarefactional pressures and spatial peak temporal average intensities I_{SPTA} [59]

Modality	frequency(MHz)	Peak rarefactional pressure (MPa)	$I_{SPTA}(W/cm^2)$
B- mode	1-15	0.45-5.5	0.0003-0.
PW Doppler	1-10	0.67-5.3	0.17-9.1
Physiotherapy	0.75-3.5	0.3	3
High-intensity focused ultrasound (HIFU)	1-10		1000-10,000
Lithotripsy	0.5-10	5-15	

Table 3.1 gives examples of frequencies, peak rarefractional pressures and spatial peak temporal average intensities I_{SPTA} used for the different modalities. It can be seen that, therapeutic systems requires higher peak negative pressures and time-averaged intensities than those of diagnostic systems.

There is lost of intensity as the sound wave propagates through the medium due to attenuation. For a homogeneous media, the waves are attenuated with distance as a result of absorption whereby in an inhomogeneous medium, acoustic scattering contributes to the lost of energy. Thus the intensity of the a plane wave propagating in the z-direction will reduce to;

$$I = I_0 e^{-2}\alpha_a z \tag{3.8}$$

Whereby in an inhomogeneous medium, it reduces to;

$$I = I_0 e^{-2\alpha z} \tag{3.9}$$

where α_a is the amplitude of the absorption coefficient and I_0 is the initial intensity of the wave in the medium. $\alpha = \alpha_a + \alpha_s$ where α is the total attenuation coefficient and α_s is the scattering attenuation coefficient but because attenuation due to scattering is relatively less than that of the absorption, it is assumed $\alpha = \alpha_a$.

3.1.1.2 *Transmission and reflection*

Changes in the acoustic media influences the propagation of ultrasound in that media. When the ultrasound waves are transmitted into a tissue, the wave will be partially reflected and transmitted at the boundaries or interface due to the relative change in acoustic impedance of the the two media. Acoustic impedance can be defined as,

$$Z = \rho c$$

which means that acoustic impedance is dependent on the density ρ of the medium and the propagation velocity of the wave in that medium. This leads to three component of the wave (reflected wave, transmitted wave and the incident wave). Thus an incoming forward wave, a reflected backward wave and a transmitted forward wave. The pressure reflection coefficient (thus the ratio of reflected to incident pressure amplitude) of a wave in two media can therefore be written as;

$$R = \frac{Z_2 - Z_1}{Z_2 + Z_1} \tag{3.10}$$

where by the transmission coefficient (ratio of transmitted to incident pressure amplitude) can be expressed as;

$$T = \frac{2}{1 + Z_1/Z_2} \tag{3.11}$$

where $Z_2 = \rho_2 c_2$ and $Z_1 = \rho_1 c_1$ are the acoustic impedance of medium 2 and 1 respectively and ρ_2, ρ_1, c_2, c_2 are the densities and propagation velocities of medium 2 and 1 respectively. If the peak compressional pressure is larger than the rarefractional pressures than $\rho_2 < \rho_1$. This implies that the reflected wave will be inverted, but if $\rho_2 > \rho_1$ then the pressure transmission coefficient will be greater than unity. If the overall energy is conserved then ;

$$\frac{Z_2}{Z_1} T^2 + R^2 = 1 \tag{3.12}$$

3.1.1.3 *Nonlinear propagation*

Propagation of the ultrasound in materials can be nonlinear although it is often assumed to be a linear process. When the pressure in the material (for example fluid) arises, the

linear relationship between compression and pressure is no longer valid, which means the compressibility function can be expressed as a second order approximation as expressed in the equation below; The relationship between compression and pressure then becomes;

$$\frac{\delta v}{\Delta V_o} = -\frac{\partial \psi}{\partial z} = \kappa P - \beta_n (\kappa P)^2 \tag{3.13}$$

where β_n is the compressibility nonlinearity parameter given as ; $\beta = 1 + \frac{B}{2A}$ (where A and B are constants). Using Taylor's expansion, the nonlinear wave equation can be written as;

$$\begin{aligned} \nabla^2 \varphi - \left[\kappa \rho \left(1 - 2\beta_n \kappa \frac{\partial \varphi}{\partial t} \right) \frac{\partial^2 \varphi}{\partial t^2} \right] = 0 \\ \Rightarrow \nabla^2 \varphi - \frac{1}{c(p)^2} \frac{\partial^2 \varphi}{\partial t^2} = 0 \end{aligned} \tag{3.14}$$

where;

$c(p) = \frac{1}{\sqrt{\kappa\rho\left(1-\beta_n \kappa \frac{\partial \varphi}{\partial t}\right)}} \approx c_o(1 + \kappa\rho(1-\beta_n) \approx c_o(1 + \beta_n \kappa \rho)$ which is pressure dependent.

Thus, the propagation velocity is no longer constant (c_0) but the wave travels with a new velocity $c(p)$. The pressure dependent propagation velocity can produce acoustic shock, where the negative spatial (and positive temporal) gradient becomes infinite. In other words, the nonlinearity leads to distortion of waves as it propagates through the material. As a result of higher local pressure and resulting higher propagation velocity, the positive peak of a pulse will travel slightly faster than the negative peak. This will therefore accumulate as the wave travels resulting in further distortion but in the end, the positive peak will catch up with the negative. This process can result in the generation of shock-like waveform with sudden changes in pressure over short distances in the wave field. This waveform distortion can also result in the generation of harmonic frequencies as the wave propagates. This effect can be well demonstrated by water due to its low absorption where by it is not possible with acoustical waves in tissues.

3.2 Secondary Physical Effects

This section is also cited from [26, 5]. Ultrasonic field can also generate some secondary effects like, radiation pressure and acoustic streaming. The effect are generally small in magnitude and increase in proportion to intensity. However, they have the potential to produce forces and motions at much lower frequencies.

3.2.1 *Radiation pressure*

This is a steady small pressure exerted on the surfaces or media interfaces and it acts in the direction of the wave propagation. It occurs as a result of the nonlinearity of the acoustic equations. For a plane wave incident normally on a perfect absorber, radiation pressure can be defined as;

$$P_{rad} = \langle \epsilon \rangle = \frac{1}{2}\frac{p^2}{\rho_0 c_0^2} = \frac{I}{c_0} \tag{3.15}$$

Where ϵ is the time-averaged energy density of the wave at the surface. If the dimensions of the object is out side that of the acoustic beam, then the total radiation force F_{rad} on the target is given as;

$$F_{rad} = \frac{P}{c_0} \tag{3.16}$$

Where P is the power in the acoustic beam. Radiation pressure for a continuous wave is a steady constant pressure whereby it varies periodically at the modulating frequency for a pulsed wave. Also, the direction and amplitude of radiation force depends on the elastic properties of the materials involved for non-absorbing interfaces and small particles.

3.2.2 *Acoustic streaming*

Attenuation of ultrasonic beam with distance can give rise to a radiation pressure gradient in the fluid which can in turn cause a net body force on each element of the fluid which give rise to a net flow of the fluid with magnitude and form depending not only on the characteristics of the beam but also the fluid and characteristics of the container [23].

The radiation pressure gradient of a plane wave is given by;

$$\frac{dP_{rad}}{dz} \approx \frac{1}{c_0}\frac{dI}{dz} \approx \frac{\alpha I}{c_0} \tag{3.17}$$

Where α is the amplitude attenuation coefficient associated with all processes of acoustic loss. The maximum axial streaming velocity, v_{max} for an unfocused circularly symmetric beam of sound or weakly focused beam of intensity, I, and beam radius ,r, is given as;

$$v_{max} \approx \frac{\alpha I}{c_0 \mu} r^2 G \tag{3.18}$$

Where μ is the shear viscosity of the fluid and G is a constant that depends on the geometry of the beam and vessel containing the fluid.

3.3 Ultrasound and Drug Delivery

Ultrasound-mediated biological phenomena has been grouped into two categories namely: thermal and non-thermal effects. Thermal effects refers to the the absorption of acoustic energy by fluids and tissues, example heating. The later is associated with bubble oscillations known as Cavitation.

3.3.1 *Ultrasonic heating*

The deposition of acoustic energy into the propagation medium due to absorption leads to heating. Thus the first direct effect of ultrasound on medium in which it propagates is heating. The rate per unit volume of heat deposited in the material is given as;

$q_v = 2\alpha_a I$, where I is the intensity of the wave and α is the attenuation coefficient.

The temperature rise associated with this heat deposition can therefore be expressed as;

$$\frac{\partial T}{\partial t} = \frac{2\alpha_a I}{\rho_0 C_p} \tag{3.19}$$

where C_p is the specific heat capacity of the medium at constant pressure. Heat will then be transfered from warmer regions to cooler regions due to the rise in temperature as well as convection, conduction and radiation. In tissues , however, perfusion will occur, thus, heat will be removed from warmer regions by blood flowing through capillaries and blood vessels and redistributed to cooler regions. These processes can be described mathematically by;

$$\frac{\partial T}{\partial t} = \kappa \Delta^2 T - \frac{(T - T_0)}{\tau} + \frac{q_v}{\rho_0 C_p} \tag{3.20}$$

where κ, τ, and T_0 are the thermal diffusivity, time constant for perfusion and initial or ambient temperature respectively. This equation is called the Pennes bio-heat transfer equation used to describe the above mentioned processes in tissues. The first term in this equation accounts for diffusion using temperature gradient where by the second term accounts for perfusion using diffusion time constant and the heat term q_v is dependent on the nature of field produced by the transmitting transducer. For a uniform tissue, the rate of temperature rise is dependent on the field and the frequency (initially greatest where the intensity is greatest). This means that for a focused transducer, it will be greatest at the focus region. This therefore leads to steeper transverse temperature gradient due to the narrow cross-section of the beam at the focus. It also results in the rate at which the temperature rise decreases due to the diffusion term. However, the highest temperature often occurs at regions closer to the transducer surface even though it may be lower in the beginning.

3.4 Cavitation

The theory in this section is cited from [14]. Cavitation is the formation and/or activity of gas-filled bubbles in a medium exposed to ultrasound [12]. It is said to be a complex phenomena that involves the creation, oscillation, growth and collapse of bubbles within a medium [35, 34] but the exact behavior is said to depend on frequency, pressure amplitude, bubble radius and environment [26]. Cavitation can be divided into two types, thus, stable or non-inertial cavitation (involves oscillation but not collapse of bubbles) and transient or inertial cavitation (involves growth and collapse of bubble). When a gas bubble in a liquid is exposed to an ultrasound field, the nature of its response changes as the pressure amplitude in its vicinity increases. That is, the nature and vigor of bubble response depends on the pressure amplitude if the ultrasound wave is continuous and is dependent on features of a waveform (display of acoustic pressure versus time) if the wave is pulsed. The waveform shows alternating positive and negative intervals of the acoustic pressure, where the medium is compressed during the positive interval and expanded during the negative interval. The maximal valve of the positive pressure is denoted as p_+ whereby the minimal valve of the negative pressure is p_-. During nonlinear propagation, p_+ and p_- are unequal whereby they are equal at low pressure amplitudes [52]. Cavitation therefore can occur in a fluid when the local pressure drops below the vapour pressure (p_v) of the fluid. The two main roles that cavitation plays in drug delivery are; Disrupting the structure of drug carriers and releasing the drug and finally making cell membranes and capillaries more permeable to drugs [49].

3.4.1 *Creation of bubbles within a medium (liquid)*

The creation or formation of bubbles in a liquid medium is known as nucleation and is the onset of a phase transition in a small region. This process can be controlled by stochastic events, which means that the observation time is a determining factor. That is, there is a greater probability that, over a long period of time, vacancies will combine to form a finite vapour pocket which will eventually lead into nucleation. However, it is also possible for a liquid to form vapour bubbles when placed in a state of tension (negative pressure). The process of nucleation is of two types, that is, homogeneous and heterogeneous nucleation. When nucleation occurs as a result of thermal motion within liquid which forms temporary microscopic voids that can constitute a nuclei, the process is called homogeneous nucleation but nucleation which is as a result of major weakness that occurs at the boundary between the liquid and the solid wall of the container or between the liquid and small particles suspended in the liquid it is called heterogeneous nucleation.

3.4.2 *Dynamics of bubble growth and collapse*

The response of bubbles exposed to pressure amplitudes of order 0.1 MPa is said to be highly nonlinear [52] but generally the response can be linear or nonlinear. When acoustic waves move through a liquid, it produces variations in the pressure of the liquid so that when the liquid's pressure drops below the vapour pressure during the low-pressure portion of the acoustic wave, small evacuated areas, or cavities are formed. These cavities becomes filled with gas and/or vapour which are then set into motion by the acoustic wave. These tiny bubbles can expand and contract in the liquid and can become larger that it can be seen by the unaided eyes. A lot of theories has been proposed on the dynamics of bubble growth and collapse which are basically based on laws of conservation of mass, momentum and energy, assumptions for equations of states for liquid and gaseous media and then transfer of heat between gas and liquid [52]. An example is the Rayleigh-Plesset equation. This equation is said to be the most popular nonlinear equation for the nonlinear response of a gas bubble in liquid to a driving pressure field. The equation is based on the following assumptions: The liquid is said to be incompressible (thus constant density ρ_L with infinite velocity of sound) with a spherical bubble of radius R(t) (where R is a function of time) as illustrated in Fig.3.2.

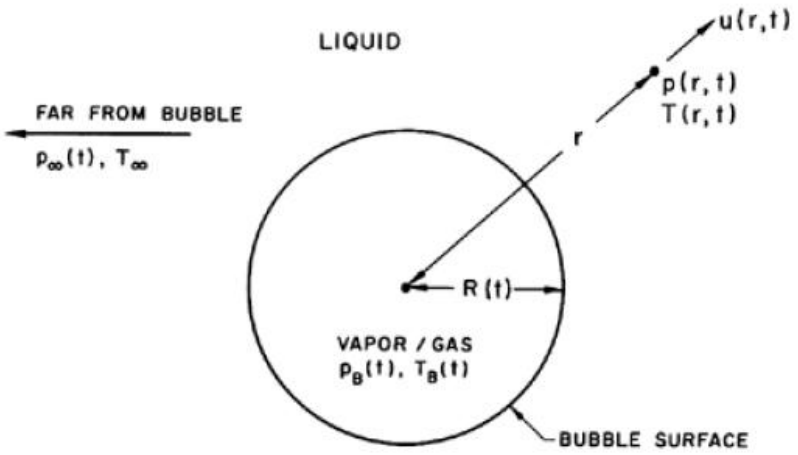

Figure 3.2: Schematic of a spherical bubble in an infinite liquid [14]

The temperature and pressure of the liquid far from the bubble are T_∞ and $P_{\infty(t)}$ respectively. The temperature T_∞ is constant (thus, temperature gradient and uniform heating of the liquid due to internal heat sources or radiation are not considered) and the pressure $P_\infty(t)$ is a known input function which regulates the growth or collapse of the bubble. In other words, it could be obtained from a determination of the pressure history that a nucleus would experience as it travels along a streamline. The dynamic viscosity

μ_L of the liquid is constant and uniform. The content of the bubble is homogeneous which means the temperature, $T_B(t)$, and pressure, $p_B(t)$ within the bubble are always uniform. The Rayleigh-Plesset equation of motion can therefore be written as [14];

$$\frac{p_v(T_\infty) - p_\infty(t)}{\rho_L} + \frac{p_{G0}}{\rho_L}\left(\frac{R_0}{R}\right)^{3k} = R\frac{d^2R}{dt^2} + \frac{3}{2}\left(\frac{dR}{dt}\right)^2 + \frac{4\nu_L}{R}\frac{dR}{dt} + \frac{2S}{\rho_L R} \tag{3.21}$$

Where ν is the kinematic viscosity, P_{G0} is the pressure of the gas (contaminant) inside the bubble at a reference bubble size R_0 and temperature T_∞, S is the surface tension, k is approximately constant and p_v is the saturated vapour pressure. For a bubble with a small perturbation in size from R = R_E to $R = R_E(1+\epsilon)$, where $\epsilon << 1$. The partial pressure of the gas remains the same at p_{GE} and the mass of gas in the bubble and the temperature (T_B) also remains the same. Rayleigh-Plesset equation then becomes;

$$R\ddot{R} + \frac{3}{2}(\dot{R})^2 + 4\nu_L\frac{\dot{R}}{R} = \frac{\epsilon}{\rho_L}\left[\frac{2S}{R_E} - 3nkp_{GE}\right] \tag{3.22}$$

This then implies that a bubble in stable equilibrium requires;

$$p_{GE} = \frac{m_G T_B K_G}{\frac{4}{3}\pi R - E^3} > \frac{2S}{3kR_E} \tag{3.23}$$

where m_G and K_G are the mass of the bubble and gas constant respectively. According to Blake [13],the critical radius for a given mass of gas can be calculated from;

$$R_C = \left[\frac{9km_G T_B K_G}{8\pi S}\right]^{\frac{1}{2}} \tag{3.24}$$

All bubbles with radius $R_E < R - C$ can exist in stable equilibrium, whereby those of radius $R_E > R_C$ must be unstable. By decreasing the the ambient pressure from p_∞ to the critical value, $p_{\infty c}$, this critical size can be reached. This critical pressure can also be calculated from the Blake threshold pressure which is given by;

$$p_{\infty c} = p_v - \frac{4S}{3}\left[\frac{8\pi S}{9km_G T_B K_B}\right]^{\frac{1}{2}} \tag{3.25}$$

3.4.3 *Dynamics of oscillating bubbles*

The radius of a bubble varies when exposed to an ultrasonic field due to the force exerted by the acoustic pressure on the bubble. The behaviour of the bubble can be liken to an oscillator with a stiffness and inertia. Where stiffness is as result of the gas in the bubble (the gas in the bubble provides a force that resists the compression) and the inertia is

provided by the liquid surrounding the bubble moves the bubble wall [26]. The response of a bubble to an acoustic pressure field can be classified into three namely linear, stable and transient as a result of the amplitude of the pressure field. Thus as the amplitude of the pressure field increases, the response moves from linear to stable and then to transient. There are other factors that also contribute to the response of bubbles to acoustic pressure filed. These factors are; the relationship between the frequency, ω, of the imposed oscillations and the natural frequency,ω, of the bubble, the second factor is the relationship between the pressure oscillation amplitude,$\tilde{p}$, and the mean pressure,$\bar{p}_\infty$. For example, there will not be any cavitation if $\tilde{p} < \bar{p}_\infty$.

3.4.3.1 *Linear response*

For small pressure amplitude pressure, the response of the bubble is linear. The linearized dynamic solution when the pressure at infinity consist of a mean value, $\bar{p_\infty}$ is given as;

$$p_\infty = \bar{p_\infty} + R_e\left\{\tilde{p}e^{j\omega t}\right\} \tag{3.26}$$

where $\tilde{p}$ is a small oscillatory pressure amplitude superimposed on $\bar{p_\infty}$ and ω is the radian frequency. The linear dynamic response of the bubble will then be;

$$R = R_E\left[1 + R_e\left\{\varphi e^{j\omega t}\right\}\right] \tag{3.27}$$

Where R_E is the equilibrium size at the pressure $\bar{p_\infty}$, and $R_E\left|\varphi\right|$ is the amplitude of the bubble radius oscillations.

The maximum or peak response amplitude occurs at a frequency, ω_p given by;

$$\omega_p = \left[\frac{3k(\bar{p_\infty} - p_v)}{\rho_L R_E^2} + \frac{2(3k-1)S}{\rho_L R_E^3} - \frac{8\nu_L^2}{R_E^4}\right]^{\frac{1}{2}} \tag{3.28}$$

This peak frequency is inversely proportional to the damping thus;

$$\left|\varphi\right| = \frac{\bar{p}}{4\mu_L}\left[\omega_p^2 + \frac{4\nu_L^2}{R_E^4}\right]^{\frac{-1}{2}} \tag{3.29}$$

whereby the natural frequency of oscillation of the bubbles at ω_p for zero damping is given by;

$$\omega_N = \left[\frac{1}{\rho_L R_E^2}\left\{3k(\bar{p_\infty} - p_v) + 2(Sk-1)\frac{S}{R_E}\right\}\right]^{\frac{1}{2}} \tag{3.30}$$

Fig. 3.3 shows a graph of the peak frequency as function of R_E for several values $\bar{p_\infty} - p_v$

In other to create cavitation in water using acoustic pressure, one has to use frequencies that lies in the frequency range of the natural frequency of the bubble. For example, typical nuclei commonly found in water has been estimated to be from 1 to 100μm [14] which corresponds to natural frequencies of order 5 to 25kHz.

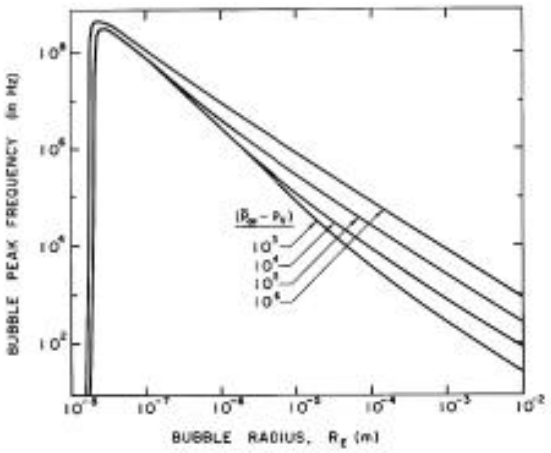

Figure 3.3: A graph of bubble peak or resonance frequency in water at $300°K$ as a function of bubble radius [14]

.

3.4.3.2 *Stable cavitation*

An increase in the amplitude of bubble oscillation can result in nonlinearity in the bubble response due to the nonlinearity in the governing equations (Rayleigh-Plesset equation). If the bubble continues to oscillate stably inspite of the effect of the nonlinearity, then the phenomena is termed "stable acoustic cavitation". In order words, stable cavitation occurs when the bubbles continues to oscillate over a relatively long period of time without collapsing. Stable or non-inertia cavitation creates a circulating fluid flow (called microstreaming) around the bubble with velocities and shear rates proportional to the amplitude of the oscillation [37, 19, 43]. At higher amplitudes, the shear force is capable of shearing open red blood cells and vesicles such as liposomes [49]. When a nucleus is excited at its resonance frequency, ω_p, it will exhibit a response whose amplitude is a function of the damping as given in Eq. 3.29. This can lead to very large amplitudes which might in turn cause the nucleus to exceed its critical size,R_C. highly nonlinear behavior with very large amplitude would result. To attain $R_{E|\varphi|} = R_C - R_E$ the amplitude of the pressure must be;

$$\bar{p}_C \approx 4\mu_L \left[\omega_N^2 - \frac{4\nu_L^2}{R_E^4}\right]^{\frac{1}{2}} \left[\left\{1 + \frac{\rho_L \omega_N^2 R_E^3}{2S}\right\} - 1\right] \tag{3.31}$$

Different nonlinear phenomena like subharmonics, rectified diffusion etc, can affect stable acoustic cavitation. For example, the bubble equilibrium radius grows with time during

rectified diffusion. Thus the surface area of the bubble is larger on the expansion phase than on the compression phase and this results in more gas diffusing into the bubble when the pressure inside is low than the amount of gas that diffuses out when the pressure is high.

3.4.3.3 *Inertial cavitation*

At higher oscillation amplitudes as a result of increase in acoustic intensity, the inward moving wall of the fluid gains sufficient inertia that it cannot reverse direction when the acoustic pressure reverse direction, the gas in the bubble is then compressed to a very small volume which creates extremely high pressures and temperatures [49]. The bubble will eventually collapse to a minute fraction of its original size, at which point the gas within dissipates into the surrounding liquid via a rather violent mechanism, which releases a significant amount of energy in the form of an acoustic shock-wave and as visible light (a process known as sonolumonesecene). At the point of total collapse, the temperature of the vapour within the bubble may be several thousand of kelvin, and the pressure several hundred of atmospheres. Inertial cavitation can cause serious damage to cells or vesicles because of the very high shear stresses in the region of collapse, the shock waves by the collapse and the free radicals produced by the high temperatures. Consider now a bubble of size, R_E with mass of gas m_G subjected to mean pressure, $\bar{p}_\infty$, with superimposed oscillation frequency ω and amplitude $\tilde{p}$.

Now, if $\omega << \omega_N$, then the inertia of the liquid is insignificant and it so will not involve the dynamics of bubble growth. The bubble will then respond quasistatically. For transient cavitation to occur under this condition, a critical amplitude ($\tilde{p}_c$) must be reached.

Where;

$$\tilde{p}_c = \bar{p}_\infty - p_v + \frac{4S}{3}\left[\frac{8\pi S}{9m_G T_B K_G}\right]^{\frac{1}{2}} \tag{3.32}$$

This condition will therefore be reached when the minimum instantaneous pressure,$(\bar{p}_\infty - \tilde{p}_c)$, just reaches the critical Blake threshold pressure. If on the other hand, $\omega >> \omega_N$, then the inertia of the liquid will involve bubble dynamics. Under this condition, as stated by Apfel [6], transient cavitation can only occur if the ambient pressure (p_∞) falls below the vapour pressure for part of the oscillation cycle. The negative pressure will be equal to $(\bar{p}_\infty - \tilde{p}_c)$. If the pressure then exceeds the quasistatic Blake threshold then the bubble growth rate can be approximated to asymptotic growth rate given in Eq. 3.23 so that combination of this equation and the grow time gives the maximum bubble radius given by,

$$R_M = f(\beta)\frac{\pi}{\omega}\left[\frac{\tilde{p}_c - \bar{p}_\infty}{\rho_L}\right]^{\frac{1}{2}} \tag{3.33}$$

where $\beta = (1 - \frac{\bar{p}_\infty}{\tilde{p}_c})$ and the function function $f(\beta)$ account for some details like fraction of half-period $(\frac{\pi}{\omega})$ and is given as;

$$f(\beta) = \left(\frac{4}{3\pi}\right)(2\beta)^{\frac{1}{2}}\left\{1 + \frac{2}{3(1-\beta)}\right\}^{\frac{1}{3}} \tag{3.34}$$

Transient cavitation will therefore occur when $R_M \rightarrow 2R_E$, when the bubble reaches a size approximately twice the original size or more in a relatively few cycle. With this criterion the critical pressure will then be given as;

$$\tilde{p}_C = \bar{p}_\infty + \frac{4\rho_L R_E^2 \omega^2}{\pi^2 f^2} \tag{3.35}$$

It can therefore be deduced from this express that for a particular spherical bubble, the occurrence of inertial cavitation depends on the acoustic pressure amplitude, the acoustic frequency and bubble radius. From the work done by Apfel and Holland [7], it has been shown that for any frequency there is a minimum peak rarefractional pressure p_{opt} that is required to generate inertial cavitation , and this only occurs for bubbles with an initial radius R_{opt} as shown in Fig. 3.4. Apfel and Holland investigated the relationship between p_{opt} and frequency, f, for water and blood using bulk properties for the two fluids to be [7] ;

$$\frac{p_{opt}^a}{f} = b \tag{3.36}$$

where p_{opt} is in MPa, f is in MHz, $a = 2.10$ for water 1.67 for blood and $b = 0.06$ for water and 0.13 for blood. If a is approximately taken to be 2 then a mechanical index MI can be defined as [7];

$$MI = \frac{p_r}{\sqrt{f}} \tag{3.37}$$

where p_r is the rarefactional pressure in MPa and f is in MHz. MI is considered to be an indicator of the likelihood of inertial cavitation and it is therefore assumed that if MI of 0.7 is not reached then the probability of inertial cavitation is negligible. In diagnostic ultrasound the allowed MI is 1.9 [26]. Another study by Sponer [58] shows that there is a linear dependence of the threshold pressure on the acoustic frequency for cavitaion to take place. This dependence may be expressed as;

$$p_r = 0.06 + 0.05f \tag{3.38}$$

Where f and p_r are in MHz and MPa respectively.

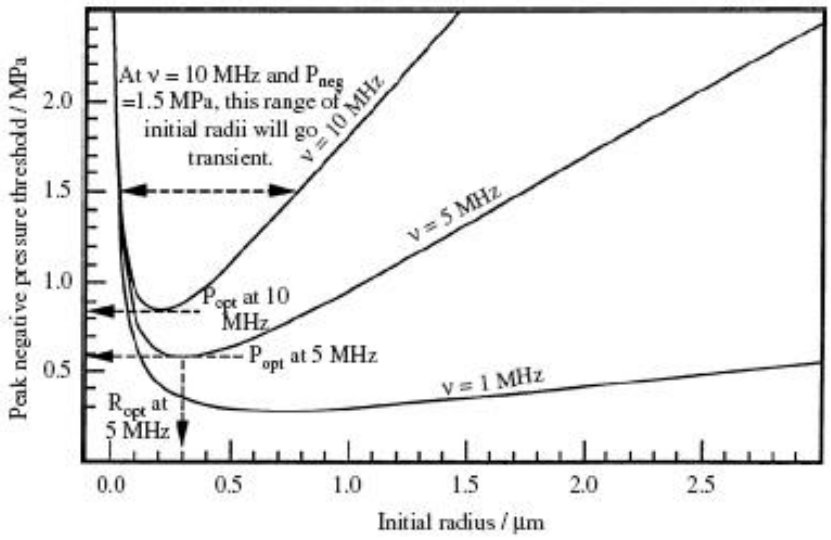

Figure 3.4: A graph of minimum peak negative (rarefractional) pressure require to produce inertial cavitation within one period verses initial bubble radius and frequency [7].

3.5 Ultrasound Transducer

An ultrasound transducer is a device which converts electrical energy to acoustical energy or acoustical energy to electrical. This conversion is done by a piezoelectric material and the phenomenon of conversion of mechanical acoustical energy or vice versa is called piezoelectricity. When a suitable voltage is applied to the transducer and the frequency of the input voltage reaches the resonance frequency for thickness vibrations of the piezoelectric material, the piezoelectric material will vibrates and these vibration is transmitted as ultrasonic pressure waves [42]. The main components of a transducer are active element and backing. The active element can be a piezo or ferroelectric material (such as polarized ceramics) which converts electrical energy into ultrasonic energy. Backing is normally done with a highly attenuative material with high density used to control the vibration of the transducer by absorbing the energy radiating from the back face of the active element. If the acoustic impedance of the active element does not match (mismatch) with that of the backing, more sound energy is reflected back into the test material and this will result in transducer with lower resolution but higher in signal amplitude or greater sensitivity. However, if the acoustic impedance of these two materials (backing and the active element) matches the result will be a heavily damped transducer with good range resolution but lower in signal amplitude[45] .

The rest of the theory in this part has been taken from chapter 2 and 3 of [5]. If a transmitting transducer is driven with a voltage generator $v_s(t)$ which has an internal

impedance of $Z_s(w)$. The transducer's input impedance is Z_L. The driven voltage on the electrical port of the transducer is given as;

$$V_L(w) = H_{ti}(w)V_g(w) \tag{3.39}$$

Where;

$$H_{ti}(w) = \frac{Z_L}{Z_L + Z_s(w)}, \tag{3.40}$$

is the transmitter impedance transfer function and Eq. 3.39 is in the frequency domain. The output is transducer's velocity u(t) which is also given in the frequency domain as;

$$U_t = H_{tt}(w)V_L \tag{3.41}$$

Where $H_{tt}(w)$ is the transmit transducer function. The transmitted wave will then have a pressure amplitude of ;

$$P(w) = U(w)Z \tag{3.42}$$

Where Z is the characteristic impedance. The electrical power of a Voltage driven and current driven transducer is therefore given as;

$$\begin{aligned} P_V &= |V|^2 \frac{Re\{Y_i\}}{2} = |V|^2 \frac{|Y_i|\cos\theta_i}{2} = |V|^2 \frac{\cos\theta_i}{2|Z_i|} \\ P_I &= |I|^2 \frac{Re\{Z_i\}}{2} = |I|^2 \frac{|Z_i|\cos\theta_i}{2}, \end{aligned} \tag{3.43}$$

respectively. $Y_i = \frac{1}{Z_i}$ is the admittance of the electrical port and $Z_i = |Z_i| e^{i\theta_i}$ is the electrical input impedance. Also acoustic power can be given as;

$$P_{ac} = \frac{p^2}{2Z_0} = \frac{|H|^2}{2Z_0}|V|^2 \tag{3.44}$$

Where Z_0 is the acoustic impedance of the material, p is the maximum pressure given as $p = HV$, H is the transfer function and V is the voltage used to drive the transducer. From Eq. 3.43, the voltage can be derived as;

$$|V| = \frac{2|Z_i|}{P_V}\cos\theta_i \tag{3.45}$$

Substituting Eq. 3.45 into Eq. 3.44 yields;

$$\begin{aligned} P_{ac} &= \frac{|Z_i||H|^2 P_V}{\cos\theta_i Z_0} \\ P_{ac} &= \frac{Re\{Z_i\}|H|^2 P_V}{Z_0} \end{aligned} \tag{3.46}$$

Hence the acoustic energy is given as;

$$E_{ac} = P_{ac}t, \tag{3.47}$$

where t is the time taken or exposure time.

3.5.1 *Radiation field from single element ultrasound transducer*

The theory at this section has been taken from chapter 1 and 5 of [5]. Analysis of the radiated beam can be done by using Huygens' principle by considering each point on the surface as a source of a spherical wave. The partial waves will then interfere and generate to form a beam profile as can be seen in Fig. 3.5. The beam profile depends on the length of the transmitted pulse.

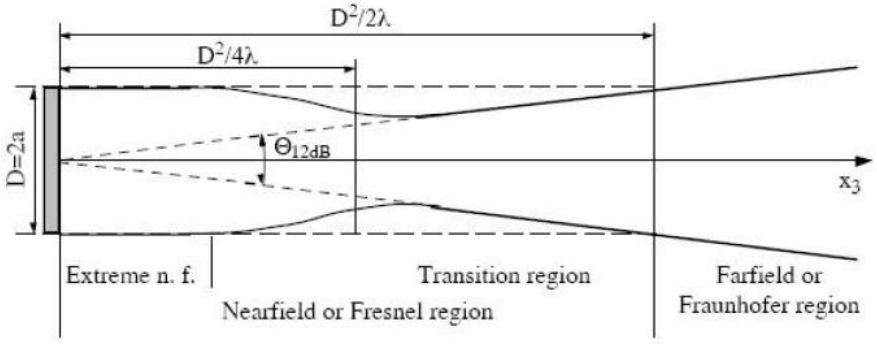

Figure 3.5: Schematic illustration of the beam profile of a plane circular transducer. D is the diameter of the transducer, a is the radius and λ is the wavelength of the radiation [5]

A continuous vibration of the surface has a continuous wave beam pattern whereby a pulsed vibration has pulsed wave. As can be seen in the diagram, a plane transducer has distinct regions of the beam namely;

1. The farfield or Fraunhofer region. This is where $r > \frac{D^2}{2\lambda}$. Where $D = 2a$ is the diameter of the transducer and r is the distance from the center of the transducer. In this region the beam expands with a fixed opening angle as a result of diffraction and so the beam is composed of central main lobe with side lobes as skirts around. The width of the main lobe can be defined as where the amplitude has fallen XdB off from the axial value. The dual sided opening angle of the main lobe for a plane transducer can then be defined as; $\Theta_{XdB} = k_X \frac{\lambda}{D}$. Also for a plane transducer, the distance along the axis to the start of the farfield region is given as; $x_3 = 2a^2/\lambda = D^2/2\lambda$

2. The nearfield or Fresnel region. This is where $r < D^2/2\lambda = Da/\lambda$. Thus the region between the transducer and the farfield. This region is divided into two namely; extreme near field and the transition region. The extreme near field is the region where $r < \frac{0.25D^2}{2\lambda}$ whereas the transition region is the region between extreme near and the farfield. At the transition region, the highest intensity of the beam for a focused transducer is nearer to the transducer than the geometric

focus. This is due to diffraction focusing, thus a phenomenon whereby there is a slight contraction of the central portion of the beam before it starts to diverge in the farfield.

For a focused transducer as shown in Fig. 3.6, the beam is focused by forming the transducer as spherical shell with radius of curvature F also known as the focal distance or length. The F-number of a focused transducer can be defined as; $FN = F/D$ whereas the focal diameter of the beam for a circular aperture is;

$$D_F(XdB) = \Theta_{XdB} = k_X F\lambda/D = k_X \lambda FN \tag{3.48}$$

For efficient focusing, it is required that;

$$F < D^2/2\lambda = Da/\lambda \Leftrightarrow FN < D/2\lambda = a/\lambda \tag{3.49}$$

where $\Theta_F = \Theta_1 2dB$. This implies that the focus must be in the nearfield of a plane transducer with the same diameter. The Fresnel parameter is defined as;

$$S = \frac{F\lambda}{a^2} \tag{3.50}$$

The maximum intensity occurs closer to the transducer than for higher values of S. The region where the beam diameter is limited as a result of diffraction is known as depth of focus. The point at which the on-axis transmitted amplitude has dropped by XdB from the maximum possible value is called focal depth. Therefore the focal depth for 1dB is given as;

$$L_F \approx 2D_F(12DB)FN \tag{3.51}$$

where FN is the F-number.

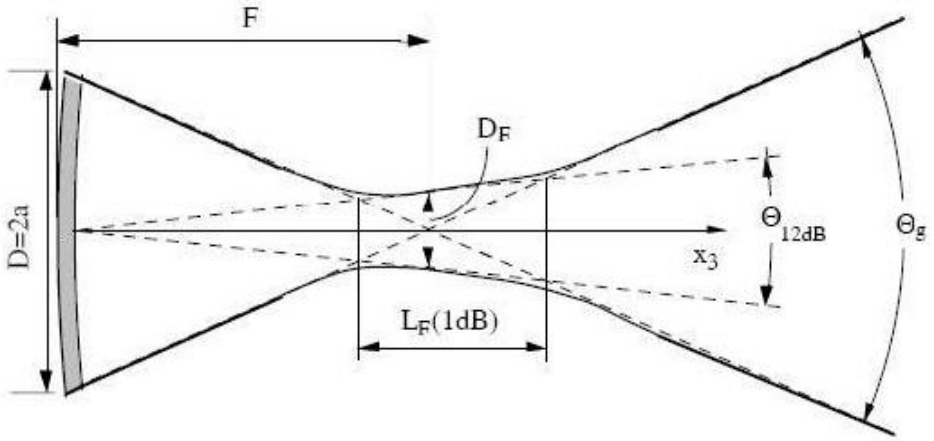

Figure 3.6: Schematic illustration of the beam profile of a focused circular transducer. D is the diameter of the transducer, a is the radius, λ is the wavelength of the radiation, F is the radius of curvature, L_F is the depth of focus and D_F is the focal diameter [5]

The spatial frequency response for the particle velocity and pressure can be expressed as;

$$\begin{aligned} U(r,w) &= H_u(r,w)F(r,w) \\ P(r,w) &= H_p(r,w)F(r,w) \end{aligned} \tag{3.52}$$

Where $H_u(r,w) = -\rho^{-1}\nabla H(r,w)$ and $H_p(r,w) = iwH(r,w)$. The spatial frequency response, H(r,w), at the surface of the transducer (st)can also be written as;

$$H(r,w) = \int_{st} d^2 r_0 \frac{e^{-ik|r-r_0|}}{2\pi\,|r-r_0|} Mn(r_0) \tag{3.53}$$

Where r_0 is the point from the source or surface of the transducer, r is the point in space, $Mn = \rho(r)U_n(r_0)$, $Un(r_0)$ is the particle velocity, and ρ is the density. Solving this integral the spatial frequency response then becomes;

$$H(r,w) = \frac{2\rho}{k} e^{ik\left\{(a^2+x_3^2)+x_3\right\}/2} \sin \frac{k\left\{(a^2+x_3^2)^{\frac{1}{2}} - x_3\right\}}{2} \tag{3.54}$$

Where $(x_3^2+a^2)^{\frac{1}{2}} - x_3$ is the difference in the propagation distance for a wave starting at the edge of the transducer and a wave starting in the center. This implies the pressure and the velocity will then yield;

$$\begin{aligned} H_p(x_3) &= \rho c \left\{ e^{-ikx_3} - e^{-ik(x_3^2+a^2)^{\frac{1}{2}}} \right\} \\ &= i2\rho c e^{ik\left\{(a^2+x_3^2)+x_3\right\}/2} \sin \frac{k\left\{(a^2+x_3^2)^{\frac{1}{2}} - x_3\right\}}{2} \end{aligned} \tag{3.55}$$

and

$$H_u(x_3) = e^{-ikx_3} - \frac{x_3}{(a_2 + x_3)^{\frac{1}{2}}} e^{-ik(a^2+x_3^2)^{\frac{1}{2}}} \tag{3.56}$$

The complex radiation intensity on the axis is given as;

$$I_{mc}(x_3) = H_p(x_3)H_u^*/2 \tag{3.57}$$

and the time average intensity in the center of the transducer, x_3, where $\frac{a}{\lambda} = 20$ then becomes;

$$I_m(0) = Z_0 \sin^2 \frac{ka}{2} \tag{3.58}$$

Where $Z_0 = \rho c$ is the characteristic impedance. The pressure amplitude varies with position as a result of interference so the time average intensity varies from $0 - Z_0$. The time average intensity then becomes;

$$I_m \approx Z_0/2 \tag{3.59}$$

This shows that the intensity has zeros when;

$$k\left[(x_3^2)^{\frac{1}{2}} - x_3\right] = 2n\pi \tag{3.60}$$

and maxima when;

$$k\left[(x_3^2)^{\frac{1}{2}} - x_3\right] = (2n+1)\pi \tag{3.61}$$

Where $n = 0, 1, 2, 3, ...$ It can therefore be seen that we get zeros when the wave at the center and those from the edge are in phase while the maxima occurs when the two waves are are 180° out of phase.

Now substituting $k = 2\pi/\lambda$ in the above equation, for the zeros, the equation becomes;

$$(x_3^2)^{\frac{1}{2}} - x_3 = n\lambda \tag{3.62}$$

and for maxima;

$$(x_3^2)^{\frac{1}{2}} - x_3 = \frac{(2n+1)\lambda}{2} \tag{3.63}$$

Solving these equation yields;

$$x_{3n} = \frac{a^2}{2n\lambda} - \frac{n\lambda}{2} x_{3n} = \frac{a^2}{(2n+1)\lambda} - \frac{(2n+1)\lambda}{4} \tag{3.64}$$

for the zeros and maxima values respectively. The pressure at the focus is given as;

$$P_F = \frac{\omega \pi a^2}{c 2\pi F} = \frac{\pi a^2}{\lambda F} P_t = \frac{\pi}{S} P_t \tag{3.65}$$

Where S is the Fresnel parameter for a focused transducer.

Chapter 4

SPECTROSCOPY

Spectroscopy is the use of the absorption, emission, or scattering of electromagnetic radiation (light) by matter to qualitatively or quantitatively study the matter or to study physical processes. In other words spectroscopy can be defined as a branch of light interactions which deals with the study of independence of light absorption or emission on the wavelength of light. The matter can be atoms, molecules, atomic or molecular ions, or solids. The interaction of radiation with matter can cause redirection of the radiation and/or transitions between the energy levels of the atoms or molecules. Spectrometry refers to when a spectroscopic technique is used to assess the concentration or amount of a given species. The instrument that performs such measurements is a spectrometer or spectrograph. A spectrum is a plot of the strength of transition as a function of wavelength or frequency.

This chapter gives a brief description of the various processes involved when light interacts with matter and the various types of spectroscopy base on these interaction. Thus the first section deals with absorption and emission and the second section explains how these processes can be used to obtain information from the substance. The information in this Chapter was taken from Chapter 4 of [50].

4.1 Absorption and Emission

The information at this section was taken from Chapter 4 of [50]. Absorption is a process whereby an atom or molecule moves from a lower level (generally the ground state) to a higher level with transfer of energy from the radiation field to the atom, molecule, or solid. The energy gap between these two energy levels (higher energy level and the lower energy level) is equivalent to the photon energy given by $\Delta E = E_f - E_i$. If the initial energy level is an excited state then the process is called excited state absorption. However, a transition from a higher level to a lower level with transfer of

energy from the emitter to the radiation field is called emission. If no radiation is emitted, the transition from higher to lower energy levels is called non radiative decay. In this process, the excited-state energy is dissipated as heat or in producing a chemical reaction (photochemistry). Emission can be in two forms, namely: spontaneous and stimulated emission. Spontaneous emission is a process whereby a molecule returns from an excited state to its lower energy state by emission of a photon whose energy correspond to the energy gap between these two energy states. In stimulated emission, an incident photon of energy equivalent to the energy between two energy levels (final and initial energy level) is used to trigger an emission. This implies that only spontaneous emission will take place in the absence of any incident photon.

The de-excitation (return of a photon from a higher energy level to a lower energy level) process can occur either by non-radiative process namely: internal conversion and intersystem crossing (without emission of light) or by two processes namely: fluorescence and phosphorescence with emission of light [16]. These phenomena has been explained in Fig. 4.1. The S state are the singlet state (in the order of increasing energy from the ground-state, S_0, S_1, S_2) of the molecule whereby the T states are the excited triplet states. The horizontal closely spaced lines represent the vibrational levels. Suppose a molecule is excited to a higher electronic singlet state S_2, the de-excitation process will start from a non-radiative crossing from the S_2 state to S_1. This type of crossing between two electronic states of the same spin multiplicity is called internal conversion(IC).The next step is a rapid vibrational relaxation where excess vibrational energy is dissipated into heat which takes the molecule to the lowest zero-point vibration level of the S_1 electronic state. It then moves from this state(s_1) to the ground electronic state S_0 by an emission process called fluorescence. S_1 and S_0 are of the same spin multiplicity and the process is spin-allowed (thus observes the rule of no change of spin value). The excitation may cross from S_1 to T_1 (instead of S_1 to S_0) by a non-radiative process called intersystem crossing (ISC). This transition is between two states of different spin and so it violates the rule of no change of electronic state and is thus called a spin-forbidden transition. The process is then followed by a rapid vibrational relaxation to the zero-point vibrational level of the T_1 state. The final step to the ground state (S_0) is a radiative process called phosphorescence. This process is spin-forbidden and the emission is weak so it has a longer lifetime.

Absorption and emission cross-section of a photon depends on the spatial overlap of the final and initial wave function. For absorption, the transition from the ground state S_0 with the lowest vibrational state to an excited state vibrational state within the electronic excited state has the largest probability whereas the reverse is true for emission. Thus the transition with the largest probability for emission is from the lowest vibrational level in the the electronic excited state to a higher vibrational level in the ground level. The reason being that vibrational relaxation and internal conversion occurs faster than fluorescence and so fluorescence emission spectra are shifted to lower energies (longer wavelengths) than the absorption spectra. Also phosphorescence spectra are of lower energies than the fluorescence spectra as illustrated in Fig. 4.2. This is what is known

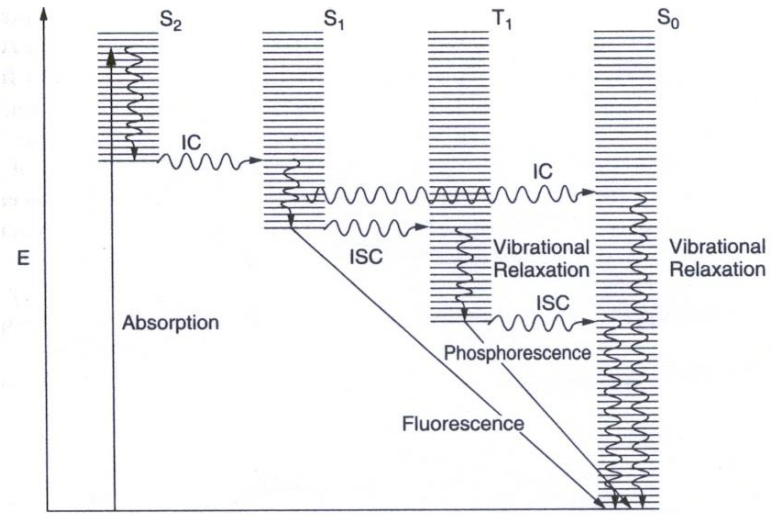

Figure 4.1: Jablonski diagram showing possible fates of excitation [50]

as Stokes shift [16].

4.2 Types of Spectroscopy

The information in this Section was taken from Chapter 4 of [50]. There are various types of spectroscopy but the type depends on the physical quantity measured, where it is normally intensity of energy absorbed or produced. However, spectroscopic methods are differentiated based on whether or not they apply to atoms (atomic) or molecules (molecular). Along with that distinction, they can be classified on the nature of their interaction:

4.2.1 *Electronic absorption spectroscopy*

This method is often used for a quantitative analysis of a sample. It uses the range of the electromagnetic spectra in which a substance absorbs to study radiation spectra absorbed by atoms or molecules that change energy levels. The underlining principle is a linear absorption of light from a conventional lamp (Xenon lamp) which provides a continuous distribution of the electromagnetic radiation from UV to near IR. UV-visible spectrometer is used for this method and it measures linear electronic absorption which can be described using the Beer-Lambert's law. According to this law, an incident beam of intensity I_0 at a frequency ν can be described by;

$$I(\nu) = I_0 e^{-k(\nu)bc} = I_0(\nu)10^{-\epsilon(\nu)bc} \tag{4.1}$$

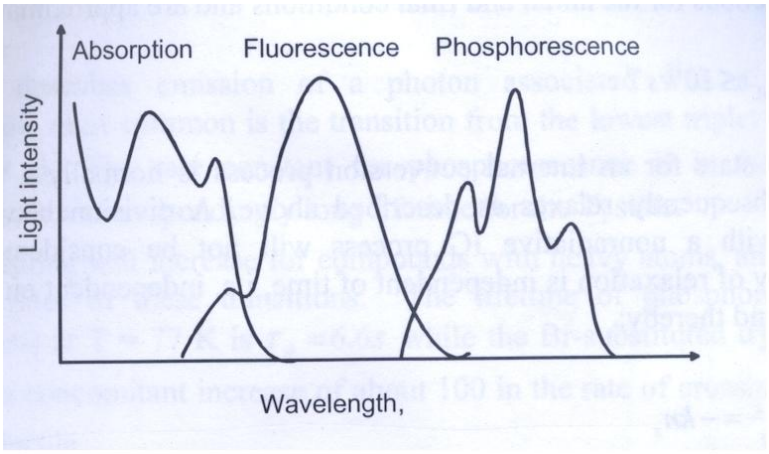

Figure 4.2: Strokes shift of fluorescence and phosphorescence spectra relative to absorption spectra. [16]

Where I is the output intensity,ϵ and k are the molar extinction coefficients, c is the molar concentration and b is the optical path depth. Absorption spectroscopy includes atomic absorption spectroscopy and various molecular techniques, such as infrared spectroscopy in that region and nuclear magnetic resonance (NMR) spectroscopy in the radio region. Examples of absorption spectroscopy are: absorption of infrared radiation spectroscopy, Atomic absorption spectroscopy, UV/visible spectroscopy, Mossbauer spectroscopy etc.

4.2.2 *Electronic Emission spectroscopy*

Emission spectroscopy deals with emission associated with a transition from an excited electronic state to a lower state. It make use of a substance that can absorb energy and radiate (emit) in a range of electromagnetic spectrum. The absorbed energy can be from a variety of sources and that determines the name of the subsequent emission, like luminescence. Generally, this method deals with visible light and shorter wavelengths, due to the fact that fluorescence is less likely to happen with long wavelengths. At room temperature, biological molecules exhibit fluorescence but under certain conditions, they can emit phosphorescence. The fluorescence band produced by one photon absorption is red-shifted so the shift between the absorption peak and the emission band (fluorescence) is the Stokes shift. The amount of stokes shift is a measure of the relaxation process occurring in the excited state populated by absorption and the difference in energy of the absorbed photon and the emitted photon correspond to the energy loss due to non-radiative process. Stokes shift may be as result of environmental effector as a change in the geometry of the emitting excited state. Examples of emission spectroscopy are: Fluorescence spectroscopy, Flame emission spectroscopy, X-ray fluorescence spectroscopy, Stellar spectroscopy etc.

4.2.2.1 *Fluorescence spectroscopy*

Fluorescence spectroscopy is also known as fluorometry or spectrofluorimetry. It is a type of electromagnetic spectroscopy which analyzes fluorescence from a sample. The spectrum is obtained by exciting the molecules in a medium using a conventional lamp (Xenon lamp or mercury xenon lamp) and the excitation is done by using a broad-band filter to select a wavelength range that corresponds to the absorption band so that only light at frequencies higher than that of emission are allowed. Thus, the specimen is first excited, by absorbing a photon of light, from its ground electronic state to one of the various vibrational states in the excited electronic state so that as the molecules may drop down into any of several vibrational levels in the ground state, the emitted photons will have different energies, and thus frequencies. Therefore, by analyzing the different frequencies of light emitted in fluorescent spectroscopy, along with their relative intensities, the structure of the different vibrational levels can be determine. The fluorescence spectrum consisting of fluorescence intensity as a function of frequency or wavelength is obtained in a fluorescence spectrometer. An excitation spectrum is measured by recording a number of emission spectra using different wavelengths of excitation light. Fluorescence excitation spectra can also give information on the absorption of the state that produces maximum fluorescence. Generally, a fluorometer has three basic items namely; a source of light, a sample holder and a detector. It also has excitation filter for selecting the wavelength of the incident radiation and an emission monochromator for analyzing the emission of the sample [48](see Fig.4.3).

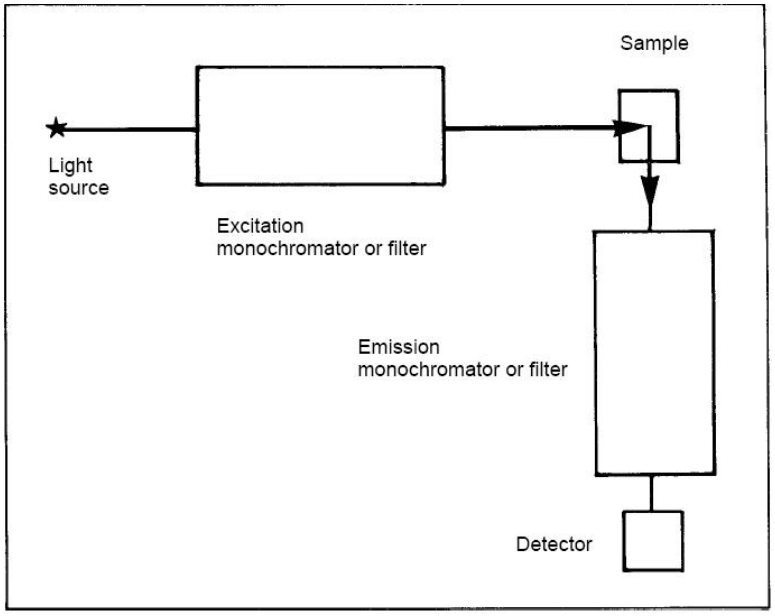

Figure 4.3: Essential component of a fluorescence spectrometer [48]

Part II

MATERIALS AND METHOD

Chapter 5

CONTROL RELEASE EXPERIMENT

This chapter consists of two main parts. That is, part one describes the materials and equipment for the experiment- design of the experimental setup used for the insonification, characterization of the transducers and then chemicals used in the experiment. The second part deals with the method used for preparation and treatment of the sample.

5.1 Materials and Equipment

This section describes all the materials and chemicals used in this research work. More detailed description of some of the equipment (transducer) and apparatus can be found at Appendix.A.

5.1.1 *Design of experimental setup for the ultrasonic insonation*

The experimental setup was designed in cooperation with Ing. Tonni Johansen. The ultrasound probes used in this experiment were chosen to cover a broad spectra of frequencies in order to find the optimal frequency. The tip of a condom was used as a sample holder and was assumed to be cylindrical with $10mm$ diameter and height. In order to insonify the whole sample volume ($1ml$), the beam diameter (D_F) and the focal depth (L_f) (defined by Eq.3.48 and Eq.3.51 respectively) for all transducers were chosen to be not less than $10mm$. This led to four transducers with different active diameters and focal length: $200kHz$ with an active diameter of $38mm$ and a focal length of $76mm$, $500kHz$ with an active diameter of $25mm$ and a focal length of $50mm$, $1MHz$ with an active diameter of $25mm$ and focal length of $85mm$ and finally $2MHz$ with active diameter of $19mm$ and a focal length of $125mm$. Detailed specification of these transducers can be found in Table A.1 at Appendix.A. Based on the specifications, a plexiglass chamber with dimensions of $300mm$ x $200mm$ (rectangular) was made for the exposure of the sample to the ultrasound beam (ultrasonication bath)(see Fig.5.1a).

This dimension makes it more flexible to be used for all transducers irrespective of the focal length. The short end of the chamber or the ultrasonication bath has a hole with the same diameter as that of the total diameter of the transducer. Different transducers can be mounted by replacing the short end ($200mm$) of the chamber with plexiglass plates (of the same size) that have holes of different diameters ($25mm$, $32mm$ and $45mm$,) corresponding to the total diameter of the transducer.

The sample chamber is made up of a very thin condom ($0.05mm$ in thickness) wrapped around a $5cm$ plexiglass glass tube (for support) with the tip of the condom (approximately $1cm^3$) serving as the actual sample holder. In order words the sample ($1ml$ of liposome in HEPES buffered sucrose solution or PBS) was placed at the tip of the condom for the ultrasound exposure. With the help of a syringe air could be blown into the condom from the top of the plexiglass tube in order for the condom to be firm when immersed in the water bath. Finally, to hold the sample chamber fixed at one position in the water bath during ultrasound exposure, an outer cylinder was made which can be placed on a plexiglass bridge made across the water chamber so that only the tip of the condom is exposed to the ultrasound beam. This can be seen in Fig.5.1a. During exposure, the water chamber was filled to cover the whole surface area of the transducer.

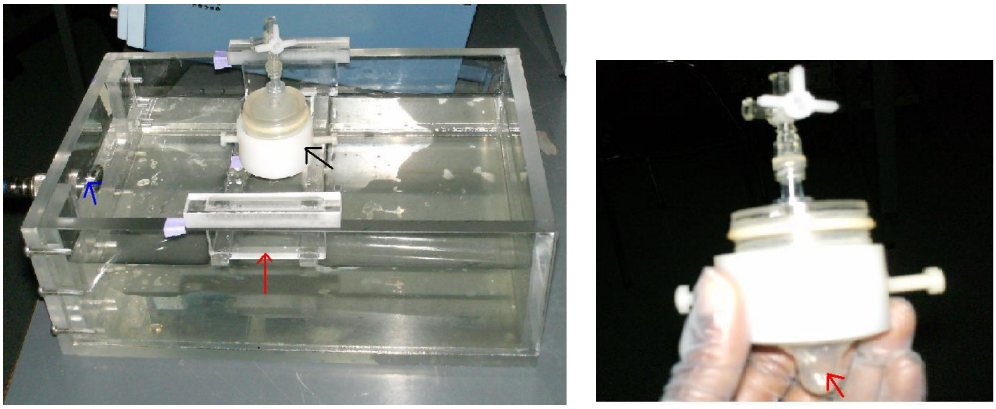

(a) (b)

Figure 5.1: (a) Water chamber ($300mm$ x $200mm$ rectangular box) used for the insonification with the sample chamber (black arrow) on the bridge (red arrow) and the transducer (blue arrow). (b) Sample chamber with the condom (red arrow).

5.1.2 *Characterization of transducers*

In order to know the specifications (especially the acoustic pressure and power) of the transducers used in this project the transducers were tested using the method described below. All transducers used in this project (total of four) were supplied by Ultran group U.S.A. Detailed description of these transducers (that is diameter, focal length, focal depth etc.) can be found in Table A.1 at Appendix.A. A signal generator (Waveform

generator WW2571, Tabor Electronics) controlled by a computer programmer called ArbConnection (Tabor Electronics v4.0) was used to generate a sinus signal of amplitude $333.3mV_{pp}$ with 10 periods and a pulse repetition frequency of $100Hz$. This was connected to a $400MHz$ oscilloscope (LeCroy waveSurfer $42X_2$) for monitoring of signal. The output of the signal generator was connected to a $50dB$ RF power amplifier (2100L ENI, Rochester, NY $10kHz - 12MHz$, 50Ω). The output signal from the amplifier was then used to drive the transducer with nominal frequency of $200kHz$, $38mm$ active diameter and a focal length of $76mm$. The transducer was immersed in a water tank as shown in Fig. 5.2.

A needle hydrophone $0.2mm$ (Precision Acoustics, number SN 887, and ID 1222) controlled by a robot connected to the computer (matlab program) was placed directly opposite the transducer in the water tank (see Fig.5.2b) to pick up the acoustic signal. This signal was amplified with a $25dB$ booster amplifier and then read on the oscilloscope connected to it. **Note:** SN 887 was used for the measurement of the $200kHz$ and the $500kHz$ transducers whereby the ID 1222 was used for the $1MHz$ and the $2MHz$ transducers. The matlab program was used to calculate the maximum pressure, the pressure at the focus and the corresponding acoustic powers. This was repeated with different input voltages ($333.3mV_{pp}$ and $666.7mV_{pp}$) on the signal generator and the values of the pressure at these voltages were also recoded. The whole process was then repeated for the other transducers ($500kHz$, $1MHz$, $2MHz$). The impedance of these transducers were measured afterwards with an Hp 4194A Impedance/Gain-Phase analyzer. Although the same procedure was used for all transducers, different number of periods and pulse repetition frequencies (PRF) were used for each transducer. Thus for $1MHz$ and $2MHz$, 10 periods with $500Hz$ PRF was used for all input voltages, whereas for $500kHz$, 3 periods with $100Hz$ was used for $333.3mV_{pp}$ and then 5 periods with $50Hz$ PRF was used for $666mV_{pp}$. **Note:** No measurement was taken at $200mV_{pp}$ for the $500kHz$ and the $200kHz$ transducers. The manufactures of these transducers gave a voltage limitation of $50Vrms$ for continuous wave which implies that for a pulse wave the limit will be given by;

$$V_{pw} = V_{cw}/\sqrt{D} \tag{5.1}$$

Where V_{pw}, V_{cw} and D are voltages of pulse wave, continuous wave and duty cycle respectively.

5.1.3 *Equipment for ultrasonic insonation*

The experimental setup used for the exposure of sample to the ultrasound beam is as shown in Fig.5.3. A waveform generator (Hewlett Packard, $15MHz$, 33120A) was used to generate a sine wave of $200mV_{pp}$ with 10 periods and a pulse repetition frequency (PRF) of $500Hz$. This was connected to an oscilloscope ($60MHz$ Tektronix TDS 2002) in order to monitor the signal that is being sent to the amplifier. The signal was then

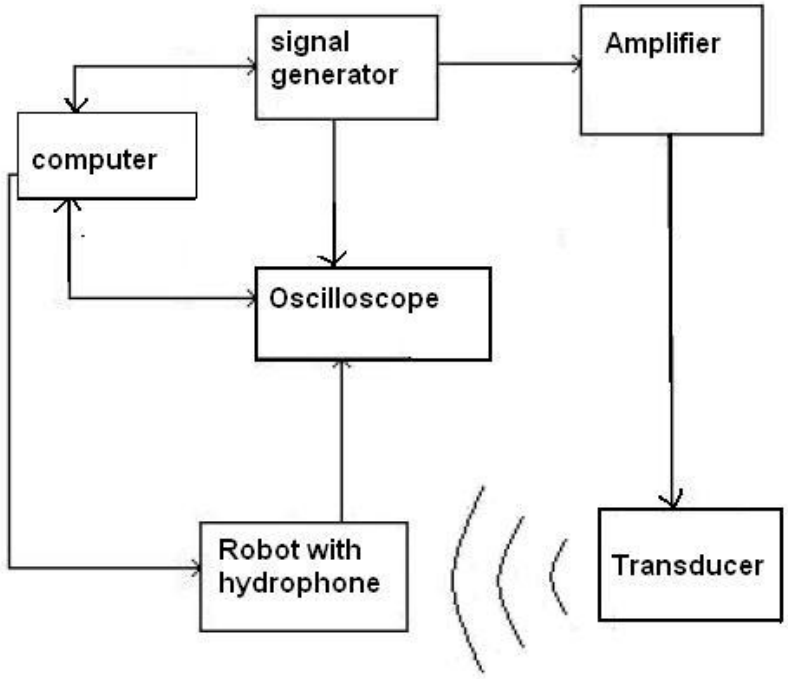

(a)

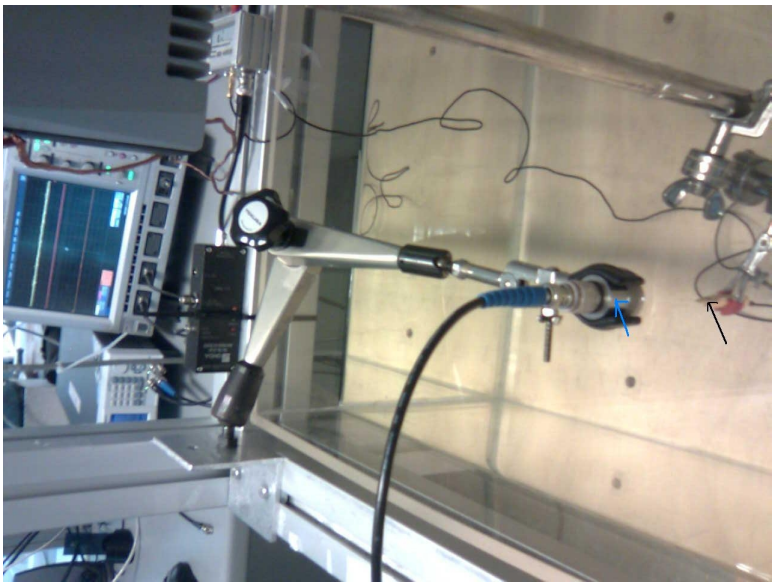

(b)

Figure 5.2: (a) Schematic illustration of the experimental setup for the characterization of transducers. (b) A figure showing the experimental setup for the characterization of transducers where black arrow and blue arrows shows the hydrophone and transducer respectively placed opposite to each other in the water tank.

amplified by an RF power amplifier with a gain of $50dB$ (240L ENI, $20KHz - 10MHz$, 50Ω, Rochester, NY) and then used to drive the transducer placed in the water chamber for treatment of sample as can be seen in Fig.5.1b. The same equipment were used for the $200kHz$ and the $500kHz$ transducer whereas, for the $1MHz$ and $2MHz$ transducer, a $50dB$ RF power amplifier (2100L ENI, Rochester, NY $10KHz - 12MHz$, 50Ω,) together with a $400MHz$ oscilloscope (LeCroy waveSurfer $42X_2$) were used.

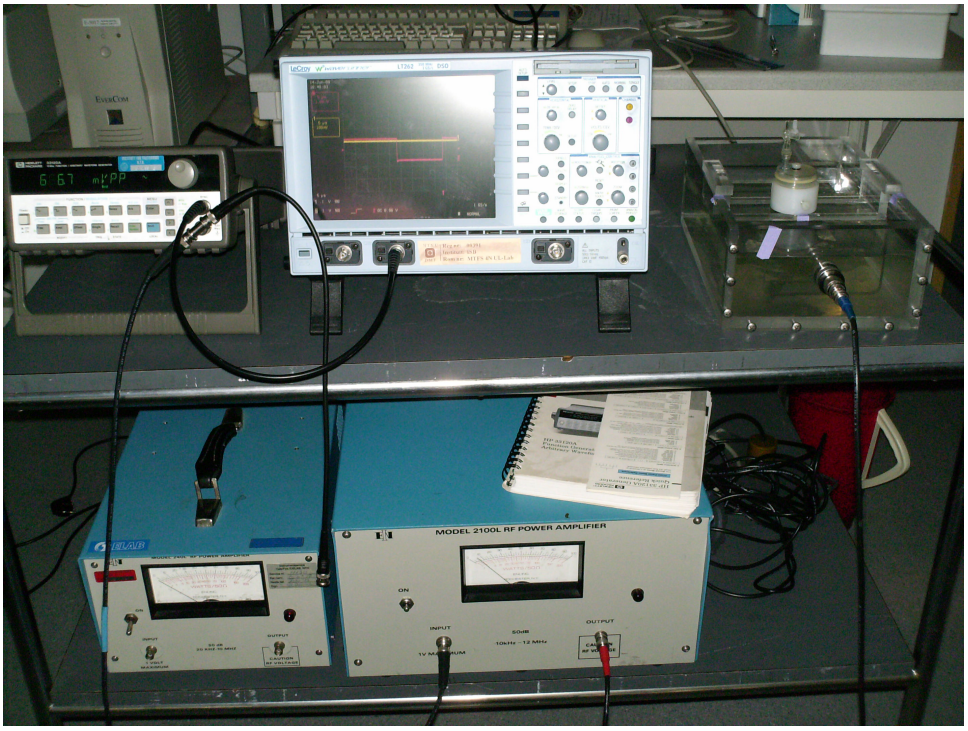

Figure 5.3: A figure showing the experimental setup used for the ultrasound treatment of the sample.

5.1.4 *Calcein liposomes*

As a model for drug delivery, acoustically active liposomes filled with calcein, a small fluorescent molecule was used as the sample. All liposomes were supplied by Epitarget, Oslo Norway and was kept at $2 - 8°C$.

Description of liposomes: Calcien liposomes of batch numbers #CCD6-23rep, #CCD-23dup. Three batches were provided but the third one has the same name and composition as CCD6-23dup. These batches had the following properties:

- Membrane composition; DSPE:DSPC:DSPE-PEG2000:Chol (mole%; $62 : 7,5 : 5,5 : 25$)

- Concentration of lipid (nominal) = 16 mg/mL
- Composition of intraliposomal phase; 50 mM calcein and 10 mM HEPES solution with pH = 7.4.
- Composition of extraliposomal phase; 10 mM HEPES and 0.02% (w/v) sodium azide sucrose solution with pH = 7.39.
- liposome physiochemical properties: size = $87nm$ (CCD-23rep) and $85nm$ (CCD-23dup), Zeta potential = $-19mV$ with pH = 7.1 for CCD-23rep and polydispersity index =$0.1 for CCD-23dup$

5.1.5 *The photospectrometer*

For measuring the effects of ultrasound on release, a photospectrometer (fluoromate, Spex industries.) was used. This measures the release of calcein (a small fluorescent molecule) by registering the intensity of emitted light. Due to self quenching (quenching of emitted light from nearby calcein molecules) caused by the high intraliposomal concentration of calcein, the fluorescence intensity displayed by intact liposomes is low but the intensity increases when they are released from the liposomes. Since calcein absorbs light with wavelength of $494nm$ and emits light with a peak at $515nm$, the excitation and the emission wavelength were set to $460nm$ and $500-600nm$ respectively. The output was a spectrum of intensity (in cps) against wavelength (nm).

5.2 Method for Drug Release Experiment

This section deals with the step by step procedure used in preforming the experiment. That is, the procedure for the preparation of the two dilution media has been described in the first part whereby the second part of this section describes the procedure for preparing the sample, the exposure to the ultrasound beam, the method used in the measurement of the fluorescence intensity and calculation of percentage release.

5.2.1 *Method for preparation of dilution medium*

5.2.1.1 *Preparation of sucrose /10 mM HEPES solution (2l)*

This solution was prepared for dilution purposes - used for diluting the liposomes to $1:500v/v$. The materials used in the preparation can be found at AppendixA. First $11.922g$ of HEPES (MW $238.3g/mol$, pH = $6.8-8.2$, pKa = 7.54, 99.5%titration, Sigma H3375 Batch# 88H5446, USA) was dissolved in 400ml of distilled water. 1M NaOH was then added to this solution until the pH was 7.4. This was followed with deionised water

to make a total volume of $500ml$ which resulted in a $100mM$ HEPES buffer solution with pH of 7.4. The sucrose solution was prepared by dissolving $193.98g$ of sucrose (MW 342.30 g/mol, BDH AnalaR prod 102745C, Lot#$K32050486405$ BH15 England) in $1000ml$ of deionised water while stirring with a magnetic stirrer . $212ml$ of the $100mM$ HEPES buffer solution was added to the sucrose solution followed by 0.41 of Sodium azide (BDH AnalaR prod 10369 Lot#$K2237000548$). Finally water was added to the mark and the final pH of the solution was measured to be 7.39.

5.2.1.2 *Preparation of Phosphate Buffered Saline (PBS)*

This solution was prepared by dissolving 1 tablet of Phosphate Buffered Saline (PBS) from Sigma Aldrich in $200ml$ of deionised sterilfiltered water. Where 1 tablet consist of Sodium chloride crystals (NaCl), Sodium phosphate, Dibasic, Anhydrous, Potassium chloride (KCl) and Potassium phosphate, monobasic, anhydrous (KH2PO4).

5.2.2 *Procedure for drug release experiment*

The liposomes were diluted to $1 : 500v/v$, that is, $28\mu l$ of liposomal calcein diluted with $14ml$ of $10mM$ HEPES buffered Sucrose solution (pH = 7.39) stored at $2 - 8°$C or Phosphate buffered saline (PBS). The solution was kept at room temperature (20°) until it was $\approx 19°$, then without ultrasound exposure, the fluorescence intensity of 1 ml of the solution was taken with the fluorometer described above. 1 ml of the sample was placed in the sample chamber (tip of the condom) as described in the previous Section 5.1.1. The sample chamber was placed on the bridge on top of the water bath at a distance (from the surface of the transducer to the sample) equivalent to the focal length of the transducer being used so that the sample was totally immersed in the water (20°). For example, the sample was placed at $76mm$ for the $200kHz$ transducer. The sample was then exposed to the ultrasound beam for $30s$ using the setup described in Section 5.1.3 with an initial input voltage of $200mV_{pp}$, 10 periods (20 and 40 periods for $1MHz$ and $2MHz$ respectively) and PRF of $500Hz$. It must be noted that different number of pulses were used for the different transducers so as to get the same duty cycle (although this was partially meet) and at the same time not to exceed the voltage limitation (50Vrms continuous wave) given by the manufacturer.

A finnpipette was used to remove the sample from the sample chamber into a cuvette after the $30s$ of ultrasound exposure and then the fluorescence intensity measured with the fluorometer. The process was repeated for six times ($1ml$ each) by increasing exposure time ($60s$, $90s$, $120s$, $240s$, $360s$ and $600s$) and the fluorescence intensity taken for each sample with the same settings. 10% Triton $X - 100$(Sigma U.S.A $\#T - 8787$,Lot $\#19H2611$) in H_2O was added to the sample with the highest ultrasound exposure ($600s$) in order to get the total release. The solution was whirl mixed and heated to 65°C for $5min$ in a water bath (DT Hetotherm , 220V, No. 91060917) and then cooled

to room temperature before taken the fluorescence measurement. **Note** : New samples (from one complete batch of diluted liposomes- $1/500v/v$) were used for each exposure time but the process was repeated (thus, for $200mV_{pp}$) with a flesh sample (new batch of diluted liposomes - $1:500v/v$) under the same conditions.

The input voltage was increased to $333.33mV_{pp}$, $666.7mV_{pp}$ ($500mV_{pp}$ maximum for $200kHz$) and the whole process was repeated twice for each voltage. The same procedure was used for all the other transducers, thus, $500kHz$, $1MHz$ and $2MHz$ as can be seen in Table 5.1 and Fig. 5.4. Although all experiments were conducted under the same conditions, different liposomes were used based on availability. That is, CCD6-23rep was used for investigating each of the transducer whereby CCD6-23dup was used for investigating effect of PBS and HEPES on release when using the $1MHz$ and the $2MHz$.

The ultrasound mediated release of calcein into the extraliposomal phase was determined by a marked increase in fluorescence intensity due to an overall reduced quenching effect. To quantify the release, the % release can be calculated from [21, 25];

$$\%release = \frac{F_u - F_b}{F_T - F_b} \times 100 \tag{5.2}$$

where F_u,F_b, and F_T are the fluorescence intensities of the sample before ultrasound exposure, after ultrasound exposure and after solubilisation with surfactant (Triton X-100). The average percentage release was then calculated for each voltage by finding the mean for the two experiment for each voltage.

Table 5.1: Summary of ultrasound settings used for the insonification of the sample in the control release experiment. Experiment was repeated twice for each input voltage.

Frequency[MHz]	Input voltage[mV_{pp}]	PRF[Hz]	Number of Periods
0.2	200	500	10
	333.33	500	10
	500	500	10
0.5	200	500	10
	333.3	500	10
	666.7	500	10
1	200	500	20
	333.3	500	20
	666.7	500	20
2	200	500	40
	333.3	500	40
	666.7	500	40

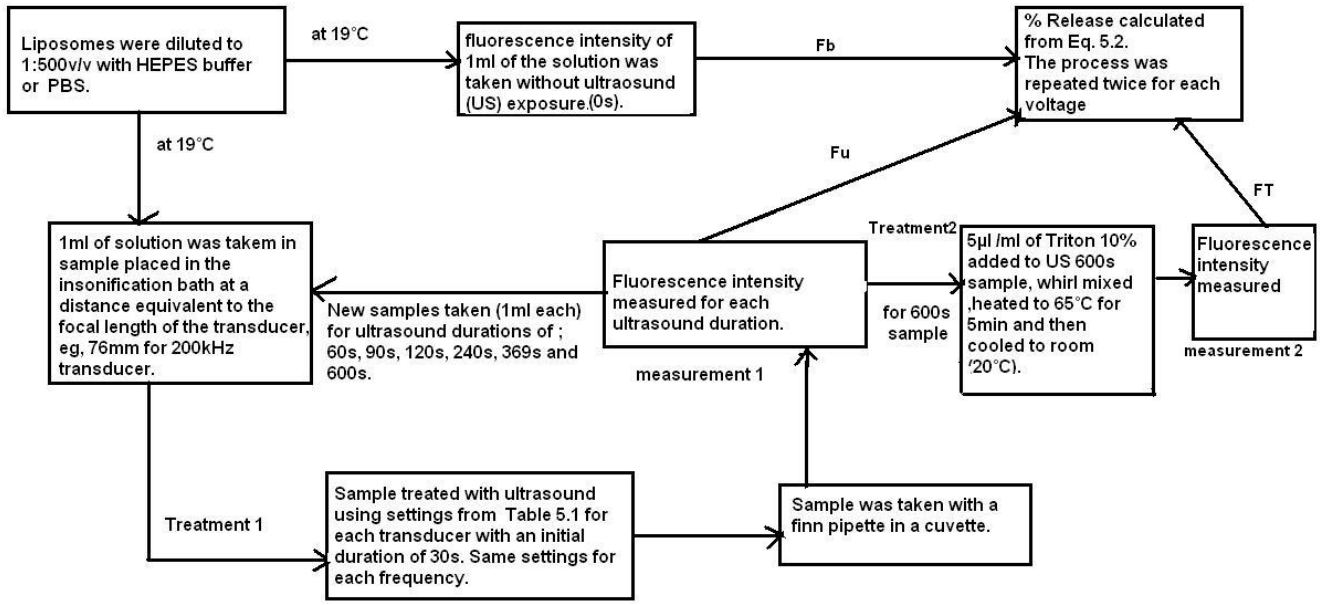

Figure 5.4: A chart describing the step by step experiment procedure used in the control release experiment. All experiments were repeated twice for each voltage. Where Fb, Fu, and FT are the fluorescence intensity before ultrasound treatment (0s), after ultrasound treatment and after ultrasound and Triton treatment.

Part III

RESULTS

Chapter 6

RESULTS

6.1 Characterization of Transducers

Generally these transducer were found to have very low acoustic powers and intensities. The highest acoustic power, negative pressure at the focus, mechanical index (MI) and intensity obtained was $18.9mW$, $611kPa$, 0.611 and $1.0mW/cm^2$ respectively with the $1MHz$ transducer (see Table 6.3). The transducers were found to be having impedances with very high magnitude and phase angles and also non was matched. It was observed that the output voltage from amplifier was more than what was expected for a 50dB amplifier (see Section B.1 and B.2). The acoustic intensity, mechanical index (MI) and electrical power for all transducers were calculated from Eq. 3.7, Eq. 3.37 and Eq. 3.43 respectively.

6.1.1 *200kHz transducer*

This transducer has a focal length of $76mm$, an active diameter of $38mm$ and an area of $45.4cm^2$. It has impedance with magnitude 118Ω and phase angle of 15.1° as shown in Fig. B.1 which gives $113.28 + j30.68\Omega$. The result obtained from the water tank measurement (characterization of transducers) has been summarized in the Table 6.1.The input voltage and the corresponding acoustic pressure, power and intensity, etc were found to be linearly relate. The highest acoustic power, pressure at the focus, intensity, MI obtained were $2.19mW$, $145kPa$, $0.048mW/cm^2$ and 0.32. The transducer was not characterized at $200mV_{pp}$ so the acoustic properties (power, intensity,MI, etc.) were estimated from the values of the other input voltages using $p = HV$ (where H is the transfer function and V is the voltage) and assuming a linear relationship. In continuous mode, an electrical power of $74.5W$ was used but the transducer was not characterized using continuous mode so no information was given on the acoustic properties.

Table 6.1: Measurement taking with 200kHz transducer with a focal length of 76mm in water, active diameter of 38mm and impedance of $113.28 + j30.68\Omega$. The same duty cycle (1/200) was used for all measurements.

Input Voltage[mV_{pp}]	200	333.3	500
Output Voltage from amplifier[V_{pp}]	176	276	330
PRF[Hz]	100	100	100
Number of periods	10	10	10
Electrical power[W]	0.68	1.68	2.40
Acoustic power at the focus[mW]	0.33	0.80	2.19
Acoustic pressure at the focus[kPa]	-59 and 66	-93 and 103	-145 and 170
Maximum acoustic pressure[kPa] at 34mm	-123 and 138	-193kPa and 217	-561 and 712
Average acoustic intensity at the focus[mW/cm^2]	0.01	0.02	0.05
Mechanical Index at the focus	0.13	0.21	0.32

6.1.2 *500kHz transducer*

The focal length of the transducer is 50mm with active diameter of 25mm an and area of 19.6mm. The impedance was measured to be $22.7 - j361.2\Omega$, thus 361.9Ω in magnitude with a phase angle of $-86.4°$ as shown in Fig.B.2. The results for the characterization can be found at Table 6.2. The highest acoustic negative pressure at the focus, MI, and acoustic power obtained are 378kPa , 0.54 and 0.75mW respectively. The transducer was not characterized at 200mV_{pp} so the acoustic parameters (power, intensity,MI, etc.) were estimated from the values of the other input voltages using $p = HV$ (where H is the transfer function and V is the voltage) and assuming a linear relationship. It was observed during the measurement that, acoustic power for the 312kPa was higher than that of 378kPa (see Table 6.2).

Table 6.2: Measurement taking with $500kHz$ transducer with a focal length of $50mm$ in water, active diameter of $25mm$ and impedance of $22.7 - j361.2\Omega$. Different duty cycles were used for the two voltages $333.3mV_{pp}$ (1/1000) and $666.7mV_{pp}$ (1/2000).

Input Voltage $[mV_{pp}]$	200	333.3	666.7
Output voltage from amplifier$[V_{pp}]$	172	282	400
PRF[Hz]	100	100	50
Number of periods	5	5	5
Electrical power[W]	0.65	1.75	1.76
Acoustic power at the focus[mW]	0.38	0.75	0.64
Acoustic pressure at the focus[kPa]	-190 and 206	-312 and 338	-378 and 443
Maximum acoustic pressure at [kPa]	-237 and 259	-389 and 425 at 35mm	- 457 and 512 at 36mm
Average acoustic intensity at the focus$[mW/cm^2]$	0.01	0.04	0.03
Mechanical Index at the focus	0.34	0.45	0.54

6.1.3 *1MHz transducer*

This transducer has a focal length of $85mm$ in water, an active diameter of $25mm$ and an area of $19.6mm$. It has an impedance of $32.4 - j158.5\Omega$, 162Ω in magnitude with a phase angle of $78.3°$ (see Fig. B.3). A summary of the result from characterization measurement can be found in Table 6.3. An increase in the input voltage resulted in an increase in acoustic pressure, power and intensity. This transducer gave the highest acoustic power, pressure, intensity etc as stated above.

Table 6.3: Measurement taking with 1MHz transducer with a focal length of $50mm$ in water, active diameter of $25mm$ and impedance of $32.4 - j157.5\Omega$. Duty cycle for voltages was 1/200.

Input Voltage [mV_{pp}]	200	333.3	666.7
Output Voltage from amplifier[V_{pp}]	120	200	400
PRF[Hz]	500	500	500
Number of periods	10	10	10
Electrical power[W]	1.11	3.09	12.35
Acoustic power at the focus [mW]	1.44	4.30	18.87
Acoustic pressure at the focus[kPa]	-196 and 210	-325 and 363	-611 and 760
Maximum acoustic pressure [kPa]	-237 and 247 at 62mm	-389 and 417 at 63mm	-718 and 833 at 67mm
Average acoustic intensity at the focus [mW/cm^2]	0.07	0.22	1.00
Mechanical Index at the focus	0.20	0.33	0.61

6.1.4 *2MHz transducer*

The focal length of the transducer is $125mm$ with an active diameter of $19mm$ and an area of $11.3cm^2$. The impedance was measured to be $12.4 + j57.8\Omega$ with a magnitude of 59.23Ω and a phase angle of $-77.5°$ as shown in Fig. B.4. The same duty cycle (1/400) was used for all voltages. Table 6.4 gives the result obtained from the water tank measurement and it can be seen that all acoustic parameters increased with increase in input voltage. With the same number of pulses (10) and PRF ($500Hz$), the highest acoustic pressure, power, intensity and MI obtained are $386kPa$, $4.21mW$, $0.37mW/cm^2$ and 0.27 respectively.

Table 6.4: Measurement taking with 2MHz transducer with a focal length of $50mm$ in water, active diameter of $25mm$ and impedance of $12.4 + j57.8\Omega$. The duty cycle used for all voltages was 1/400.

Input Voltage[mV_{pp}]	200	333.3	666.7
Output Voltage from amplifier[V_{pp}]	60	100	200
PRF[Hz]	500	500	500
Number of periods	10	10	10
Electrical power[W]	0.36	1.01	4.03
Acoustic power at the focus [mW]	0.3	1.0	4.2
Acoustic pressure at the focus [kPa]	-143 and 172	-233 and 318	-386 and 669
Maximum acoustic pressure[kPa]	-202 and 223 at 81mm	-327 and 385 at 81mm	-551 and 748 at 91mm
Average acoustic intensity at the focus[mW/cm^2]	0.03	0.08	0.37
Mechanical Index at the focus	0.10	0.17	0.27

6.2 Control Release Experiment

This section is in six parts, 1 to 4 deals with the results obtained for each transducer whereas the remaining three parts is a comparison between these four transducers and the two dilution medium. Generally, different number of pulses were used for these transducers but the same PRF was used in all the cases. This is to obtain the same duty cycle for all transducers (although this was partially met) and at the same time prevent damage to the transducer by exceeding the limitation given by the manufacturer. Thus, 1/40 duty cycle was used for the 200kHz transducer whereas 1/100 was used for the rest of the transducers. This implies that the acoustic parameters used in the control release experiments might be higher than what was obtained from the characterization measurement since very low duty cycles were used for the characterization (see Section 6.1). The results for all frequencies were plotted in three forms- average percentage release as a function of ultrasound duration, average percentage release as function of the product of the square of the negative pressure and the true time (product of irradiation time and duty cycle). This parameter $p_{neg}^2 T_c$ is also a measure of the mechanical index or a form of energy.

Finally, the maximum release for each intensity was plotted as a function of acoustic intensity calculated from Eq. 3.7 Furthermore, the data was fitted to a theoretical curve and the first -order rate constant (k) for each intensity calculated using;

$$I = I_o(1 - e^{-kt}) \tag{6.1}$$

Where I is intensity as time t, I_0 is the maximum intensity, $k = 1/T_{release}$ is the rate constant and t is the ultrasound duration (see Section B.4 for example of the matlab code used for the calculations and the figures generated for the errors and the rate constants). **Note:** HEPES was used for all experiments except at Section 6.2.6 where PBS was use in order to compare data. The value of k was chosen from the minimum value of the error.

6.2.1 *200kHz transducer*

Inspite of experimental errors, the maximum average percentage release of calcein obtained with this transducer was $\sim 12\%$ for pulse wave at an acoustic negative pressure of $145kPa$ whereas a maximum of $\sim 22\%$ was obtained for a continuous wave with electrical power of $74.5W$ as shown in Fig. 6.1. The maximum release was found to increase as the intensity of the beam was increased, thus, the average maximum % release of calcein from the liposomes increased from 7.5% to 12% as the acoustic intensity of the beam was increased from $0.01mW/cm^2$ to $0.05mW/cm^2$. It can also be seen from Fig. 6.1b and Section B.3.2 that, release is also pressure dependent although for shorter exposures it is not well seen and $145kPa$ and $93kPa$ seems to be practically the same even at higher exposures with a slight difference at the maximum exposure ($600s$). Nevertheless, with the same pressure and intensity, release was found to increase with exposure time (see Fig. 6.1) and is more evident between the $93kPa$ and the $59kPa$ and also between $145kPa$ and $59kPa$ but for $145kPa$ and $93kpa$ the amount of calcein released seems to be practically the same. The rate constants for these pressures were found to be; $k_{59kPa} = 0.0111s^{-1}, k_{93kPa} = 0.0077s^{-1}, k_{145kPa} = 0.0063s^{-1}$. Also, Fig. 6.1c shows a graph of average percentage release as function of ultrasound duration for a continuous wave with electrical power of $74.5W$ with a maximum average release of 21.5%. In this graph the amount of calcein released was also found to increase with exposure time. The first-order rate constant was found to be; $k_{cont} = 0.0050^{-1}$.

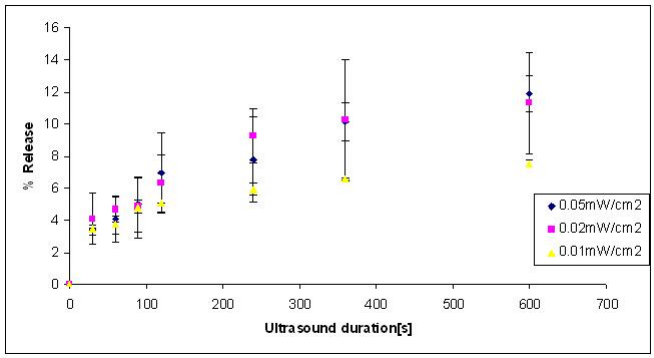

(a)

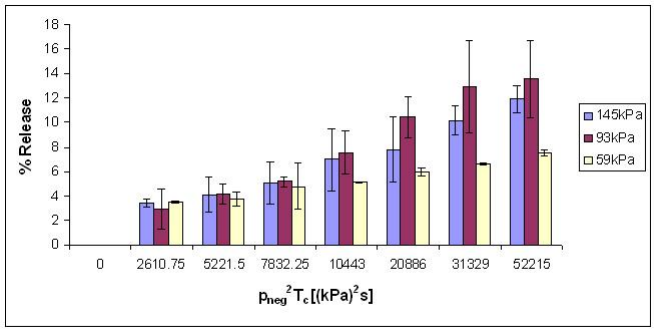

(b)

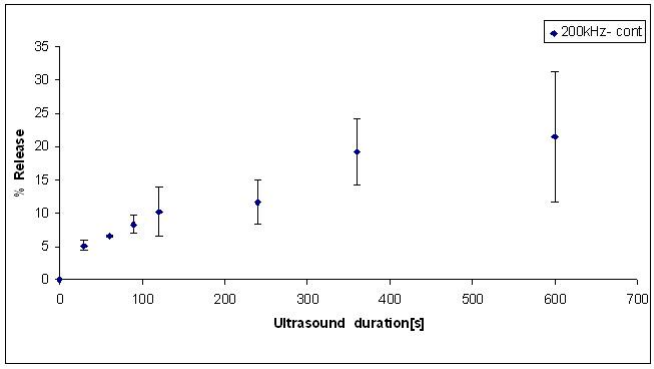

(c)

Figure 6.1: (a)Average percentage release of calcein as a function of ultrasound duration at 200kHz for three different acoustic intensities of $0.05mW/cm^2$,$0.02mW/cm^2$ and $0.01mW/cm^2$. with a duty cycle of 1/40. The first-order rate constants were found to be ; $k_{59kPa} = 0.0111s^{-1}, k_{93kPa} = 0.0077s^{-1}, k_{145kPa} = 0.0063s^{-1}$. (b) Average percentage release of calcein as a function of the product of the square of the negative acoustic pressure ($145kPa, 93kPa$ and $59kPa$) and the true time ($p_{neg}^2 T_c$) with a duty cycle of 1/40. (c) Average percentage release of calcein as a function of ultrasound duration for a continuous wave with an electrical power of $74.5W$(100% duty cycle). Error bars shows standard deviation (n = 2) from the mean of the percentage release.

6.2.2 *500kHz transducer*

The maximum release obtained from this transducer is $\sim 15\%$ at an acoustic negative pressure of $312kPa$. This can been seen in Fig. 6.2. Also, the maximum percentage release increased from 6.1% to 14.9% with intensities from $0.01mW/cm^2$ to $0.04mW/cm^2$ which implies it increases with increase in intensity. In Fig. 6.2b average percentage release was plotted as a function of the product of the square of the negative pressure and the true time (exposure time multiplied by the duty cycle). This also shows that the average percentage release increases as the the pressure increases although this is not see so well until at $90s$ and also between $312kPa$ and $378kPa$. Finally, with same negative pressures and intensities, the average percentage release was found to be dependent on exposure time especially for $312kPa$ and $378kPa$ as shown in Fig. 6.2. The first-order rate constant for each negative pressure was found to be ; $k_{190kPa} = 0.0125s^{-1}$, $k_{312kPa} = 0.0071s^{-1}$, $k_{378kPa} = 0.0048s^{-1}$.

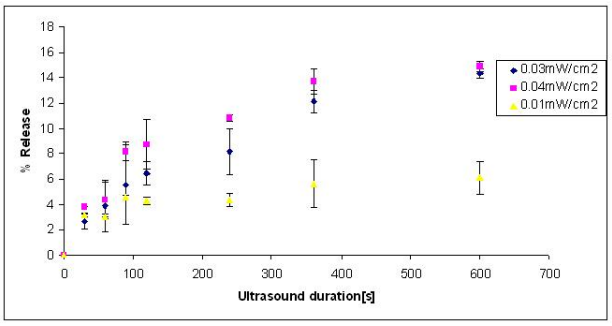

(a)

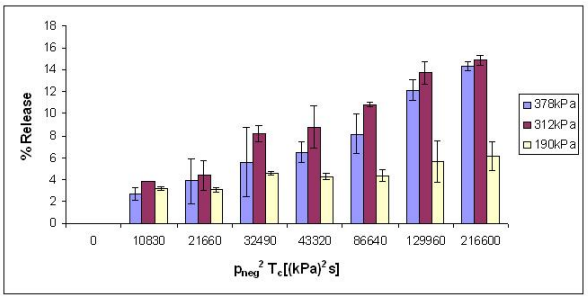

(b)

Figure 6.2: (a)Average percentage release of calcein as a function of ultrasound duration at $500kHz$ for three different acoustic intensities of $0.03mW/cm^2$,$0.04mW/cm^2$ and $0.01mW/cm^2$ with a duty cycle of 1/100. (b) Average percentage release of calcein as a function of the product of the square of the negative acoustic pressure ($378kPa, 312kPaand190kPa$) and the true time with a duty cycle of 1/100. Error bars shows standard deviation (n = 2) from the mean of the average percentage release and the first-order rate constants were found to be $k_{190kPa} = 0.0125s^{-1}$, $k_{312kPa} = 0.0071s^{-1}$, $k_{378kPa} = 0.0048s^{-1}$.

6.2.3 *1MHz transducer*

In Fig. 6.3 it can be seen that the maximum average percentage release given by this frequency was found to be $\sim 9\%$ at an acoustic negative pressure of $611kPa$. Like the first two transducers, the percentage release increased as the duration of the ultrasound increased at constant pressure and intensity. Also, average percentage release increased with an increase in the negative pressure although there some slight deviations as shown in Fig. 6.3. From Fig. 6.3a it can seen that percentage release increased from 5.8% to 8.5% (although not that much increase) with an increase in acoustic intensity from $0.07mW/cm^2$ to $1.00mW/cm^2$. The first-order rate constant for each negative pressure was found to be ; $k_{196kPa} = 0.0091s^{-1}$, $k_{325kPa} = 0.0083s^{-1}$, $k_{611kPa} = 0.0056s^{-1}$.

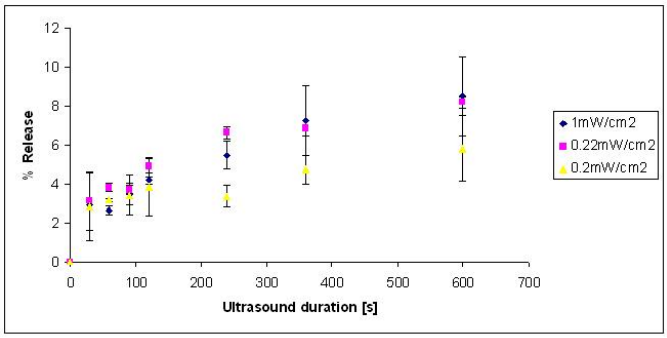

(a)

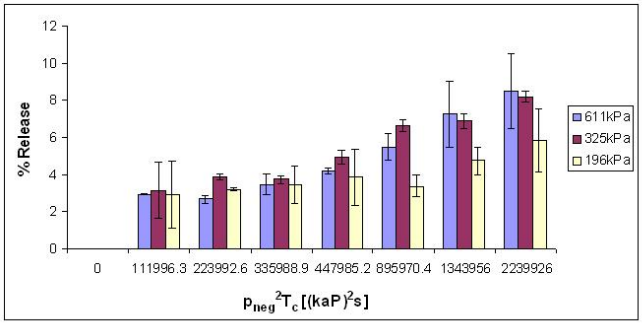

(b)

Figure 6.3: (a)Average percentage release of calcein as a function of ultrasound duration at $1MHz$ for three different acoustic intensities of $1.0mW/cm^2$, $0.22mW/cm^2$ and $0.07mW/cm^2$ with a duty cycle of 1/100. (b) Average percentage release of calcein as a function of the product of the square of the negative acoustic pressure ($611kPa, 325kPa$ and $196kPa$) and the true time with a duty cycle of 1/100. Error bars shows standard deviation (n = 2) from the mean of the percentage release and the first-order rate constant for each negative pressure was found to be; $k_{196kPa} = 0.0091s^{-1}$, $k_{325kPa} = 0.0083s^{-1}$, $k_{611kPa} = 0.0056s^{-1}$.

6.2.4 *2MHz transducer*

With a duty cycle of 1/100 (40 pulses with $500Hz$ PRF) unlike what was used in the characterization measurement (1/400, thus 10 pulses with $500Hz$), the maximum average percentage release of calcein obtained with this transducer was 7.3% for pulse wave at an acoustic negative pressure of $386kPa$ as shown in Fig. 6.4. This transducer gave the minimum percentage release. Release was found to increase from 5.2% to 7.3% as the intensity of the beam was increased from $0.03mW/cm^2$ to $0.4mW/cm^2$. It can also be seen in Fig. 6.4a that, generally release increased with increase in negative pressure although there were some few deviations from $30s$ to $90s$. Release was also found to be dependent on the exposure time, thus, at constant pressure and intensity, the amount of calcein release increased with an increase in ultrasound duration or exposure. This is clearly seen at $600s$ - maximum or terminal release. The first-order rate constant for each negative pressure was found to be ; $k_{143kPa} = 0.0056s^{-1}, k_{233kPa} = 0.0063s^{-1}, k_{386kPa} = 0.0048s^{-1}$.

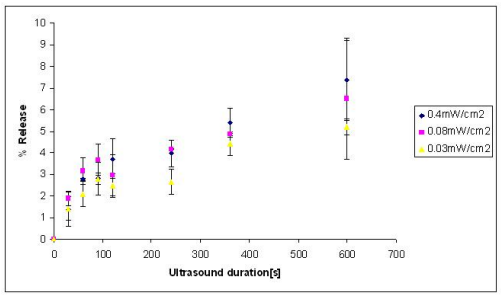

(a)

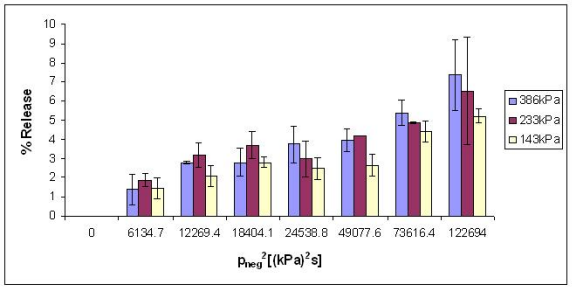

(b)

Figure 6.4: (a)Average percentage release of calcein as a function of ultrasound duration at 2MHz for three different acoustic intensities of $0.27mW/cm^2$, $0.17mW/cm^2$ and $0.1mW/cm^2$ with a duty cycle of 1/100. (b) Average percentage release of calcein as a function of the product of the square of the negative acoustic pressure ($386kPa, 233kPa$ and $143kPa$) and the true time with a duty cycle of 1/100. Error bars shows standard deviation ($n = 2$) from the mean of the average percentage release and the first-order rate constant for each negative pressure was found to be ; $k_{143kPa} = 0.0056s^{-1}, k_{233kPa} = 0.0063s^{-1}, k_{386kPa} = 0.0048s^{-1}$.

6.2.5 *Results from all transducers*

As stated in the previous sections three of the transducers ($500MHz$, $1MHz$ and $2MHz$) have the same duty cycles, that is, 1/100 whereas the $200kHz$ have 1/40. Inspite of all experimental errors, the maximum average release from all the transducers was found to be $\sim 15\%$ at an acoustic negative pressure of $312kPa$ with the $500kHz$ transducer at an acoustic intensity of $0.04mW/cm^2$. Generally, it can be seen from Fig. 6.5 that release increases with ultrasound duration and acoustic pressure. That is, release decreases as the frequency increases but is dependent mechanical index. For example, with a MI of 0.5, the release from the $500kHz(15\%)$ was higher than that of $200kHz$ with MI of 0.3 (12%). From Fig. 6.5b it can also be seen that the amount of calcein release is dependent on frequency especially at low intensities but deviates a bit at higher intensities. For all frequencies, thus keeping the frequency constant, maximum percentage release increased with increase in acoustic intensity with some slight deviation in the 500kHz transducer. Finally, it was noticed that, $200kHz$ at continuous wave gave higher release than all (see Fig. 6.5 and Fig. 6.1c

6.2.6 *Effect of HEPES and PBS on release*

The HEPES and PBS were investigated to find out which of the two gives the maximum release. Three different transducer were used for this experiment namely $500kHz$, $1MHz$ and $2MHz$. In all these experiments with the different transducers, PBS was found to give the maximum release under the same experimental conditions.

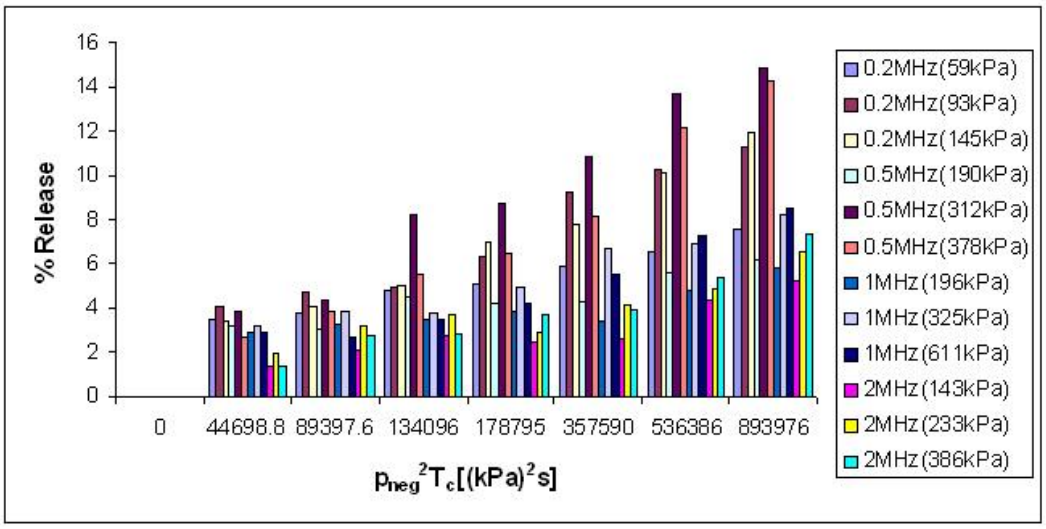

(a)

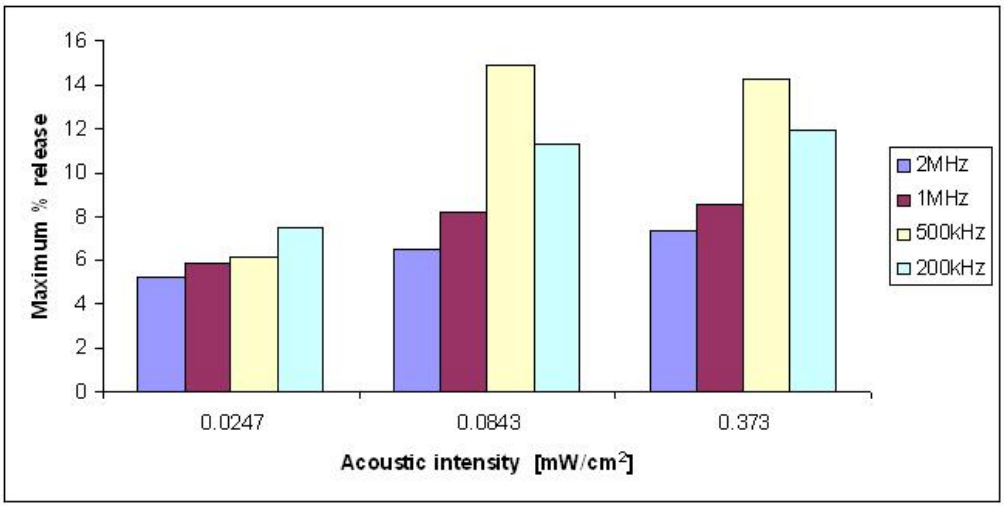

(b)

Figure 6.5: Average percentage release of calcein as a function of the product of the square of the negative acoustic pressure and the true time with a duty cycle of 1/40 (200kHz) and 1/100 (500kHz, 1MHz and 2MHz) for all transducers. (b) Maximum percentage release of the various intensities of frequency as a function of acoustic intensity. Error bars shows standard deviation from the mean (n = 2).

6.2.6.1 PBS and HEPES: 500kHz transducer

Using CCD-23rep liposomes and $500kHz$ transducer with a duty cycle of 1/100 (10 periods with $500Hz$ PRF) and a negative pressure of $312kPa$, PBS was found to give a maximum release of $\sim 40\%$ when the sample was placed at the focus ($50mm$) of the beam whereas it gave a maximum of $\sim 30\%$ when placed at $40mm$ away from the transducer. However, when the same liposomes, the same transducer with the same duty cycle and acoustic negative pressure ($312kPa$) under the same experimental conditions was used with HEPES as a dilution medium, the maximum release at the focus was found to be 15.2% and 8.8% at $40mm$ which is even less than half that of PBS in both cases. It can also been seen that, in both media, release increases with exposure time. Thus, the longer the ultrasound duration, the higher the release (see Fig. 6.6). Again, the amount of calcein released was higher when sample was placed at the focus for both PBS and HEPES. These experiment were done once unlike all the other experiments where they were repeated and the average taken. The first-order rate constant for both PBS and HEPES was found to be ; $k_{PBS} = 0.0077s^{-1}$ at the focus $k_{PBS} = 0.010s^{-1}$ at 40mm, $k_{HEPES} = 0.0067s^{-1}$ at the focus and $k_{HEPES} = 0.0091s^{-1}$ at 40mm.

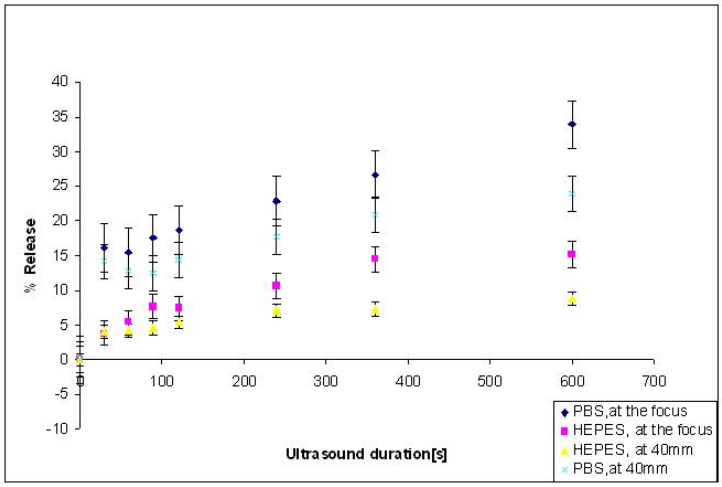

Figure 6.6: Percentage release of calcein as a function of ultrasound duration with PBS and HEPES as dilution medium at an acoustic negative pressure of $312kPa$. Sample was placed at the focus ($50mm$) of the ultrasound beam and $40mm$ away from the surface of the transducer. Error bars shows standard error. The first-order rate constant for both PBS and HEPES was found to be ; $k_{PBS} = 0.0077s^{-1}$ at the focus $k_{PBS} = 0.010s^{-1}$ at 40mm, $k_{HEPES} = 0.0067s^{-1}$at the focus and $k_{HEPES} = 0.0091s^{-1}$ at$40mm$. .

6.2.6.2 PBS and HEPES : 1MHz and 2MHz transducers

In this experiment, the $1MHz$ and $2MHz$ transducers were used together with CCD6-23dup (last batch) liposomes. The same duty cycle (1/100) was used for both the $1MHz$ (20 pulses with $500Hz$ PRF) and the $2MHz$ (40 pulses with $500Hz$ PRF) transducer. In all these experiments (with both $1MHz$ and $2MHz$), PBS was found to give the maximum average percentage release of 12.5% at a negative pressure of $325kPa$ ($1MHz$) and 8% at a negative pressure of $386kPa$ ($2MHz$) as shown in Fig. 6.7. The average percentage release with the same liposome (CCD6-23dup) and the same transducers ($1MHz$ and $2MHz$) with HEPES was found to be 7.9% at a negative pressure of $325kPa$ ($1MHz$) and 5% at a negative pressure of $386kPa$ ($2MHz$). This also gives the indication that release increases with exposure time. Thus, the longer the exposure time, the higher the release.The first-order rate constants for both HEPES and PBS were found to be ; for 1MHz; $k_{PBS} = 0.0063s^{-1}$ and $k_{HEPES} = 0.0071s^{-1}$, for 2MHz; $k_{PBS} = 0.0091s^{-1}$ at the focus and $k_{HEPES} = 0.0071s^{-1}$.

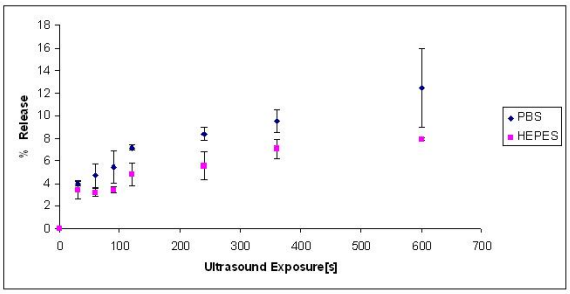

(a)

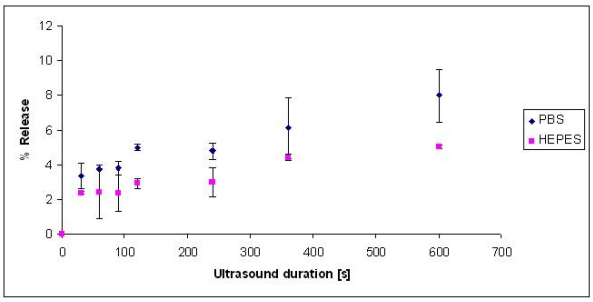

(b)

Figure 6.7: (a)Average percentage release of calcein as a function of ultrasound duration at 1MHz at an acoustic negative pressure of 312kPa with a duty cycle of 1/100 using PBS and HEPES as dilution media. (b) Average percentage release of calcein as a function of ultrasound duration at 2MHz at an acoustic negative pressure of 386kPa with a duty cycle of 1/100 using PBS and HEPES as dilution media. Error bars shows standard deviation (n = 2) form the mean of the percentage release. The first-order rate constants for both HEPES and PBS were found to be ; for 1MHz; $k_{PBS} = 0.0063s^{-1}$ and $k_{HEPES} = 0.0071s^{-1}$, for 2MHz; $k_{PBS} = 0.0091s^{-1} at the focus$ and $k_{HEPES} = 0.0071s^{-1}$

Part IV

DISCUSSION AND CONCLUSION

Chapter 7

DISCUSSION

Ultrasound has been found to trigger the release of liposomal drug and reduce the volume of tumors growing in mice [25, 21, 56, 41, 40]. It has also been found to trigger the release of different drug delivery systems, such as polymeric micelles [27, 53, 54] and polymeric matrices [33]. In the present study, four ultrasound transducers ($200kHz, 500kHz, 1MHz$ and $2MHz$) were used to investigated the effect of ultrasound on liposomal drug releas. This study also confirms that ultrasound can trigger the release of liposomal drug and is frequency and pressure dependent.

7.1 Experimental Design and Characterization of Transducers

Generally, the transducers were found to have low acoustic powers and intensities but the negative pressures of all frequencies (with the exception of $59kPa$ for $200kHz$) lies within the threshold of pressure for cavitation to occur given by Eq. 3.38. Comparing these pressures with what was used by Epitarget ($240kPa$) in their release experiment with a $40kHz$ transducer [21] (70% maximum release), it can be said that they were not that low but the difference in frequencies used makes the difference.

The low acoustic power and intensities obtained could be as a result of the very low duty cycles used during the measurement or the transducers are not for high power application which was confirmed by the manufacturers afterwards. For instance, the duty cycle for the $200kHz$ was 1/200 whereby 1/1000 and 1/2000 was used for the $500kHz$ transducer. That of the $1MHz$ and the $2MHz$ were 1/200 and 1/400 respectively. This was done because no voltage limitation was given for the pulse wave so care had to be taken in order not to damage the transducer. It might also be due to the fact that most of the energy applied was reflected since the transducers were not matched to the 50Ω system used in the experiment because the imaginary part of their impedances were found to be big (see Section6.1). From Table 6.2, it can be seen that the acoustic power obtained

for the $500kHz$ decreased from $0.75W$ to $0.64W$ even with an increased input voltage (from $333.3mV_{pp}$ to $666.7mV_{pp}$). This is as a result of the low duty cycle used for the $666.7mV_{pp}$ for fear of damaging the transducer since they will be used by another student. It was observed that at this voltage ($666.7mV_{pp}$), thus the 500kHz transducer, the signal was distorted when the PRF was increased although from calculations (using Eq. 5.1) it should be possible increase to that voltage. Also, the maximum input voltage that could be applied to the 200kHz was $500mV_{pp}$ although from the calculations it could be increased more than that. The results obtained for the measurement of the maximum positive pressure and the positive pressure at the focus for this transducer (($200kHz$) at $500mV_{pp}$) were unexpected because they were far greater than their respective negative pressures (see Table 6.1). One explanation could due to saturation of the amplifier used. Nevertheless, since the duty cycles of all the frequencies were increased (1/40 for $200kHz$ and 1/100 for $500kHz$, $1MHz$ and $2MHz$) during the control release experiment (for maximum effect), it is believed that, the intensities and the pressures might be higher than what was obtained from the characterization of the transducers.

The design of the experimental setup also has some setbacks. That is, the placing of the sample chamber in the focus of the ultrasound beam was not certain since it was done by estimation with a ruler which might be dependent on the observer. Furthermore, the water used for the ultrasonic insonation (at room temperature) was not degassed, it was obtained directly from the tap and used the following day. Again, the procedure used for the control release experiment was a bit different from the what was used by Epitarget and Huang [25, 21]. Thus, same sample was used for all the ultrasound exposure whereby in the present work new samples ($1ml$) were taken for each ultrasound duration and so the handling of the sample might have introduced some errors into the experiment. These limitations in the experimental design might have introduce some sources of errors into the experimental data. This could explain why the graphs were not that smooth since there were some few fluctuations (up and down) in the values for increased exposure time or ultrasound duration.

7.2 Drug Release Experiment

There were a lot of trials before the actual results were obtained. This was to check whether the sample chamber was reliable in getting accurate result and also in order to get the right procedure for the control release experiment. Some of the initial results can be found at Appendix B.3. In Fig. B.7a and Fig. B.7b, 200kHz transducer with 5 pulses and 1kHz PRF (1/40 duty cycle) was used to acquire the data whereby the $500kHz$ with a duty cycle of 1/100 (10 pulses and $500kHz$ PRF) was used for Fig. B.7c. Initially , the sample was not treated with Triton X-100 after irradiation so the intensity of calcein registered was plotted against the duration of the ultrasound beam as seen in Fig. B.7a. For these experiments the sample was whirl mixed before exposing it to the ultrasound beam, so the amount of calcein released might be as a result of the stirring plus the

effect of ultrasound. Also, there were a lot of fluctuations in the values which might also be due to the stirring and the positioning of the sample chamber in the focus of the beam. This was corrected for by exposing the sample to the beam without stirring and markers were used to make sure the sample was always placed at the focus before irradiation although this was not so easy. The sample was not placed at the position where maximum pressure was obtained because the beam diameter is smaller before the focus and so the beam might not cover the whole sample volume ($1ml$) if placed before the focus or at the maximum pressure point although the intensity is believed to be higher at that point.

7.2.1 *200kHz transducer*

The amount of calcein release with 100% duty (continuous wave) decreased from 28.4% to 14.5% when the experiment was repeated . It might be due to the fact that the voltage limitation for the continuous wave ($70V_{pp}$) was exceeded because the output voltage from the amplifier was found to be more than what was expected. That is, $130V_{pp}$ instead of $60V_{pp}$ although the input voltage was $200mV_{pp}$. Also, as proposed by Sponer [58], the threshold pressure for $200kHz$ would be $70kPa$- using Eq. 3.38. This gives the implication that theoretically the $200kHz$ with pressure amplitude of $59kPa$ should not have given any release (thus if cavitation is the mechanism for the release) but it gave some release according to this present work. One explanation could be that, the pressure amplitude might be more than what was estimated since the $59kPa$ is a calculated value from the values of $93kPa$ and the $145kPa$ obtained experimentally and the linear assumption made does not hold. Again, the pressure amplitude might be higher than $59kPa$ since the duty cycle used in the control release experiment was more than what was used in the characterization of the transducers. The amount of calcein released for continuous was found to be more than amount release when pulse wave was used at all intensities. One explanation could be the higher electrical power of the continuous wave was calculated to be ($74.5W$) as compare to the pulse wave (see Section 6.1). Again, with the same input voltage of $200mV_{pp}$, different output voltages form amplifier were obtain for the continuous wave ($130V_{pp}$) and the pulse wave ($176V_{pp}$.)

With the same input voltage as the other transducer using pulse wave, this transducer gave the lowest acoustic negative pressures. As seen from the previous chapter, drug release increases with increase in intensity (for the same frequency) and also the ultrasound duration especially the longest exposure. This dependence is seen in Fig. 6.1 and at Section B.3.2, in all the three intensities ($0.05mW/cm^2, 0.02mW/cm^2$ and $0.01W/cm^2$), there was an initial release of 3-4% at 30s which increased slightly with time until at 120s to the maximum when there was a significant difference or increase (about 5-6% depending on the intensity) in the amount of release. Another observation was that, the amount of calcein release for the $0.05mW/cm^2$ and $0.02W/cm^2$ was practically the same right from 30s to 600s which ended with a difference of 0.57%. This could be that the

transducer does not function well at that intensity ($0.05mW/cm^2$) as observed during the characterization process or the voltage ($330V_{pp}$) was too high for it .

7.2.2 *500kHz transducer*

The amount of calcein release was found to be time dependent but unlike the 200kHz, for all the three intensities, there was a significant increment of the amount of calcein released right from 30s to the 600s. It can also be seen that after 90s, there was clear distinction in the amount of calcein release between the three intensities (see Fig 6.2 and Section B.3.3). The highest amount of release was given by $312kPa$ which might not be in agreement with the theory given by Apfel and Sponer [6, 58]. That is for the same frequency, release should increase with pressure if the mechanism of release is cavitation (MI). This could be explained by the observation made earlier on during the characterization of the transducer, that the signal became distorted as the PRF was increased (see Section 7.1). In other words practically, the transducer does not function well when the PRF was increase from 50Hz in the characterization process to 500Hz in the control release experiment.

7.2.3 *1MHz transducer*

It was observed that like the $200kHz$ and the $500kHz$, release increased with an increase in intensity. The amount of calcein release for each intensity increased steadily to the maximum value. There was no significant difference between the amount release for each intensity from 30s to 120s but from 240s to 600s there was some slight difference especially for the $611kPa$ and $325kPa2$ (see Fig 6.3 and Section B.3.4). However, the result is in accordance with that of Huang[25] only that with the same frequency ($1MHz$), a maximum of 62% of the drug was release whereby in the present work only 9% was released. The explanation might then be the difference in duty cycles used, that is, 100% duty cycle (continuous wave) and 1%(1/100) for this experiment. Also since drug release is said to increases with intensity [56], the difference in the intensity used might also be a factor to be looked at, thus, $2W/cm^2$ verses $0.025mW/cm^2$, $0.084mW/cm^2$ and $0.373mW/cm$ in the present work. The results obtained with this transducer might have some errors because the outer cylinder of the sample chamber (see Fig. 5.1b) was broken and so was not stable when placed in the focus of the beam but this problem was fixed for subsequent experiment. Finally, this transducer gave the highest acoustic pressures, intensities, power and MI with the same input voltage as the other transducers.

7.2.4 *2MHz transducer*

This transducer gave the lowest release although it has higher acoustic pressures as compared to the 200kHz transducer and this is as result of the frequency dependence

of release. Thus, the higher the frequency, the lower the release. From Fig. 6.4 and Section B.3.5, it can be observed that the amount of calcein release was a bit higher for $233kPa$ until at 600s where the the highest release was obtained by the $386kPa$.

7.2.5 *Comparing all transducers*

Rapoport [54] has reported that low ultrasound frequency $(20 - 70kHz)$ and intensity 2 or $1W/cm^2$ gave a release of 12% from a drug contained within polymeric micelles. Epitarget [21] and Huang [25] have also shown that $40kHz$ and $1MHz$ transducer (full duty cycle) released 70% and 62% of calcein entrapped in liposomes respectively. However, in the present work, the highest release was 15% obtained with a $500kHz$ pulse wave of duty cycle 1/100 at a pressure amplitude of $312kPa$ (see Fig.6.5). This is in accordance with the theory given by Apfel and Holland [7, 6] and Sponer [58] that, cavitation is dependent on the frequency and the acoustic negative pressure (if mechanism is due to cavitation). Although it is an undeniable fact that release is frequency dependent as shown by Husseini [27, 28] it can also be seen from Fig. 6.5 that this dependence also depend on the amplitude of the pressure [58, 26]. Thus when the same number of periods and PRF was used (10 and $500Hz$), the $500kHz$ transducer was found to have higher release than the $200kHz$ (higher duty cycle than $500kHz$) with a pressure amplitude of $312kPa$ compared with that of the $200kHz$ ($145kPa$). To buttress this point, if the release mechanism is cavitation, then it depends on a lot of other factors as explained in Chapter two- like the bubble radius and environment, MI, etc [6, 26, 14]. Moreover, the mechanical index of the $312kPa$ ($500kHz$) was larger (0.5) than that of $145kP$ ($200kHz$) which was 0.3.

Release was found to increase with acoustic pressure at constant frequency (at least the maximum release) as seen from Fig. 6.5a. This might be due to cavitation, specifically stable cavitation since the mechanical indexes obtained for all transducers (see Section6.1) were not up to the threshold of inertial cavitation (0.7) proposed by Apfel and Holland [6, 7].This might explain why the amount of release was so low as compare to the result obtained by Epitarget, Schroeder and Huang [21, 56, 25] although the frequencies used are relatively lower than what was used in this experiment with the exception of Schroeder ($1MHz$). Stable cavitation is believed to cause small steady flow called microstreaming which intend creates extremely high shear stresses resulting in the release of the calcein from the liposomes [55, 44].

Also, the low duty cycle used in this experiment could play a role in the amount of calcein release. This is because for the 100% duty cycle (continuous wave for $200kHz$), the amount of calcein release was twice that of the pulse wave for the same transducer (12% for pules wave and 22% for continuous wave). Again, comparing with what was used by Epitarget, Schroeder and Huang [21, 56, 25], thus full duty cycle, these duty cycles are relatively low. Although Schroeder reported that release is independent on whether it is continuous or pulsed, the duty cycle of the pulsed wave was not given and the intensities used in both cases is far greater than what was used in the present work.

Another factor to be considered is the intensity of the beam which is believed to play a role in cavitation. It can be seen from Fig. 6.5b that for all frequencies, release increased with intensity. This is in accordance with the result obtained by Schroeder [56] who reported that release increases as the intensity of the beam increases. Again, this explains the reason low release was obtained (15%) in this experiment with $0.04mW/cm^2$ ($500kHz$) as compare to what he obtained (80%) with $3.3W/cm^2$ (20kHz). As said earlier on in this work, release was found to be dependent on the actual exposure time since the maximum release obtained for all transducers was when the sample was irradiated for 600s. This also agrees with what was reported by Schroeder [56] that the for a given liposomal drug, release is dependent on the irradiation time. Finally this can be explained by the first-order rate constants obtained which was almost the same ($\approx 0.01s^{-}1$) for all intensities.

7.2.6 *Effect HEPES and PBS on release*

These two dilution media were used to investigate whether they have any effect on the release of calcein from the liposomes. It was observed that for the same transducer with the same duty cycle and under the same experimental conditions, the amount of calcein release when PBS was used as dilution medium was higher than that of HEPES irrespective of the frequency and the intensity of the radiation (see Fig. 6.7, Fig. 6.6 and Section B.3.6). Little is actually known about why PBS gives higher release compare with that of HEPES but it might be due to the fact that PBS contains more ions than HEPES. This can be subjected to further investigation to get better explanations.

Chapter 8

CONCLUSION

The two main aims of this research was to design an experimental setup for the control release experiment and also to investigate the effect of ultrasound on release by varying the frequency, intensity, exposure time and the medium.

In the present work, the release of calcein from liposomes by ultrasound has been demonstrated using a broad spectra of ultrasound frequencies; $200kHz, 500kHz, 1MHz$ and $2MHz$ and an experimental setup has been designed for the control release experiment. All the four transducers were found to have low acoustic power and intensities. Nevertheless, the negative pressures of these transducers where within the threshold of cavitation so it was able to cause a release of calcein from the liposomes which demonstrates that ultrasound can trigger the release of drugs from liposomes. The maximum amount of calcein released was given by the $500kHz$ (15%) with an acoustic negative pressure of $312kPa$, an intensity of $0.04mW/cm^2$ and a mechanical index of 0.5, the next was the $200kHz$ (12%) with an acoustic pressure of $145kPa$, an intensity of $0.05mW/cm^2$ and mechanical index of 0.3. The third highest was the $1MHz$ (9%) with $611kPa$, intensity of $1.0mW/cm^2$ and mechanical index of 0.611 and then the $2MHz$ (8%) with a pressure of $386kPa$, an intensity of $0.4mW/cm^2$ and mechanical index of 0.27. The values of the mechanical indexes obtained with the various transducers suggests that, stable cavitation might have occurred which causes microstreaming which intend creates extremely high shear stresses resulting in the release of the calcein from the liposomes since the mechanical indexes were all below the threshold for inertial cavitation (0.7).

In conclusion, release is frequency and pressure dependent- dependent on MI. Again, for all frequencies and intensities maximum release was obtained with the longest exposure time ($600s$) which also confirms that ultrasound stimulated release is time dependent. Release was found to be dependent on the the intensities of the beam which is also dependent on the frequency of the transducer. Finally it was found that liposomes diluted with PBS gives higher release than with HEPES with the same transducer under the same experimental conditions. In the nut shell; *a*) Experimental setup has been designed which can be used to carry future research *b*) The optimal frequency was found to be $500kHz$ with acoustic pressure of $312kPa$ and intensity $0.038mW/cm^2$. *c*) The optimal

intensities of the various transducers are $0.05mW/cm^2$ for $200kHz$, $0.038mW/cm^2$ for $500kHz$, $1.0mW/cm^2$ for 1 MHz and finally $0.37mW/cm^2$ for $2MHzd$) Optimal ultrasound duration was found to be $600s$. *e*) PBS was found to give more release than HEPES sucrose buffer solution.

The contributions to the body of research in this subject that were presented in this thesis are therefore as follows: *a*) Establishing an experimental setup and protocols which includes design of ultrasound probes and construction of sample holders used during ultrasound exposure for control release experiment. *b*) Confirming that release of liposomal drug is dependent on the frequency and pressure. *c*) Confirming that for mechanical indexes below 0.7, the release mechanism is mainly stable cavitation. *d*) Confirming that release is dependent on ultrasound duration and the optimal duration found to be $600s$. *e*) Confirming that for a particular frequency, release is dependent on intensity and it increases as the frequency increases. *f*) Finding that release is dependent on the medium: PBS gives more release than HEPES sucrose buffer solution.

8.1 Recommendation and Future work

This research is just the beginning of the whole process of improving the delivery of cancer drug by the use of ultrasound although some work has already being done by others. The main recommendation is to improve the experimental design to get maximum effect together with the following other suggestions;

- The transducers can be matched to the 50Ω in order to have maximum power transfer for maximum effect to take place. Again, the sample chamber could be improved to have one designed for each transducer to make sure that the fluorescence changes measured is actually due to ultrasound effect and not other effects.
- Hydrophones could be used to locate the exact position of the focus during the control release experiment.
- Experiments under the same conditions could be conducted with a lower frequency than the ones used in this research to serve as a reference.
- Experiments could be conducted under physiological temperature - 37°C and to investigate the effect of HEPES and PBS on release.
- In order to get the exact specifications of the transducer, it is recommended that the exact application should be described to the manufacturer.

Finally, investigation and confirmation of the mechanism of drug release and the suggested type of cavitation is an important future work related to this research. This can then open the door for preclinical and clinical research in ultrasound stimulated release in the future.

Bibliography

[1] B. A.Chabner and D.L. Longo. *Cancer Chemotherapy and Biotherapy: Principles and practice*. Lippincott-Raven, Philadelphia, 1996.

[2] T. M. Allen. "Liposomes: opportunities in drug delivery". *Drugs*, 54:8–14, 1997.

[3] T. M. Allen, C. Hansen, F. Martin, C. Redemann, and A. Y. Young. "Liposome containing synthetic lipid derivative of poly(ethylene show prolonged circulation half-lives in vivo". *Biochimica*, 1991.

[4] V. C. Anderson and T. Takagishi. "Triggered release of hydrophilic agnets from plasmalogen liposomes using visible light or acid". *Biochimica et Biopysica Acta*, 1109:33–42, 1992.

[5] B. A. J. Angelsen. Waves, signals, and siginal processing vol i $ ii emantec. 2002.

[6] R. E Apfel. "Acoustic cavitation prediction". *Acoustic Society America*, 69, 1981.

[7] R. E. Apfel and C. K. Holland. "Gauging the likelihood of cavitation from short-pulse, low duty cycle diagnostic ultrasound". *Ultrasound in Medicine and Biology*, 17:179–185, 1991.

[8] M. Babincova, P. Cicmanec, V. Altanerova, C. Altane, and P. Babinec. "AC-magnetic field controlled drug release from magnetoliposomes:design of a method for site-specific chemotherapy ". *Bioelectrochemistry*, 55:17–19, 2002.

[9] A .D. Bangham, M. N. Standish, and J.C. Watkins. "Diffusion of univalent ions across the lamellae of swollen phospholipids"'. *Molecualr Biology*, 13:238–252, 1965.

[10] Y. Barenholz. "Liposome application: problems and prospects". *Current Opinion colloid interface science*, 6:66–77, 2001.

[11] Y. Barenholz, S. Amselem, and D. Goren. "Stability of liposomal-doxorubicin formulation: problems and prospects". *Medical Care Research and Review*, 13:449–491, 1993.

[12] S.B. Barnett, T. Haargr, M.C. Ziskin, W. L. Nyborg, K. Maeda, and J.Bang. "Current status of research on biophysical effects of ultrasound". *Ultrasound in Medicine and Biology*, 20:205–218, 1994.

[13] F. G Blake49. "The onset of cavitation in liquids: I. Acoustics res. lab". Technical Report 12, Harvard University, 1949.

[14] C. E. Brennen. *Cavitation and bubble dynamics*. New York Oxford University Press Oxford, New York, 1995.

[15] R. S. C. Cobbold. *Foundations of Biomedical Ultrasound*. 2002.

[16] C. Davies and B. T. Stokke. " Biophysical nanotechnologies,biophysical microtechniques ". Technical report, Norwegian University of Science and Technology (NTNU), Faculty of Natural Science and Technology; Department of Physics, 2006.

[17] C. D. Davies, L. M. Lundsrøm, J. Frengen, L. Eikenes, Ø. S. Bruland, O. Kaalhus, M. H. B Hjelstuen, and C. Brekken. "Radiation improves the disribution and uptake of liposomal doxorubicin (caelyx) in human osteosarcoma xenogrefts". *Cancer Research*, 64:547–553, 2004.

[18] D. C. Drummond, O. Meyer, K. Hong, D. B. Kirpotin, and D. Papahadjopoulos. "Optimizing liposomes for delivery of chemotherapeutic agents to solid tumors". *The American Society for Pharmacology and Experimental therapeutics*, 51:691–14, 1999.

[19] S.A. Elder. "Cavitation microstreaming". *Acoustics Society America*, 31, 1958.

[20] B. Endrich, H.S. Reinhold, J.F. Gross, and M. Intaglietta. "Tissue perfusion inhomogeneity during early tumor growth in rats,". *National cancer institute*, 62, 1979.

[21] Epitarget. Ultrasound testing of liposome formulations, 2008.

[22] J. Folkman. "Angiogenesis:an organizing principle for drug discovery.

[23] K. D. Frampton, K. Minor, and S. Martin. "Acoustic streaming in micro-scale cylindrical channels". *Applied Acoustics*, 65:1121–1129, 2004.

[24] A. Gabizon, R. Catane, B. Uziely, B. Kaufman, and T. Safra. "Prolonged circulation time and enhanced accumulation in malignant exudates of doxorubicin encapsulated in polyethylene-glycol coated liposomes.". *Cancer Research*, 54:987–992, 1994.

[25] S.L. Huang and C. MacDonald. "Acoustically active liposomes for drug encapsulation and ultrasound-triggered release". *Biochimica et Biopysica Acta-Biomembranes*, 1665:134–141, 2004.

[26] V. F. Humphrey. "Ultrasound and matter- physical interactions". *Biophysics and Molecular Biology*, 93:195–211, 2007.

[27] G. A . Husseini, G. D. Myrup, W. G. Pitt, and D. A Christensen. "Factors affecting acoustically triggered release of drugs from polymeric micelles". *Controlled release*, 69:43–52, 2000.

[28] G. A. Husseini, C. M. Runyan, and W. G. Pitt. "Barriers to drug delivery in solid tumors". *Biomedical Center*, 1:1–6, 2002.

[29] R. .K. Jain. "Barriers to drug delivery in solid tumors". *Scientific American*, 1:42–49, 1994.

[30] R.K. Jain. "Delivery of molecular medicine to solid tumors: lessons from in vivo imaging of gene expression and function.". *Controlled reslease*, 74:7–25, 2001.

[31] L. J. Kleinsmith. *Principles of Cancer Biology.* Pearson Benjamin Cummings, San Francisco, 2006.

[32] K. Kono, R. Nakai, K. Morimoto, and T. Takagishi. "Thermosensitive polymer-modified liposomes that release contents around physiological temperature". *Biochimica et Biopysica Acta*, 1416:239, 1999.

[33] J. Kost and R. Langer. "Responsive polymeric delivery systems". *Advance Drug Delivery Reviews*, 46, 2001.

[34] T. G. Leighton, A.D. Phelps, B.T. Cox, and W.L. Ho. "Theory and preliminary measurements of the rayleigh-like collapse of a conical bubble". *Acta Acoustica*, 84:801–814, 1998.

[35] T.G. Leighton. "Cavitation inception and fluid dynamics,". In *The Acoustic bubble*, pages 67–128. Academic Press, London, 1994.

[36] A. Marin, H. Sun, G. A. Husseini, W. G. Pitt, D. A. Christensen, and N. Y. Rapoport. "Drug delivery in pluronic micelles: effect of high-frequency ultrasound on drug release from micelles and intracellular uptake". *Control release*, 84:39–47, 2002.

[37] P. Marmottant and S. Hilgenfeldt. "Controlled vesicle deformation and lysis by single oscillating bubbles". *Nature*, 2003.

[38] A. Mueller, B. Bondurant, and D. F. O'Brien. "Visible-light-stimulated destabilization of peg-liposomes". *Macromolecules*, 33:4799–4804, 2000.

[39] S. Murdan. "Electro-reponsive drug delivery from hydrogels. *Control Release*, 92:1–17, 2003.

[40] G. Myhr and J. Moan. "Synergistic and tumour selective effects of chemotherapy and ultrasound". *Cancer letters*, 232:206–213, 2006.

[41] J.L. Nelson, B.L Roeder, J.C Carmen, F. Roloff, and W.G. Pitt. "Ultrasonically activated chemotherapeutic drug delivery in a rat model". *Cancer Research*, 62:7280–7283, 2002.

[42] K. Y Ng and T. O. Matsunaga. "Ultrasound-mediated drug delivery". *Drug delivery: applications and principles*, 1:245–278, 2005.

[43] W. L. Nyborg. "Ultrasonic microstreaming and related phenomena". *British Journal of cancer. Supplement*, 45, 1982.

[44] W. L. Nyborg. "Basic physics of low frequency therapeutic ultrasound". *Ultrasound Argioplasty*, 1996. edited by R. J. Siegel (Kluwer Academic, Boston).

[45] Olympus. Ultrasonic transducers technical notes. http://www.olympusndt.com/data/File/panametrics/UT-technotes.en.pdf, 2006.

[46] World Health Organization. http://www.who.int/mediacentre/factsheets/fs297/en/index.html. Fact sheetNo. 297.

[47] D. Papahadjopoulos, T.M. Allen, A. Gabizon, E. Mayhew, Matthay K, Huang SK, Lee K-D, Woodle MC, D.D Lasic, C. Redemann, and F.J Martin. "Sterically stabilized liposomes: Improvements in pharmacokinetics and antitumor therapeutic efficacy.". *Proceedings of National Academy of Science USA*, 88:195–211, 1991.

[48] PerkinElmers. Introduction to fluorescence spectroscopy, 2000. User Assistance.

[49] W. G. Pitt, G. A. Husseini, and Bryant J. Staples. "Ultrasonic drug delivery - a general review.

[50] P.N Prasad. *Introduction to Biophotonics*. John Wiley and Son, Inc, New Jersey, 2003.

[51] R.J. Price, D.M. Skyba, S. Kaul, and T.C. Skalak. "Delivery of colloidal particles and red blood cells to tissue through microvessel ruptures created by targeted microbubble destruction with ultrasound". *Circulation*, 98:1264–1267, 1998.

[52] Radiation Protection and Measurements. Exposure criteria for medical diagnostic ultrasound: II. criteria based on all known mechanisms. http://www.ncrp.com, 2002. NCRP Report No. 140.

[53] N. Rapoport. "Tumor targeting by polymeric assemblies and ultrasound activation.". In *Stimuli Sensitive Particulates and Assemblies*, volume 8. Kentus Books MML Series, R. Arshadi and K. Kono Eds, London, 2006.

[54] N. Rapoport, W.G. Pitt, H. Sun, and J.L. Nelson. "Adrug delivery in polymeric micelles: from in vitro to in vivo". *Control Release*, 91, 2003.

[55] J.A Rooney.

[56] A. Schroeder, Y. Avnir, S. Weisman, Y. Najajreh, A. Gabizon, Y. Talmon, J. Kost, and Y. Barenholz. "Controlling liposomal drug release with low frequency ultrasound mechanism and feasibility". *Langmuir*, 23:4019–4025, 2007.

[57] P. A. J. Speth, Q. G. C. M Hoesle, and C. Haanen. "Clinical pharamcokinetics of doxorubicin". *Clinical Pharmacokinet*, 15:15–31, 1988.

[58] J. Sponer. "Dependence of the cavitation threhold on the ultrasounic frequency". *Czechoslovak Journal of Physics*, 40, 1990.

[59] T. Szabo. *Diagnostic ultrasound imaging: Inside out.* Academic Press, London, 2004.

[60] V.P. Torchilin. "Drug discovery". *National review*, 4:145–160, 2005.

[61] P. N. T. Wells. "Ultrasound imaging". *Physics in Medicine and Biology*, 51:83–98, 2006.

[62] Y.Steinberg, A. Schroeder, Y. Talmon, J. Schmidt, R. L. Khalfin, Y. Cohen, J. M. Dvoissele, S. Begu, and D. Avnir. "Synergistic and tumour selective effects of chemotherapy and ultrasound". *Langmuir*, 23:12024–12031, 2007.

Part V

APPENDICES

Appendix A

MATERIALS AND EQUIPMENT FOR SAMPLE PREPARATION AND TREATMENT

This section gives a detailed description of all the materials or chemicals used in preparing the sample before exposing it to the ultrasound beam.

A.1 Chemicals for Sample Preparation

Liposome: calcein liposomes #CCD6-23rep, #CCD-23dup supplied by Epitarget, Oslo Norway. These batches have the following properties:

- Membrane composition; DSPE:DSPC:DSPE-PEG2000:Chol (mole%; $62 : 7,5 : 5,5 : 25$)
- Concentration of lipid (nominal) = 16 mg/mL
- Composition of intraliposomal phase; 50 mM calcein and 10 mM HEPES solution with pH = 7.4.
- Composition of extraliposomal phase; 10 mM HEPES and 0.02% (w/v) sodium azide sucrose solution with pH = 7.39.
- liposome physiochemical properties: size = $87nm$ (CCD-23rep) and $85nm$ (CCD-23dup), Zeta potential = $-19mV$ with pH = 7.1 for CCD-23rep and polydispersity index =0.1

Dilution medium1: 10 mM HEPES buffered Sucrose solution stored at $2 - 8^{\circ}$ with a pH of 7.39. The chemicals used in preparing this solution were:

- 1M NaOH

- HEPES (MW 238.3g/mol, pH = 6.8 − 8.2, pKa = 7.54, 99.5%titration, Sigma H3375 Batch# 88H5446, USA)
- Sucrose (MW 342.30 g/mol, BDH AnalaR prod 102745C, Lot#$K32050486405$ BH15 England)
- Sodium azide (BDH AnalaR prod 10369 Lot#$K2237000548$)
- Distilled water

Dilution medium 2: PBS - Phosphate buffered saline. This consist of Phosphate buffered saline tablets from the company Sigma Aldrich. That is, 1 tablet in 200 ml deionised sterilfiltered water. The Phosphate buffered saline tablets contains;

- Sodium chloride, crystals (NaCl)
- Sodium phosphate, Dibasic, Anhydrous,
- Potassium chloride (KCl)
- Potassium phosphate, monobasic, anhydrous (KH2PO4)
- Filtered deionized water

Detergent: 10% Triton X -100 in H_2O (Sigma U.S.A $\#T - 8787$,Lot $\#19H2611$)

A.2 Apparatus for the Preparation of Sample and Dilution Medium

- Cuvette
- Pipette
- Test tube 50ml
- Test tube 15ml
- Conical flask 500ml
- pH meter
- Thermometer
- Gloves
- Finn pipette

- Glass tube
- Water bath (DT Hetotherm , 220V, No. 91060917)
- Magnetic stirrer
- Measuring cylinder
- conical flask 1 liter
- pH meter (PW 9420)

A.3 Specifications of Transducers

Table A.1: Specifications of transducers used in the experiment, the focal length, active diameter and frequency were given by the manufacturer whereby the rest are calculated values. All transducers are immersion probes and were supplied by Ultran group, USA. GMP is Gas matrix piezoelectric, WS stands for W-Series and pf/p0 is the ratio of pressure at the focus to the pressure at the surface

Frequency [MHz]	0.2	0.5	1	2
Type	GMP	GMP	WS	WS
Wavelength (water)[mm]	7.50	3.0	1.5	0.75
Wavelength(plexiglass)[mm]	13.50	5.4	2.7	1.35
Focal distance or length (distilled water)[mm]	76	50	85	125
Active diameter[mm]	38	25	25	19
Total diameter[mm]	43	32	32	25
Fraunhofer limit[mm]	48.13	52.08	104.17	120.33
Focal depth (Lf)[mm]	51.94	48.0	96	129.85
Focal diameter Df[mm]	19.74	12	12	9.87
Fresnel number (Smax)	1.04	0.96	0.96	1.04
Geometric factor	3.26	3.01	3.01	3.36
pf/p0	3.02	3.27	3.27	3.02

Appendix B

RESULTS FROM CHARACTERIZATION AND CONTROL RELEASE EXPERIMENT

B.1 Impedance Measurements

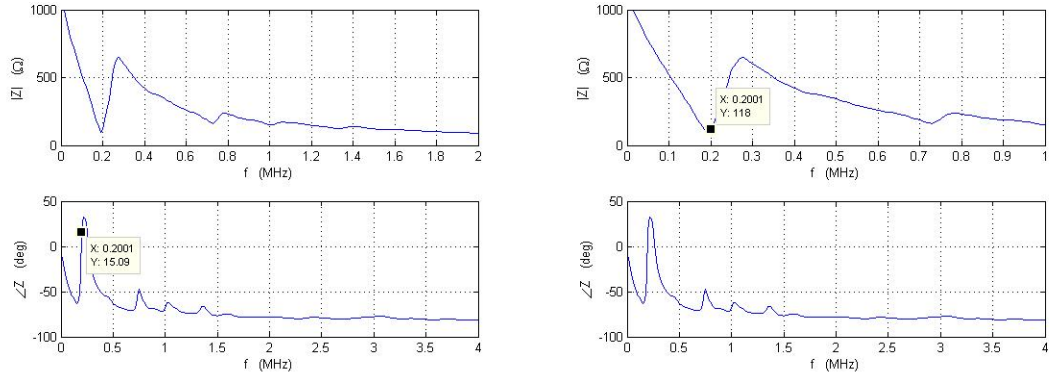

(a) (b)

Figure B.1: Impedance of the 200kHz transducer, magnitude (a) and phase angle (b)

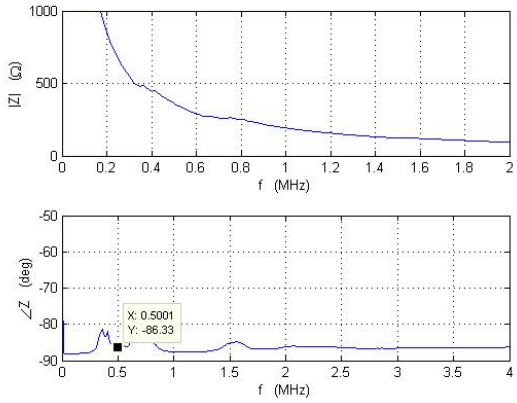

(a)

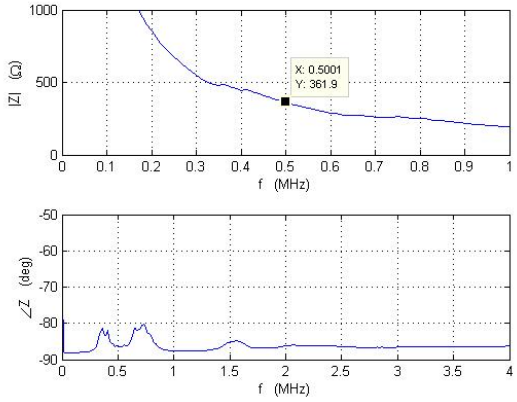

(b)

Figure B.2: Impedance of the 500kHz transducer, magnitude (a) and phase angle (b)

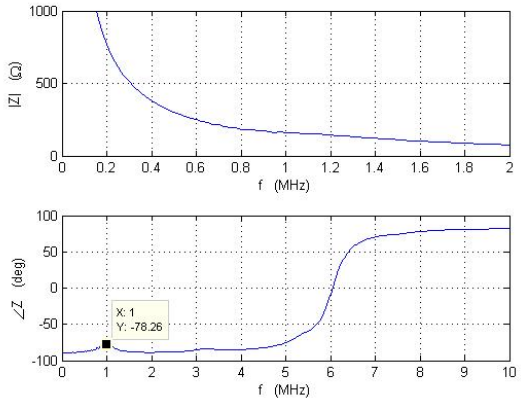

(a)

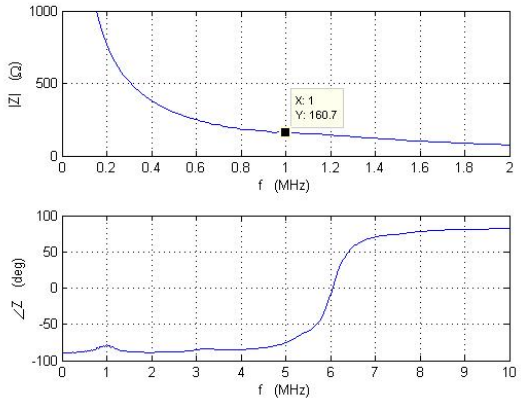

(b)

Figure B.3: Impedance of the 1MHz transducer, magnitude (a) and phase angle (b)

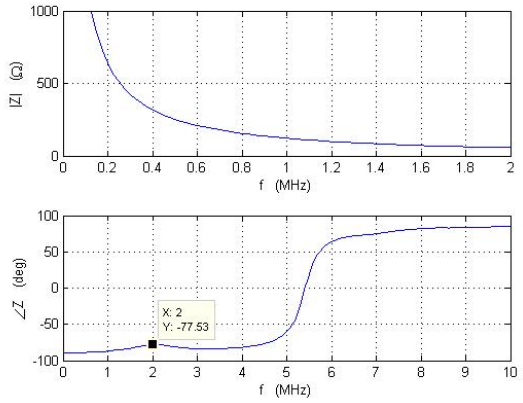

(a)

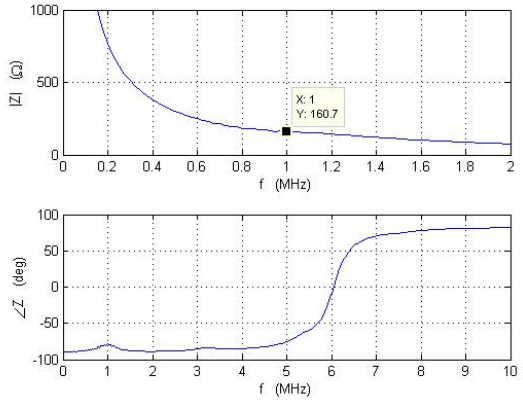

(b)

Figure B.4: Impedance of the 21MHz transducer, magnitude (a) and phase angle (b)

B.2 Measurement of Out Voltage from the Amplifier

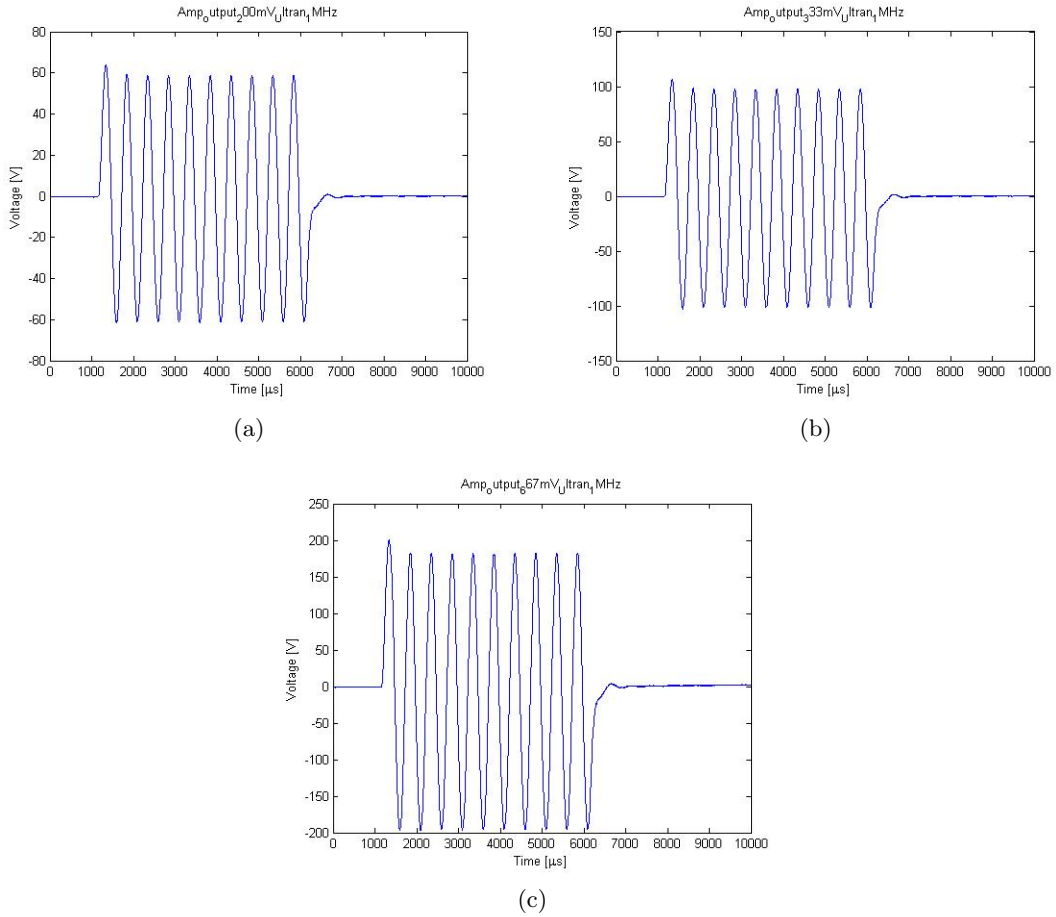

Figure B.5: Output voltage after amplification used for driving the transducer(a) input of $200mVpp$ gave an output of $\approx$ $120Vpp$ (b) input of $333.3mV$ gave an output of $\approx$ $200Vpp$ and (c) input of $666.7mVpp$ gave an output of $\approx 400Vpp$

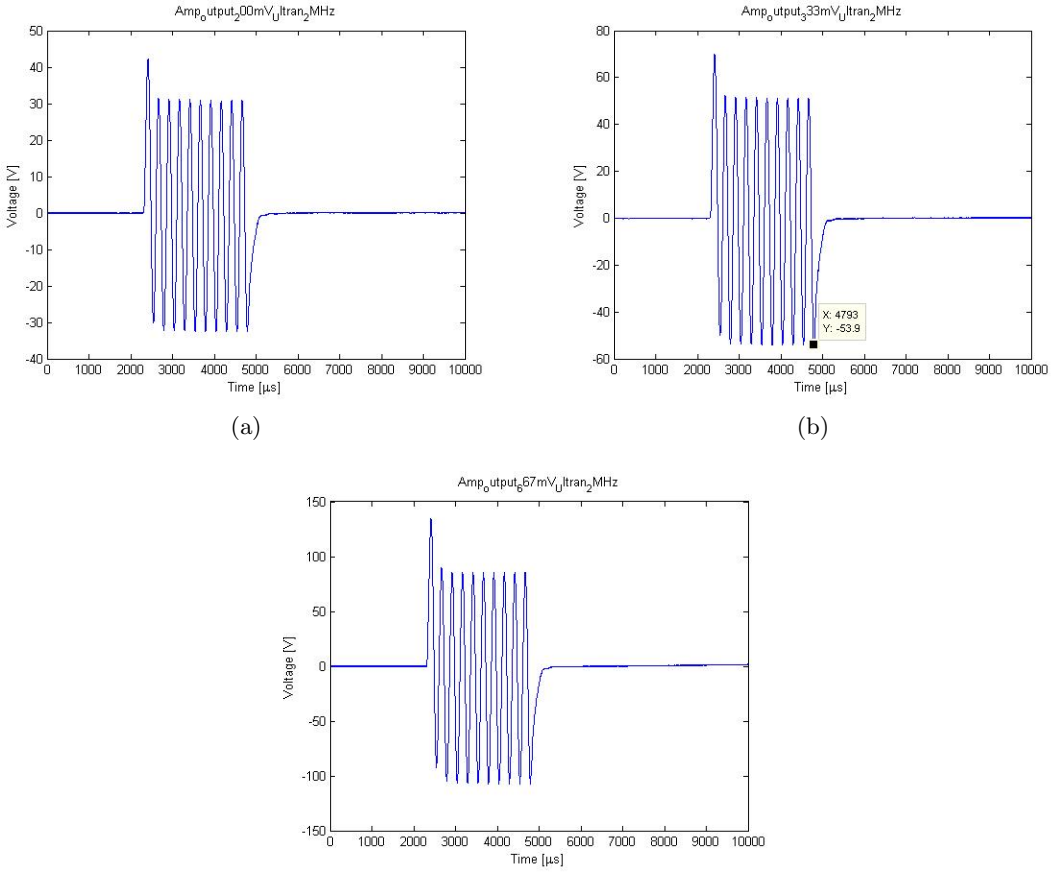

Figure B.6: Output voltage after amplification used for driving the transducer(a) input of $200mVpp$ gave an output of $\approx 60Vpp$ (b) input of $333.3mVpp$ gave an output of $\approx 100Vpp$ and (c) input of $666.7mVpp$ gave an output of $\approx 200Vpp$

B.3 Control Release

B.3.1 *Initial results*

B.3.2 *Control release at 200kHz*

Table B.1: Detailed results from the control release experiment using 200kHz transducer with continuous wave.

Ultrasound duration[s]	% release 1	% release 2	Average % release	Standard deviation
0	0	0	0	0
30	4.613937422	5.660988674	5.137463048	0.740377041
60	6.670670547	6.385973136	6.528321842	0.20131147
90	9.255465776	7.353683354	8.304574565	1.344763247
120	12.85870817	7.593724251	10.22621621	3.722905831
240	13.96326238	9.328433345	11.64584786	3.277319042
360	22.68795697	15.80823141	19.24809419	4.864700596
600	28.43712372	14.46449583	21.45080977	9.880139939
max release	100	100	100	0

Table B.2: Detailed results from the control release experiment using 200kHz transducer with 10 pulses and PRF of 500Hz (1/40 duty cycle)with an acoustic negative pressure of 59kPa.

Ultrasound duration[s]	% release 1	% release 2	Average % release	Standard deviation
0	0	0	0	0
30	3.427834204	3.500078707	3.463956456	0.051084578
60	4.129033004	3.341737054	3.735385029	0.556702305
90	6.097619558	3.464740962	4.78118026	1.861726309
120	5.078797278	5.053583087	5.066190182	0.017829126
240	6.199834073	5.704440098	5.952137086	0.350296439
360	6.60717517	6.509569568	6.558372369	0.069017583
600	7.688481941	7.348894553	7.518688247	0.240124545
max release	100	100	100	0

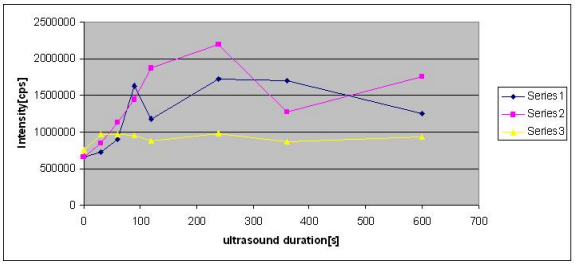

(a)

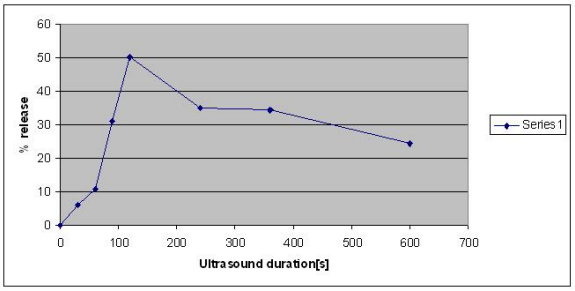

(b)

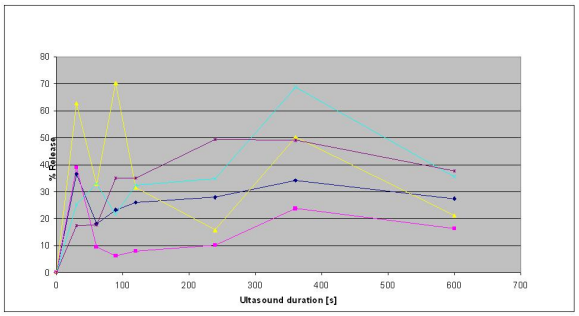

(c)

Figure B.7: Results from initial experiments (a)Intensity of calcein registered as a function of ultrasound duration using 200kHz transducer with 1kHz PRF and 5 pulses for all readings. (b)Percentage release as a function of ultrasound duration using 200kHz with 1kHz PRF and 5 pulse (c) Percentage release as function of ultrasound duration using 500kHz with 10 pulses and 500KHz PRF

Table B.3: .

Detailed results from the control release experiment using 200kHz transducer with 10 pulses and PRF of 500Hz (1/40 duty cycle) with an acoustic negative pressure of 93kPa.

Ultrasound duration [s]	% release1	% release2	Average % release	Standard deviation	$P_{ac}^2 T_{true}$ $[(kPa)^2 s]$
0	0	0	0	0	0
30	5.236152353	2.952073012	4.094112683	1.615087991	6486.75
60	5.256626278	4.118344362	4.68748532	0.804886862	12973.5
90	4.618270859	5.158680978	4.888475918	0.38212766	19460.25
120	5.083280382	7.558869845	6.321075114	1.750506096	25947
240	8.076711845	10.44615397	9.261432909	1.675448596	51894
360	7.579877939	12.91720345	10.24854069	3.774059061	77841
600	9.106083306	13.55344887	11.32976609	3.144762345	129735
max release	100	100	100	0	-

Table B.4: Detailed results from the control release experiment using 200kHz transducer with 10 pulses and PRF of 500Hz (1/40 duty cycle) with an acoustic negative pressure of 145kPa.

[H]

Ultrasound duration [s]	% release1	% release2	Average % release	Standard deviation	$P_{ac}^2 T_{true}$ $[(kPa)^2 s]$
0	0	0	0	0	0
30	3.628414173	3.207352489	3.417883331	0.297735572	15768.75
60	5.10805461	3.080163777	4.094109193	1.433935359	31537.5
90	6.224317454	3.770478609	4.997398031	1.735126087	47306.25
120	8.766263845	5.189520507	6.977892176	2.529139469	63075
240	9.687874665	5.889991091	7.788932878	2.685509229	126150
360	10.99213824	9.310407125	10.15127268	1.189163478	189225
600	12.68719902	11.11985826	11.90352864	1.108277276	315375
max release	100	100	100	0	-

B.3.3 *Control release at 500kHz*

Table B.5: Detailed results from the control release experiment using 500kHz transducer with 10 pulses and PRF of 500Hz (1/100 duty cycle) with the lowest acoustic negative pressure

Ultrasound duration [s]	% release1	% release2	Average % release	Standard deviation
0	0	0	0	0
30	3.307835985	3.061448087	3.184642036	0.174222553
60	3.195509165	2.94883504	3.072172103	0.174424946
90	4.680517277	4.437627202	4.55907224	0.171749219
120	4.49796871	4.039414566	4.268691638	0.324246745
240	3.957387149	4.732552779	4.344969964	0.548124873
360	4.269258437	6.97205184	5.620655138	1.911163544
600	5.239983172	7.05493392	6.147458546	1.283363982
max release	100	100	100	0

Table B.6: Detailed results from the control release experiment using 500kHz transducer with 10 pulses and PRF of 500Hz (1/100 duty cycle) with an acoustic negative pressure of 312kPa

Ultrasound duration [s]	% release1	% release2	Average % release	Standard deviation	$P_{ac}^2 T_{true}$ $[(kPa)^2 s]$
0	0	0	0	0	0
30	3.83928118	3.804468064	3.821874622	0.02461659	29203.2
60	5.353045038	3.413214308	4.383129673	1.3716674636	58406.4
90	7.693500163	8.730420829	8.211960496	0.733213635	87609.6
120	7.375358134	10.1488036	8.762080868	1.961122098	116812.8
240	10.67913564	10.9779029	10.82851927	0.211260353	233625.6
360	14.42965307	13.00830828	13.71898067	1.005042537	350438.4
600	15.16525693	14.5966485	14.88095271	0.402066875	584064
max release	100	100	100	0	-

Table B.7: Detailed results from the control release experiment using 500kHz transducer with 10 pulses and PRF of 500Hz (1/100 duty cycle) at an acoustic negative pressure of 378kPa

Ultrasound duration [s]	% release1	% release2	Average % release	Standard deviation	$P_{ac}^2 T_{true}$ $[(kPa)^2 s]$
0	0	0	0	0	0
30	3.083168225	2.271436845	2.677302535	0.573980763	42865.2
60	5.297618192	2.449853995	3.873736094	2.013673375	85730.4
90	7.799818377	3.332969047	5.566393712	3.158539452	128595.6
120	7.139219584	5.802188351	6.470703967	0.945423851	171460.8
240	9.420051879	6.902095191	8.161073535	1.780464249	342921.6
360	12.78255862	11.50085773	12.14170818	0.906299389	514382.4
600	14.06779619	14.58542397	14.32661008	0.366018113	857304
max release	100	100	100	0	-

B.3.4 *Control release at 1MHz*

Table B.8: Detailed results from the control release experiment using 1MHz transducer with 20 pulses and PRF of 500Hz (1/100 duty cycle) with an acoustic negative pressure of 196kPa

Ultrasound duration [s]	% release1	% release2	Average % release	Standard deviation	$P_{ac}^2 T_{true}$ $[(kPa)^2 s]$
0	0	0	0	0	0
30	2.943037611	2.935865443	2.939451527	0.005071489	11524.8
60	2.822778395	2.50914275	2.665960572	0.221773891	23049.6
90	3.086456404	3.880846509	3.483651457	0.56171863	34574.4
120	4.06781885	4.332999478	4.200409164	0.18751102	46099.2
240	6.004595831	4.995917509	5.50025667	0.713243282	92198.4
360	8.535714461	6.026908827	7.281311644	1.773993477	138297.6
600	9.962488703	7.1010717	8.531780201	2.023327367	230496
max release	100	100	100	0	-

Table B.9: Detailed results from the control release experiment using 500kHz transducer with 20 pulses and PRF of 500Hz (1/100 duty cycle) with an acoustic negative pressure of 325kPa

Ultrasound duration [s]	% release1	% release2	Average % release	Standard deviation	$P_{ac}^2 T_{true}$ $[(kPa)^2 s]$
0	0	0	0	0	0
30	2.085258589	4.195718723	3.140488656	1.492320672	31687.5
60	3.982897423	3.73211909	3.857508257	0.17732706	63375
90	3.873747994	3.597009891	3.735378943	0.195683389	95062.5
120	5.212072704	4.701800124	4.956936414	0.360817202	126750
240	6.872118934	6.444675756	6.658397345	0.30224797	253500
360	7.178773606	6.635678541	6.907226073	0.384026204	380250
600	7.985770351	8.429426585	8.207598468	0.313712332	633750
max release	100	100	100	0	-

Table B.10: Detailed results from the control release experiment using 1MHz transducer with 20 pulses and PRF of 500Hz (1/100 duty cycle) with an acoustic negative pressure of 611.

[H]

Ultrasound duration [s]	% release1	% release2	Average % release	Standard deviation	$P_{ac}^2 T_{true}$ $[(kPa)^2 s]$
0	0	0	0	0	0
30	2.943037611	2.935865443	2.939451527	0.005071489	111996.3
60	2.822778395	2.50914275	2.665960572	0.221773891	223992.6
90	3.086456404	3.880846509	3.483651457	0.56171863	335988.9
120	4.06781885	4.332999478	4.200409164	0.18751102	447985.2
240	6.004595831	4.995917509	5.50025667	0.713243282	895970.4
360	8.535714461	6.026908827	7.281311644	1.773993477	1343955.6
600	9.962488703	7.1010717	8.531780201	2.023327367	2239926
max release	100	100	100	0	-

B.3.5 *Control release at 2MHz*

Table B.11: Detailed results from the control release experiment using 2MHz transducer with 40 pulses and PRF of 500Hz (1/100 duty cycle) with an acoustic negative pressure of 143kPa

Ultrasound duration [s]	% release1	% release2	Average % release	Standard deviation	$P_{ac}^2 T_{true}$ $[(kPa)^2 s]$
0	0	0	0	0	0
30	1.046013385	1.798628619	1.422321002	0.532179335	6134.7
60	1.689646029	2.492030359	2.090838194	0.5673714	12269.4
90	2.604067468	2.989318475	2.796692971	0.2724136	18404.1
120	2.087341608	2.886480047	2.486910828	0.565076209	24538.8
240	2.25315561	3.050940716	2.652048163	0.564119259	49077.6
360	4.029782693	4.813067417	4.421425055	0.55386594	73616.4
600	5.475460784	4.956717952	5.216089368	0.366806574	122694
max release	100	100	100	0	-

Table B.12: Detailed results from the control release experiment using 2MHz transducer with 40 pulses and PRF of 500Hz (1/100 duty cycle) with an acoustic negative pressure of 233kPa

Ultrasound duration [s]	% release1	% release2	Average % release	Standard deviation	$P_{ac}^2 T_{true}$ $[(kPa)^2 s]$
0	0	0	0	0	0
30	1.65604963	2.128863846	1.892456738	0.334330139	16286.7
60	3.621563757	2.713965819	3.167764788	0.641768657	32573.4
90	4.20091594	3.193762358	3.697339149	0.712165127	48860.1
120	3.621563757	2.298343144	2.959953451	0.935658269	65146.8
240	4.164192416	4.186375544	4.17528398	0.01568584	130293.6
360	4.826424287	4.907721358	4.867072822	0.05748571	195440.4
600	8.488437629	4.533804516	6.511121072	2.796347891	325734
max release	100	100	100	0	-

Table B.13: Detailed results from the control release experiment using 2MHz transducer with 40 pulses and PRF of 500Hz (1/100 duty cycle) with an acoustic negative pressure of 386kPa

Ultrasound duration [s]	% release1	% release2	Average % release	Standard deviation	$P_{ac}^2 T_{true}$ $[(kPa)^2 s]$
0	0	0	0	0	0
30	1.948374235	0.812348877	1.380361556	0.803291234	44698.8
60	2.740542089	2.800185278	2.770363683	0.042174104	89397.6
90	3.340715593	2.277111101	2.808913347	0.752081949	134096.4
120	4.380905112	3.079879299	3.730392206	0.919964175	178795.2
240	4.385979547	3.535579668	3.960779607	0.601323521	357590.4
360	5.866949723	4.922382978	5.39466635	0.667909551	536385.6
600	8.658305667	6.03830031	7.348302989	1.852623555	893976
max release	100	100	100	0	-

B.3.6 *HEPES and PBS*

B.3.6.1 With 500kHz transducer

Table B.14: Detailed results from the control release experiment using PBS as a dilution medium and 500kHz transducer with 10 pulses and PRF of 500Hz (1/100 duty cycle) with an acoustic negative pressure of 312kPa. Sample was placed (50mm) at the focus of the transducer.

Ultrasound duration [s]	% release	$P_{ac}^2 T_{true}$ $[(kPa)^2 s]$
0	0	0
30	16.19159164	29203.2
60	15.47825531	58406.4
90	17.43846384	87609.6
120	18.65578289	116812.8
240	22.92452103	233625.6
360	26.62295107	350438.4
600	33.87712131	584064
max release	100	-

Table B.15: Detailed results from the control release experiment using HEPES as dilution medium and 500kHz transducer with 10 pulses and PRF of 500Hz (1/100 duty cycle) with an acoustic negative pressure of 312kPa. Sample was placed at the focus (50mm) of the transducer.

Ultrasound duration [s]	% release	$P_{ac}^2 T_{true}$ $[(kPa)^2 s]$
0	0	0
30	3.83928118	29203.2
60	5.353045038	58406.4
90	7.693500163	87609.6
120	7.375358134	116812.8
240	10.67913564	233625.6
360	14.42965307	350438.4
600	15.16525693	584064
max release	100	-

Table B.16: Detailed results from the control release experiment using PBS as a dilution medium and 500kHz transducer with 10 pulses and PRF of 500Hz (1/100 duty cycle) with an acoustic negative pressure of 312kPa. Sample was placed at the 40mm from the surface of the transducer.

Ultrasound duration [s]	% release	$P_{ac}^2 T_{true}$ $[(kPa)^2 s]$
0	0	0
30	14.12173346	29203.2
60	12.79571704	58406.4
90	12.51210033	87609.6
120	14.34419234	116812.8
240	17.65280924	233625.6
360	20.82193048	350438.4
600	23.90786825	584064
max release	100	-

Table B.17: Detailed results from the control release experiment using HEPES as a dilution medium and 500kHz transducer with 10 pulses and PRF of 500Hz (1/100 duty cycle) with an acoustic negative pressure of 312kPa. Sample was placed at the 40mm from the surface of the transducer.

Ultrasound duration [s]	% release	$P_{ac}^2 T_{true}$ $[(kPa)^2 s]$
0	0	0
30	4.032160129	29203.2
60	4.188629972	58406.4
90	4.578812533	87609.6
120	5.378539685	116812.8
240	7.07008337	233625.6
360	7.270613807	350438.4
600	8.771547529	584064
max release	100	-

B.3.6.2 With the 1MHz and 2MHz transducers

Table B.18: Detailed results from the control release experiment using PBS as a dilution medium and 1MHz transducer with 20 pulses and PRF of 500Hz (1/100 duty cycle) with an acoustic negative pressure of 325kPa.

Ultrasound duration [s]	% release1	% release2	Average % release	Standard deviation	$P_{ac}^2 T_{true}$ $[(kPa)^2 s]$
0	0	0	0	0	0
30	3.895381137	4.114715693	4.005048415	0.155092952	31687.5
60	5.408259977	3.964378136	4.686319057	1.020978641	63375
90	6.506082498	4.465374171	5.485728334	1.442998697	95062.5
120	7.349590268	7.06005317	7.204821719	0.204733645	126750
240	8.783302921	7.952682416	8.367992669	0.587337392	253500
360	10.20949888	8.850058144	9.529778513	0.961269764	380250
600	14.93672728	9.96422218	12.45047473	3.516092076	633750
max release	100	100	100	0	-

Table B.19: Detailed results from the control release experiment using HEPES as a dilution medium and 1MHz transducer with 20 pulses and PRF of 500Hz (1/100 duty cycle) with an acoustic negative pressure of 325kPa.

Ultrasound duration [s]	% release1	% release2	Average % release	Standard deviation	$P_{ac}^2 T_{true}$ $[(kPa)^2 s]$
0	0	0	0	0	0
30	2.841190633	3.986656619	3.413923626	0.809966766	31687.5
60	3.485828769	2.942471867	3.214150318	0.38421135	63375
90	3.252952851	3.64944189	3.45119737	0.280360088	95062.5
120	5.524485128	4.129327753	4.82690644	0.98652524	126750
240	6.461001377	4.695332397	5.578166887	1.248516509	253500
360	7.666317005	6.425274572	7.045795788	0.87754952	380250
600	8.008320876	7.847524708	7.927922792	0.11370006	633750
max release	100	100	100	0	-

Table B.20: Detailed results from the control release experiment using PBS as a dilution medium 2MHz transducer with 40 pulses and PRF of 500Hz (1/100 duty cycle) with an acoustic negative pressure of 386kPa

Ultrasound duration [s]	% release1	% release2	Average % release	Standard deviation	$P_{ac}^2 T_{true}$ $[(kPa)^2 s]$
0	0	0	0	0	0
30	9.315392066	3.876815084	6.596103575	3.845654664	44698.8
60	3.764499711	3.766306684	3.765403198	0.001277723	89397.6
90	3.535752647	4.079037938	3.807395293	0.384160713	134096.4
120	4.882212095	5.123135582	5.002673838	0.170358631	178795.2
240	4.466755017	5.136761192	4.801758105	0.47376591	357590.4
360	4.877935599	7.36309198	6.120513789	1.757270929	536385.6
600	6.918279338	9.077663631	7.997971484	1.526915277	893976
max release	100	100	100	0	-

Table B.21: Detailed results from the control release experiment using HEPES as a dilution medium and 2MHz transducer with 40 pulses and PRF of 500Hz (1/100 duty cycle) with an acoustic negative pressure of 386kPa

Ultrasound duration [s]	% release1	% release2	Average % release	Standard deviation	$P_{ac}^2 T_{true}$ $[(kPa)^2 s]$
0	0	0	0	0	0
30	2.442208623	2.329448956	2.38582879	0.079733125	44698.8
60	1.342112366	3.537096728	2.439604547	1.552088327	89397.6
90	1.611920201	3.119454892	2.365687547	1.065988003	134096.4
120	2.737273986	3.120088781	2.928681383	0.270690937	178795.2
240	2.422188442	3.586087238	3.00413784	0.823000731	357590.4
360	4.293019419	4.584370759	4.438695089	0.206016508	536385.6
600	4.975141609	5.133136919	5.054139264	0.111719555	893976
max release	100	100	100	0	-

B.4 Example of the Matlab Code for Calculations of First Order Rate Constant

```
U  = [0,30,60,90,120,240,360,600]';

A1 = [0,5.137463048,6.528321842,8.304574565,
10.22621621,11.64584786,19.24809419,21.45080977]';

A2 = [0,3.417883331,4.094109193,4.997398031,
6.977892176,7.788932878,10.15127268,11.90352864]';

A3 = [0,4.094112683,4.68748532,4.888475918,
6.321075114,9.261432909,10.24854069,11.32976609]';

A4 = [0,3.463956456,3.735385029,4.78118026,
5.066190182,5.952137086,6.558372369,7.518688247]';

% Where A1-A4 are the average percentage release at the various pressures
% for j = 1:10
% I1 = A1(end)*(1 - exp(-k1*U));
% error1 = norm(I1-A1)
% % endk1 = 1/210;
```

```
for j = 1:20
k1(j) = 1/(20 + 10*j);
I1 = A1(end)*(1 - exp(-k1(j)*U));
error1(j) = norm(I1-A1);
end
for j = 1:20
k2(j) = 1/(20 + 10*j);
I2 = A2(end)*(1 - exp(-k2(j)*U));
error2(j) = norm(I2-A2);
end
for j = 1:20
k3(j) = 1/(20 + 10*j);
I3 = A3(end)*(1 - exp(-k3(j)*U));
error3(j) = norm(I3-A3);
end
for j = 1:20
k4(j) = 1/(20 + 10*j);
I4 = A4(end)*(1 - exp(-k4(j)*U));
error4(j) = norm(I4-A4);
end

figure(1)
plot(k1,error1,'g')
hold on
plot(k2,error2,'b')
plot(k3,error3,'r')
plot(k4,error4,'y')
grid
xlabel('Rate constant[1/s]')
ylabel('Error')
hold off


[errmin,j] = min(error1);
k1 = 1/(20 + 10*j)
I1 = A1(end)*(1 - exp(-k1*U));
error1 = norm(I1-A1)
errors1 = I1-A1;

[errmin,j] = min(error2);
k2 = 1/(20 + 10*j)
I2 = A2(end)*(1 - exp(-k2*U));
```

```
error2 = norm(I2-A2)
errors2 = I2-A2;

[errmin,j] = min(error3);
k3 = 1/(20 + 10*j)
I3 = A3(end)*(1 - exp(-k3*U));
error3 = norm(I3-A3)
errors3 = I3-A3;

[errmin,j] = min(error4);
k4 = 1/(20 + 10*j)
I4 = A4(end)*(1 - exp(-k4*U));
error4 = norm(I4-A4)
errors4 = I4-A4;
```

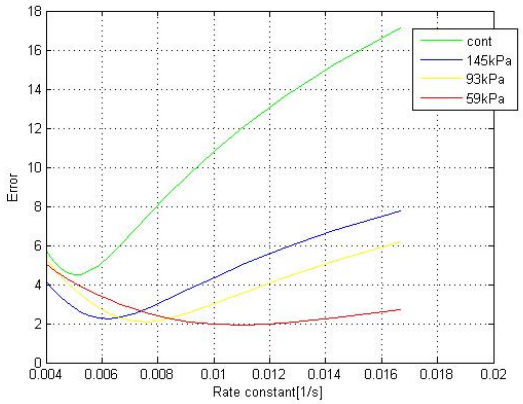

(a) 200kHz Transducer

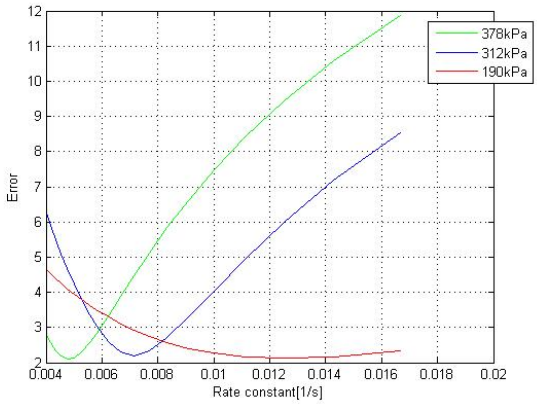

(b) 500kHz Transducer

Figure B.8: A graph of error as a function of first-order rate constant k (a) $k_{cont} = 0.005, k_{59kPa} = 0.0111s^{-1}, k_{93kPa} = 0.0077s^{-1}, k_{145kPa} = 0.0063s^{-1}$. with minimum errors of 4.5, 1.9, 2.1, 2.2 (b)$k_{190kPa} = 0.0125s^{-1}$, $k_{312kPa} = 0.0071s^{-1}$, $k_{378kPa} = 0.0048s^{-1}$ with minimum errors of 2.1, 2.2, 2.1.

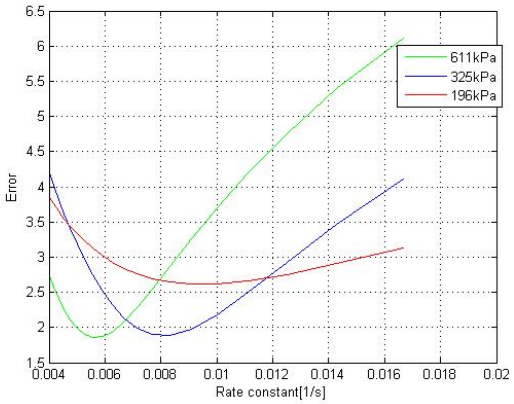

(a) 1MHz Transducer

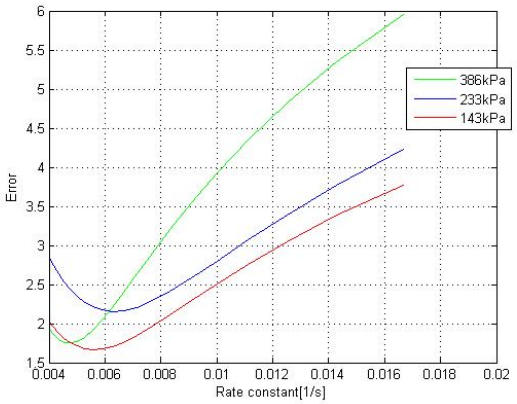

(b) 2MHz Transducer

Figure B.9: A graph of error as a function of first-order rate constant k (a) $k_{196kPa} = 0091s^{-1}, k_{325kPa} = 0.0083s^{-1}, k_{611kPa} = 0.0056s^{-1}$. with minimum errors of 2.6, 1.9, 1.9 (b)$k_{143kPa} = 0.0056s^{-1}$, $k_{233kPa} = 0.0063s^{-1}$, $k_{386kPa} = 0.0048s^{-1}$ with minimum errors of 1.7, 2.2,1.8.

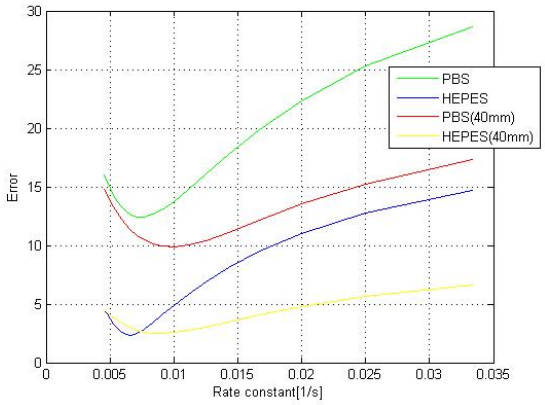

(a)

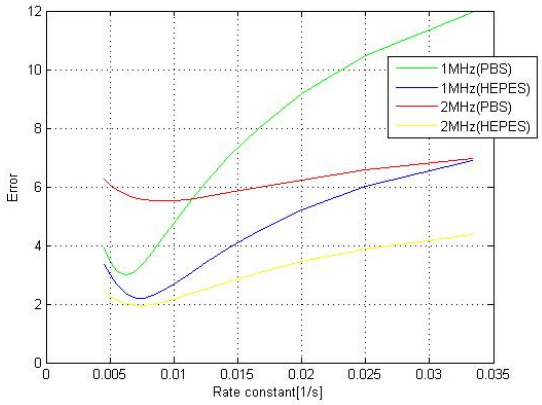

(b)

Figure B.10: A graph of error as a function of first-order rate constant k (a) 500kHz transducer for PBS and HEPES $k_{PBS} = 0077s^{-1}, k_{HEPES} = 0.0067s^{-1}, k_{PBSat40mm} = 0.010s^{-1}, k_{HEPESat40mm} = 0.0091s^{-1}$. with minimum errors of 12.4, 2.3, 9.9, 2.5 respectively (b)1MHz transducer $k_{PBS} = 0.0063s^{-1}$, $k_{HEPS} = 0.0071s^{-1}$ with minimum errors of 3.0, 2.2 respectively , for the 2MHz transducer $k_{PBS} = 0.0091s^{-1}, k_{HEPES} = 0.0071s^{-1}$ with minimum errors of 5.5, 2.0